Two Dimensional Turbulent Boundary Layer with Favorable Pressure Gradients: Similarity Type Solution of the Momentum Equation

---

A Thesis

presented to

the Faculty of the Department of Chemical Engineering

University of Houston

In Partial Fulfillment

of the Requirements for the Degree

Master of Science in Chemical Engineering

---

by

Jerry A. Bullin

May, 1970

Acknowledgments

The author would like to express his gratitude to his advisor, Dr. A. E. Dukler, whose comments and guidance were invaluable in this study. The author is also grateful to Mr. R. A. Williams and Mr. D. M. Ingels for their assistance in programming.

Finally, the author owes special thanks to his wife, Carol, for her perserverance in preparing the manuscript.

Two Dimensional Turbulent Boundary Layer
with Favorable Pressure Gradients:
Similarity Type Solution of
the Momentum Equation

An Abstract of a Thesis
presented to

the Faculty of the Department of Chemical Engineering
University of Houston

In Partial Fulfillment
of the Requirements for the Degree
Master of Science in Chemical Engineering

---

by
Jerry A. Bullin
May, 1970

Abstract

The turbulent boundary layer momentum equation was solved by using similarity variables to transform the partial differential equation into a more manageable form. Contrary to the case for laminar boundary layers, this equation contained a term involving streamwise derivatives which was not negligible. Thus, a method to estimate the streamwise term was devised.

A modification of an eddy viscosity distribution for pipe flow due to Gill and Sher was used to eliminate the Reynolds' shear stresses. The modified Gill and Sher equation was used for the so-called inner region of the boundary layer while the eddy viscosity was assumed constant in the outer region. Although the eddy viscosity distribution was not representative of the flow for adverse pressure gradients, it was quite satisfactory for zero and favorable pressure gradients involving fully developed turbulent flow. As a consequence of the eddy viscosity distribution, unacceptable results were acquired for adverse pressure gradient cases.

The present method was evaluated for zero and favorable pressure gradients by comparing the results with three different flows under various conditions. Good agreement was observed in all cases for the local and average skin friction coefficients and velocity profiles. Except for one boundary layer involving nonequilibrium flows, good results were obtained for the displacement and momentum thicknesses.

One of the major advantages of the present method was that a minimum of input information was required. That is, for any given boundary layer, only the approach velocity and the streamwise pressure gradient were needed.

Table of Contents

Chapter		Page
I.	INTRODUCTION	1
	Review of the Approaches for Solving the Turbulent Boundary Layer	3
II.	DEVELOPMENT OF THE BOUNDARY LAYER MOMENTUM EQUATION AND PARAMETERS	10
	Mathematical Statement of the Problem	10
	Transformation of Momentum Equation . .	11
	Formulation and Transformation of Eddy Viscosity Equation	15
	Transformed Momentum Equation	18
	Alternate Eddy Viscosity Formulation . .	19
	Other Boundary Layer Parameters	22
III.	METHOD OF SOLUTION	25
	Estimation of the Streamwise Terms . . .	25
	Convergence Technique for f''_o and η_δ . .	29
	Establish Inner and Outer Regions of Boundary Layer	34
	Numerical Techniques	38
	Summary	38
IV.	DISCUSSION OF RESULTS AND COMPARISON TO EXPERIMENT	39
	Results	46

Comparison of Calculated and Experimental Results 47

Results Using Alternate Eddy Viscosity Distribution 52

V. SUMMARY OF RESULTS AND RECOMMENDATIONS . . 53

BIBLIOGRAPHY 79

APPENDIX 83

A. Program for Turbulent Boundary Layer Calculations 84

B. Meissinger's Influence Function Technique 97

C. Comparison of Results Using Alternate Eddy Viscosity Distribution with Experimental Data 100

D. Nomenclature 104

List of Figures

FIGURE		Page
1-1	Boundary Layer Regions	8
1-2	Eddy Viscosity Distribution	9
2-1	Coordinate System	11
2-2	Smoothed Eddy Viscosity Distribution . . .	21
3-1	Correction for Streamwise Terms	28
3-2	Convergence Technique for f_o'' and η_δ . . .	35
3-3	Determination of Transition Point	36
3-4	Transition Point vs. Dimensionless Pressure Gradient	37
4-1	Effect of Correction for Streamwise Terms	40
4-2	Estimated Streamwise Terms vs. η for First Five Estimates	42
4-3	Distributions in a Boundary Layer with Favorable Pressure Gradients	44
4-4	Distributions in a Boundary Layer with Adverse Pressure Gradient	45
4-5	Calculated Results, u^+ vs. y^+	54
4-6	Calculated Results, u^+ vs. y^+	55
4-7	Calculated Results, u^+ vs. y^+	56
4-8	Calculated Results, c_f vs. Re	57
4-9	Calculated Results, c_f vs. Re	57
4-10	Calculated Results, c_f vs. Re	57

4-11 Calculated Results, $c_{f_{avg}}$ vs. Re 58

4-12 Comparison of Results with Experimental Data, c_f vs. Re 59

4-13 Comparison of Results with Experimental Data, $c_{f_{avg}}$ vs. Re 59

4-14 Comparison of Results with Smith and Walker Data, u^+ vs. y^+ 60

4-15 Comparison of Results with Smith and Walker Data, $u/u_\circ$ vs. η 61

4-16 Comparison of Results with Smith and Walker Data, u^+ vs. y^+ 62

4-17 Comparison of Results with Smith and Walker Data, $u/u_\circ$ vs. η 63

4-18 Velocity Profile Used to Match the Momentum Thickness at x = 2 feet (Herring and Norbury) 50

4-19 Comparison of Results with Herring and Norbury Data, u^+ vs. y^+ 64

4-20 Comparison of Results with Herring and Norbury Data, $u/u_\circ$ vs. η 65

4-21 Comparison of Results with Herring and Norbury Data, u^+ vs. y^+ 66

4-22 Comparison of Results with Herring and Norbury Data, $u/u_\circ$ vs. η 67

4-23 Boundary Layer Wall Used by Schubauer and Klebanoff 51

4-24 Comparison of Results with Schubauer and Klebanoff Data, u^+ vs. y^+ 68

4-25 Comparison of Results with Schubauer and Klebanoff Data, $u/u_\circ$ vs. η 69

4-26 Comparison of Results with Schubauer and Klebanoff Data, u^+ vs. y^+ 70

4-27 Comparison of Results with Schubauer and Klebanoff Data, u/u_o vs. η 71

4-28 Comparison of Results with Schubauer and Klebanoff Data, u^+ vs. y^+ 72

4-29 Comparison of Results with Schubauer and Klebanoff Data, u/u_o vs. η 73

4-30 Comparison of Results with Schubauer and Klebanoff Data, u^+ vs. y^+ 74

4-31 Comparison of Results with Schubauer and Klebanoff Data, u/u_o vs. η 75

C-1 Comparison of Results Using Alternate Eddy Viscosity with Experimental Data, u^+ vs. y^+ 101

C-2 Comparison of Results Using Alternate Eddy Viscosity with Experimental Data, u^+ vs. y^+ 102

List of Tables

Table		Page
4-1	Affect of Successive Approximations of Streamwise Terms on Boundary Layer Parameters	41
4-2	Comparison of Experimental (Smith and Walker) and Calculated Boundary Layer Parameters	76
4-3	Comparison of Experimental (Herring and Norbury) and Calculated Boundary Layer Parameters	77
4-4	Comparison of Experimental (Schubauer and Klebanoff) and Calculated Boundary Layer Parameters	78
A-1	Definition of Symbols in Computer Program	95
C-1	Comparison of Calculations Using Alternate Eddy Viscosity with Experimental Data	103

Chapter I

Introduction

In 1904, Prandtl (12) introduced the concept by which the flow past a body is divided into two regions: a very thin layer near the body where frictional effects are very important and the remaining flow outside this layer where frictional effects may be neglected. The thin viscous layer near the wall is generally referred to as a boundary layer and may be entirely laminar or may be turbulent with an extremely thin laminar sublayer.

In introducing the boundary layer concept, Prandtl simplified the Navier-Stokes equations for the case of a fluid flowing along a solid surface to obtain the well known boundary layer equation. This equation and the continuity equation are nonlinear partial differential equations whose exact solution can be accomplished only for certain specific situations. The existence of a known relationship between the local shear stress and the local velocity gradients makes the exact solution mathematically possible for these specific situations which occur in laminar flow.

In 1908, Blasius (1) obtained the first solution of the boundary layer equations for the case of laminar flow over a horizontal flat plate with no pressure gradient. In this classical solution a method called the similarity transformation was used. Blasius observed that the velocity profiles at all points along the plate for this particular flow could be reduced to a single profile if plotted using suitable scales. Thus, if the dimensionless quantity, u/u_0, where u_0 is the free stream velocity, is plotted as a function of a dimensionless variable, η, where η is the distance normal to the plate and is scaled by the boundary layer thickness, a velocity profile independent of position along the plate is obtained. As a result, the boundary layer equations are reduced to ordinary differential equations. Since Blasius' first solution, the method of similarity transformation has been successfully applied to many cases in laminar flow especially since the advent of high speed computers. Schlichting (16) has shown that the similarity method may be used for all laminar boundary layers where the free stream velocity varies along the plate as x^m where x is the distance from the leading edge of the boundary layer and m is a constant dependent upon geometry.

On the other hand, due to only limited understanding of the highly complex turbulent processes, exact solutions of the boundary layer equations are not possible for turbulent flows. The momentum equation for turbulent boundary layers contains a shear stress term which does not occur in the laminar boundary layer equation. For a two dimensional boundary layer, this term involves the time averaged product of two fluctuating velocities and is known as the turbulent shear stress as contrasted to the shear stress which results from the mean velocities. As one would expect, the fluctuating and mean velocities result from a decomposition of the velocity field into fluctuating and mean components.

The turbulent shear stress has not been theoretically related to the mean velocity gradient (or any other quantity which can be effectively used). As in most cases where rigorous theoretical relationships are not available, the solution must depend on some empirical information. Thus, the turbulent shear stress is empirically correlated with the most convenient parameter - the mean velocity gradient. Other methods use different empirical correlations to obtain solutions.

Review of the Approaches for Solving the Turbulent Boundary Layer

The objective of any method for solving the boundary layer equations is the prediction of certain mean properties of the flow such as the velocity, the skin friction, displacement thickness (which is a measure of the boundary layer thickness), and the location of the point at which the boundary layer separates from the wall or body. Information which almost all methods require for any particular boundary layer are the free-stream pressure gradient or the free-stream velocity distribution in the streamwise direction and information which specifies the conditions which exist at the point along the plate where the calculations are to be started. Since the calculations are very sensitive to the streamwise pressure gradient, a very high degree of accuracy is required in specifying this data. In addition, certain specialized information such as detailed velocity profiles at the starting point and turbulence data is essential to some methods.

A unique classification of the approaches to the solution of the boundary layer equation has recently been presented (4). The approaches are categorized into two broad groups based upon the form of the equation used to represent the boundary layer, that is,

A.) Methods based on the solution of a system of ordinary differential equations derived from integral equations.

B.) Methods based on the solution of the partial differential equations.

The momentum equation for a turbulent boundary layer in partial differential form is

$$u\frac{\partial u}{\partial x} + v\frac{\partial u}{\partial y} = u_o\frac{du_o}{dx} + \nu\frac{\partial^2 u}{\partial y^2} - \frac{\partial}{\partial y}(\overline{u'v'}) \tag{1-1}$$

where the bar denotes time average, u' and v' are fluctuating velocities and u_o is the free stream velocity. If Equation 1-1 is integrated across the boundary layer, the momentum integral equation which is used in the former group is obtained

$$\frac{d}{dx}(u_o^2\theta) + \delta^* u_o\frac{du_o}{dx} = \frac{\tau_w}{\rho} \tag{1-2}$$

Essentially all of the integral methods use the momentum integral equation, a second integral equation, and an assumed velocity distribution such as Coles "law of the wake". The assumed velocity profile is used to determine θ and δ^*. In addition, some methods require an empirical equation for the wall shear stress.

The nature of the second integral equation can be used to further classify the integral methods. The most significant difference between the integral methods is in the structure of this second equation. As pointed out by Reynolds (14), the three major integral techniques are the dissipation integral method, the entrainment method, and the moment of momentum method.

The dissipation integral method uses the mean energy integral equation, which is obtained by multiplying the momentum equation (Equation 1-1) by u before integrating, as the second equation. The mean energy equation is

$$\frac{d}{dx}(u_o^3 \delta^{**}) = 2D \tag{1-3}$$

$$D = \int_o^{\delta} \left\{ \overline{-u'v'} + \nu\left[\frac{\partial u}{\partial y}\right] \right\} \frac{\partial u}{\partial y}\, dy \tag{1-4}$$

where D is called the dissipation integral and δ^{**} is the dissipation energy thickness. The dissipation integral represents the rate of energy transfer from the mean velocity energy to the turbulence. An addition assumption involving either the local Reynolds' stress distribution or the dissipation integral and the properties of the mean flow is required in order to solve Equations 1-2 and 1-3.

The second method is based on the process of entrainment of nonturbulent fluid into the turbulent boundary layer region. The entrainment rate may be obtained from the continuity equation

$$\text{Entrainment rate} = \frac{d}{dx} \int_o^{\delta} u\, dy \tag{1-5}$$

An assumption about the relationship between the entrainment rate and either the mean flow or the turbulence is necessary for closure.

An additional method involves the moment of momentum integral equation which is acquired by multiplying the momentum equation by y. An assumption is required about the term in the moment of momentum integral equation which contains the integral of the turbulent shear stress. Other moment of momentum equations may be generated by multiplying the momentum equation by different weighting functions.

It should be noted that there are many variations of the above integral methods. All of the methods attempt to consider the turbulence either implicitly or explicitly.

The differential methods, on the other hand, may be classified according to the manner in which the Reynolds' stresses are represented. One category relates the Reynolds' stresses to the turbulence while the other uses the mixing length and eddy viscosity approach. The former method uses the turbulent kinetic energy equation with the appropriate boundary layer approximations as an additional equation. However, some assumptions are still necessary for closure, for example, an assumption is required about the relationship between the Reynolds' stresses and the mean turbulent energy.

The second method introduces an eddy viscosity according to the following equation:

$$-\overline{u'v'} = \varepsilon\frac{\partial u}{\partial y} \tag{1-6}$$

The equation defining the mixing length approach is very similar to Equation (1-6). In fact, they are related by

$$\varepsilon = L^2 \frac{du}{dy} \tag{1-7}$$

where L is the mixing length. This approach is used in the present analysis, thus, further development is in order.

Application of the Similarity Transformation Method to the Eddy Viscosity-Mixing Length Approach:

The difficulty in handling the equations in the eddy viscosity-mixing length approach has led investigators to use similarity variables to transform the partial differential equations into ordinary ones. As a result of the similarity type solutions of the turbulent boundary layer momentum equation, three universal velocity distribution laws have been proposed. These three laws have been analyzed in some detail by Telles and Dukler (23).

In the region of the boundary layer near the wall, the "law of the wall" proposes that the velocity profiles are independent of position along the wall when the velocity is measured in terms of its scale, that is,

$$u^+ = u/u_* = u^+(y^+) \tag{1-8}$$

where

$$y^+ = u_* y/\nu$$

and $$u_* = (\tau_w/\rho)^{1/2} = \text{friction velocity}$$

Since large deviations between the law of the wall and experiment were observed at large values of y^+, Coles (4) proposed a purely empirical correction to the wall law, that is,

$$u^+ = A + B \ln y^+ + K_1 \, W(y/\delta) \tag{1-9}$$

Based on experimental evidence Coles considered this equation to be universal and presented numerical values of W for various values of y/δ.

In a manner similar to the wall law, a "velocity defect law" has been proposed for the fully developed turbulent region of the boundary layer. This law suggests that the mean velocity is a unique function of its difference from the free stream velocity, that is,

$$\frac{u_o - u}{u_*} = u_D = u_D(y/\delta) \qquad (1\text{-}10)$$

The major limitations to these "universal" laws are that they are asymptotic in character and apply only over limited regions.

Two Layer Approach:

In the present approach to the solution of the turbulent boundary layer momentum equation, the boundary layer is regarded as a composite layer characterized by inner and outer regions as shown in Figure 1-1.

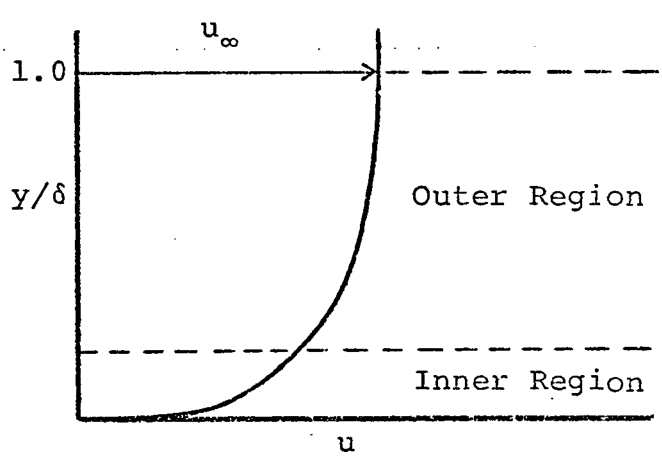

Figure 1-1

Boundary Layer Regions

According to Clauser (13), the inner region contains about 10 to 20% of the total thickness. The thickness depends primarily on the wall shear stress and fluid viscosity. In this region, the eddy viscosity varies almost linearly with distance from the wall.

For the outer region, on the other hand, the flow is completely independent of viscosity but is highly dependent on the streamwise pressure gradient. In addition, the flow is affected by the wall shear stress.

As in the inner region, the turbulent shear stress is related to the mean velocity distribution by the eddy viscosity. However, in this region the eddy viscosity is assumed constant as suggested by Clauser. The eddy viscosity distribution for an entire boundary layer is shown in Figure 1-2.

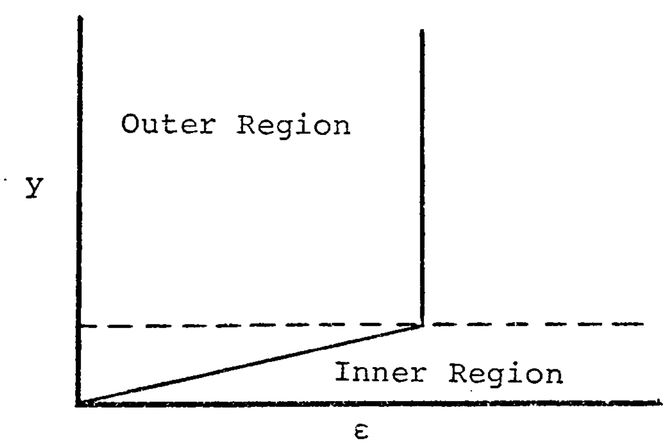

Figure 1-2

Eddy Viscosity Distribution

Chapter II

Development of the Boundary Layer Momentum Equation and Parameters

Mathematical Statement of the Problem

For an incompressible fluid, the equations for conservation of mass and momentum in a turbulent boundary layer are

continuity:

$$\frac{\partial u}{\partial x} + \frac{\partial v}{\partial y} = 0 \tag{2-1}$$

momentum:

$$u\frac{\partial u}{\partial x} + v\frac{\partial u}{\partial y} = \nu\frac{\partial}{\partial y}\left[(1 + \varepsilon/\nu)\frac{\partial u}{\partial y}\right] - \frac{1}{\rho}\frac{\partial P}{\partial x} \tag{2-2}$$

where the coordinate system is defined by Figure 2-1.

Once the eddy viscosity has been specified, a unique solution of these equations satisfying the following boundary conditions is desired:

$$\begin{aligned} y = 0: &\qquad u = v = 0 \\ y = \infty: &\qquad u = u_\infty \end{aligned} \tag{2-2a}$$

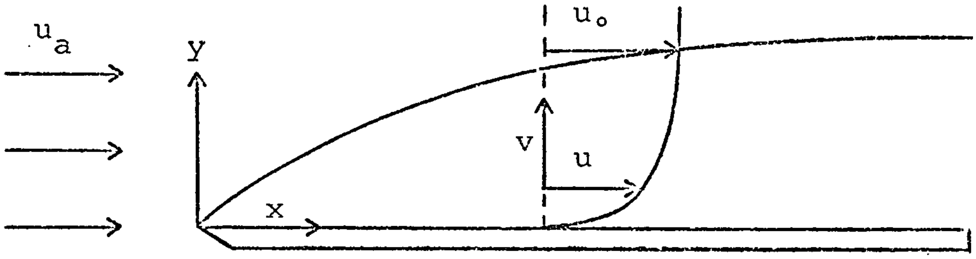

Figure 2-1

Coordinate System

Transformation of Momentum Equation

Before attempting to solve Equations 2-1 and 2-2, it is convenient to transform them into a more manageable form by defining new independent and dependent variables. These variables are generally called similarity variables. The principle guidelines for defining similarity variables are that the partial differential equations are transformed to ordinary differential equations and that the resulting equations and boundary conditions are as simple as possible.

After considering the above requirements the following similarity transformation due to Meksyn (10) is used. To satisfy the continuity equation (2-1), a stream function ψ is introduced such that

$$u = \frac{\partial \psi}{\partial y}, \qquad v = -\frac{\partial \psi}{\partial x}. \tag{2-3}$$

The variables (x,y) are first changed to (ξ, η_1), where

$$\xi = \int_0^x \frac{u_o}{u_a}\, dx \tag{2-4}$$

and

$$\eta_1 = \frac{u_o}{u_a}\, y \tag{2-5}$$

ξ and η_1 correspond to the velocity potential and the stream function of the inviscid flow at the edge of the boundary layer for unit free stream velocity.

Following a procedure similar to Blasius the variables are changed to

$$\eta = \left[\frac{1}{2\nu u_a \xi}\right]^{1/2} u_o\, y \tag{2-6}$$

$$\psi = (2\nu u_a \xi)^{1/2}\, f(\xi, \eta) \tag{2-7}$$

Thus the new coordinates are ξ and η as expressed by Equations 2-4 and 2-6.

All quantities in Equations 2-1 and 2-2 can be expressed in terms of these new variables as shown below:

$$u = \left(\frac{\partial \psi}{\partial y}\right)_x = u_o f' \tag{2-8}$$

$$-v = \left(\frac{\partial\psi}{\partial x}\right)_y = u_\circ\left[\frac{1}{2Re}\right]^{1/2}\left\{f + 2\xi\left(\frac{\partial f}{\partial \xi}\right)_\eta - (1+\lambda)\eta f'\right\} \tag{2-9}$$

$$\left(\frac{\partial u}{\partial x}\right)_y = -\frac{u_\circ^2}{2\xi u_a}\left\{\lambda f' - 2\xi\left(\frac{\partial f'}{\partial \xi}\right)_\eta + (1+\lambda)\eta f''\right\} \tag{2-10}$$

$$\left(\frac{\partial u}{\partial y}\right)_x = \frac{u_\circ^2}{u_a}\left[\frac{Re}{2}\right]^{1/2} f'' \tag{2-11}$$

where the prime denote differentiation with respect to η at constant x and λ and Re are defined by

$$\lambda = -2\frac{u_a}{u_\circ^2}\frac{du_\circ}{dx} = \frac{-2\xi}{u_\circ}\frac{du_\circ}{d\xi} \tag{2-12}$$

$$Re = \frac{u_a\xi}{\nu} \tag{2-13}$$

The density (ρ) and viscosity (μ) are assumed constant for any given boundary layer.

Upon substituting Equations 2-8 through 2-11 into Equation 2-2 and simplifying, the following is obtained

$$\frac{\partial}{\partial \eta}[(1 + \varepsilon/\nu)f''] = -ff'' + \lambda(1 - f')^2$$
$$+ 2\xi \left[\frac{\partial f'}{\partial \xi}\right]_\eta f' - 2\xi \left[\frac{\partial f}{\partial \xi}\right]_\eta f''$$

(2-14)

Taking the indicated derivative on the left side of the above equation and rearranging yields

$$f''' = \frac{-ff'' + \lambda(1-f'^2) - f'' \dfrac{\partial(\varepsilon/\nu)}{\partial \eta} + 2\xi \left[f' \dfrac{\partial f'}{\partial \xi} - f'' \dfrac{\partial f}{\partial \xi}\right]}{(1 + \varepsilon/\nu)}$$

(2-15)

For similarity to exist the streamwise terms must be negligibly small as suggested by Prandtl. However, for turbulent flow these terms are not negligible as will be shown in Chapter IV. Therefore, similarity does not apply for turbulent flow and the similarity variables should be regarded only as a convenient change of variables.

The streamwise derivatives may be stated in another form. Differentiating the Reynolds number as defined by Equation 2-13 with respect to ξ yields

$$\frac{dRe}{d\xi} = \frac{u_a}{\nu} \qquad (2\text{-}16)$$

Substituting Equation 2-16 into the streamwise term gives

$$2\left\{f'\left(\frac{\partial f'}{\partial \xi}\right)_\eta - f''\left(\frac{\partial f}{\partial \xi}\right)_\eta\right\} = 2Re\left\{f'\left(\frac{\partial f'}{\partial Re}\right)_\eta - f''\left(\frac{\partial f}{\partial Re}\right)_\eta\right\} \quad (2\text{-}17)$$

Thus, the streamwise derivatives may be expressed in terms of Reynolds' number.

Formulation and Transformation of Eddy Viscosity Equation

In order to solve Equation 2-15, an eddy viscosity distribution must be specified. A theoretical expression for the eddy viscosity is not available. Furthermore, experimental data for eddy viscosity are very rare due to the difficulties encountered in measuring the time average velocity gradients, especially in the outer region of the boundary layer where they are very small. The only data which could be located were found in Hinze (8). The eddy viscosity formulation that will be used in this study is basically the same as that used by Padilha (12). The boundary layer is considered as a composite layer consisting of inner and outer regions.

In the inner region, a modification of the Gill and Sher (6) equation for pipe flow is used. This correlation is an alteration of Prandtl's mixing length theory in that the mixing length is given by an expression to account for the viscous sublayer close to the wall, that is,

$$L = ky(1 - e^{-\phi y/y_m}) \quad (2\text{-}18)$$

where $\phi = \frac{y_m^+ - a}{b}$

y_m = maximum value of y

a = turbulent damping factor

b = constant

Thus,

$$(\varepsilon/\nu)_i = k^2 y^2 \frac{du}{dy} (1 - e^{-\phi y/y_m})^2 \quad . \tag{2-19}$$

The advantages in using correlations such as Equation 2-19 are that they predict a continuous velocity profile and have the ability to describe the transition region from laminar to turbulent flow.

In the outer region, the eddy viscosity is assumed constant. Studies made by Clauser (3) indicate that the eddy viscosity is constant for the outer 80 to 90% of the layer and is given by

$$(\varepsilon/\nu)_\circ = \frac{k_2 u_\circ \delta^*}{\nu} \tag{2-20}$$

where $k_2 = 0.018$.

Now the problem is reduced to determining the transition point between the inner and outer regions.

The point at which the inner region ends and the outer region begins will be known as the transition point. The criterion used to define the transition point is the continuity of the eddy viscosity, that is, the transition point is that point where $(\varepsilon/\nu)_i = (\varepsilon/\nu)_\circ$. Hence, the eddy viscosity for the inner region is given by Equation 2-19 and, once the transition point is known, the eddy viscosity for the outer region is given by

$$(\varepsilon/\nu)_o = (\varepsilon/\nu)_i \quad \text{at transition point.} \qquad (2\text{-}21)$$

The next step in the solution of Equation 2-15 is the transformation of the eddy viscosity equations into Meksyn coordinates. Using Equations 2-4 and 2-6 in 2-19 transforms the eddy viscosity equation to

$$(\varepsilon/\nu)_i = k^2(2\mathrm{Re})^{1/2}\eta^2 f''(1 - e^{-\phi\eta/\eta_\delta})^2 \qquad (2\text{-}22)$$

where

$$\phi = \frac{(2\mathrm{Re})^{1/4}(f_o'')^{1/2}\eta_\delta - a}{b} .$$

The constant a is interpreted as a turbulent damping factor which describes the points where transition from laminar to turbulent flow takes place. The constant b is evaluated by choosing the value which gives the best overall fit. A value of 25.0 was used.

The eddy viscosity equation for the outer region remains the same as given by Equation 2-21 since it is constant for this region.

Since the determination of the transition point requires Clauser's Equation 2-20, it must also be transformed. After using the transformed variables and rearranging, the following results:

$$(\varepsilon/\nu)_o = k_2(2Re)^{1/2}\int_o^\infty (1-f')\,d\eta \qquad (2\text{-}23)$$

Transformed Momentum Equation

The momentum Equation 2-15 may now be expressed entirely in terms of transformed variables once the derivative of the eddy viscosity with respect to η has been computed. Performing the differentiation yields

For the inner region:

$$\frac{\partial(\varepsilon/\nu)_i}{\partial\eta} = f''' \left[\beta\eta^2(1-e^{-\phi\eta/\eta_\delta})^2\right] + \beta\eta f''\left\{(1-e^{-\phi\eta/\eta_\delta}) + \frac{\phi\eta}{\eta_\delta}e^{-\phi\eta/\eta_\delta}\right\}(1-e^{-\phi\eta/\eta_\delta}) \qquad (2\text{-}24)$$

where $\beta = 2k^2(2Re)^{1/2}$

For the outer region:

$$\frac{\partial(\varepsilon/\nu)_o}{\partial\eta} = 0 \qquad (2\text{-}25)$$

The final equation results when Equations 2-17, 2-21, 2-22, 2-24, and 2-25 are substituted into 2-15. Since the derivative of the eddy viscosity in the outer region is zero, the momentum equation for this region is simplier than for the inner region. Therefore, the momentum equation is

For the inner region:

$$f''' = \frac{-ff'' + \lambda(1-f'^2) - \beta\eta(f'')^2\left[1+(\phi\eta/\eta_\delta - 1)e^{\frac{-\phi\eta}{\eta_\delta}}\right](1-e^{\frac{-\phi\eta}{\eta_\delta}})}{(1 + 2\varepsilon/\nu)}$$

$$+ \frac{2Re[f'\left[\frac{\partial f'}{\partial Re}\right]_\eta - f''\left[\frac{\partial f}{\partial Re}\right]_\eta]}{(1 + 2\varepsilon/\nu)} \qquad (2\text{-}26a)$$

For the outer region:

$$f''' = \frac{-ff'' + \lambda(1-f'^2) + 2Re[f'\left[\frac{\partial f'}{\partial Re}\right] - f''\left[\frac{\partial f}{\partial Re}\right]_\eta]}{(1 + \varepsilon/\nu)} \qquad (2\text{-}26b)$$

The boundary conditions given in Equation 2-3 are stated below in terms of η and f:

$$\text{at } \eta = 0 \begin{cases} f = 0 \\ f' = 0 \end{cases} \qquad \text{and as } \eta \to \infty \begin{cases} f' \to 1.0 \\ f'' \to 0 \end{cases} \qquad (2\text{-}27)$$

To avoid confusion, it is stressed again that the equation for the outer region is a simplification of the equation for the inner region since the derivative of the eddy viscosity in the outer region is zero.

Alternate Eddy Viscosity Formulation

Another eddy viscosity formulation which was considered gave results almost as good as the aforementioned formulation. This alternate distribution used Equation 2-22 for the eddy viscosity in the inner region while the eddy viscosity in the outer region was modified by an intermittency factor as suggested by Klebanoff (9), that is, for the inner region

$$(\varepsilon/\nu)_i = k^2(2Re)^{1/2}\eta^2 f''(1-e^{-\phi\eta/\eta_\delta})^2 \qquad (2\text{-}28)$$

and for the outer region

$$(\varepsilon/\nu)_o = \gamma(\varepsilon/\nu)_i \text{ at transition point} \qquad (2\text{-}29)$$

Furthermore, the transition point was assumed constant at 0.16 for this formulation and the streamwise terms were assumed to be negligible.

Although the intermittency factor (9) is given by

$$\gamma = 1/2[1 - \text{erf } 5(y/\delta - 0.78)], \qquad (2\text{-}30)$$

the derivative of the eddy viscosity for the outer region, which is given by

$$\frac{d}{d\eta}(\varepsilon/\nu)_o = -\left[\frac{5}{(\pi)^{1/2}\eta_\delta}e^{-[5(\eta/\eta_\delta-0.78)]^2}\right](\varepsilon/\nu)_{i,\eta/\eta_\delta=0.16} ,$$

(2-31)

was assumed to be zero for this particular distribution. When the derivative of $(\varepsilon/\nu)_o$ was included, the results were unsatisfactory for no apparent reason even after correcting for the streamwise terms.

Attempts to smooth the various eddy viscosity distributions at the transition point, as shown in Figure 2-2, produced no significant improvement in the results and, therefore, were dropped.

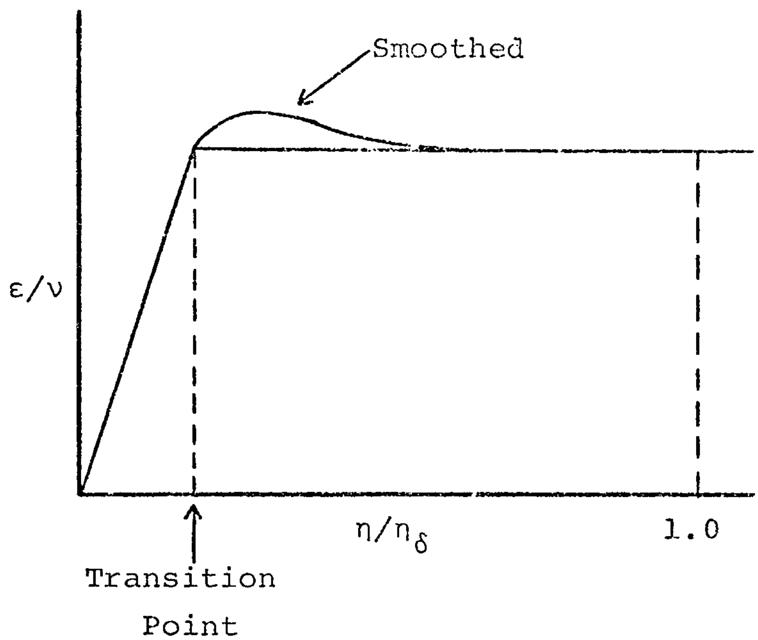

Figure 2-2

Smoothed Eddy Viscosity Distribution

Other Boundary Layer Parameters

Once the momentum equation has been solved for any given case, other boundary layer parameters, such as the skin-friction coefficient, displacement thickness, momentum thickness, and the velocity profile in term of dimensionless coordinates, can be calculated. These parameters expressed in terms of both regular and transformed variables are as follows:

Local skin-friction coefficient:

$$c_f = \frac{\tau_w}{1/2\rho u_o^2} \tag{2-32a}$$

or, in terms of transformed variables, ξ and η,

$$c_f = \left(\frac{2}{Re}\right)^{1/2} f''_o \tag{2-32b}$$

Displacement thickness:

$$\delta^* = \int_o^\infty \left(1 - \frac{u}{u_o}\right) dy \tag{2-33a}$$

or, in terms of ξ and η,

$$\delta^* = \left(\frac{2}{Re}\right)^{1/2} \frac{u_a \xi}{u_o} \int_o^\infty (1-f')\, d\eta \tag{2-33b}$$

Momentum thickness:

$$\theta = \int_0^\infty \frac{u}{u_o} \left(1-\frac{u}{u_o}\right) dy \tag{2-34a}$$

or, in terms of ξ and η,

$$\theta = \left(\frac{2}{Re}\right)^{1/2} \frac{u_a \xi}{u_o} \int_0^\infty f'(1-f')\, d\eta \tag{2-34b}$$

Dimensionless coordinates for velocity profiles are

$$u^+ = u/u_* \tag{2-35a}$$

$$y^+ = \frac{u_* y}{\nu} \tag{2-35b}$$

or, in terms of ξ and η,

$$u^+ = \frac{(2Re)^{1/4}}{(f_o'')^{1/2}} f' \tag{2-36a}$$

$$y^+ = (2Re)^{1/4} (f_o'')^{1/2} \eta \tag{2-36b}$$

Once the displacement and the momentum thicknesses are computed the shape factor H can be determined from

$$H = \delta^*/\theta \tag{2-37}$$

In addition, the average skin-friction coefficient can be calculated for a boundary layer on a flat plate with no pressure gradient using

$$c_{favg} = 2\theta/\xi \tag{2-38}$$

Chapter III

Method of Solution

The method used to solve the momentum equation consists of integrating Equation 2-26 while ignoring the streamwise terms, then based on these results, estimating the streamwise terms and re-solving the momentum equation using the correction for the ξ-derivatives. Other methods (16) have linearized the momentum equation before solving in order to overcome the long computation time when the boundary layer becomes very thick. However, this problem is easily resolved by using a larger integration step in the region away from the wall. No additional error is introduced since changes in velocity are small for thick boundary layers in the region away from the wall.

Estimation of the Streamwise Terms

The streamwise terms may be evaluated by two different methods - a finite difference solution of the boundary layer or by the estimation technique described below. The major disadvantage of the finite difference method is that the entire boundary layer must be solved using closely spaced points in the streamwise direction in order to obtain a solution at any given point.

The present technique for approximating the streamwise terms uses Equation 2-17 which expresses these terms in the most convenient form, that is,

$$\Delta_c = \frac{2\text{Re}\ [f'\left[\frac{\partial f'}{\partial \text{Re}}\right]_\eta - f''\left[\frac{\partial f}{\partial \text{Re}}\right]_\eta]}{(1 + \varepsilon/\nu)} \tag{3-1}$$

where Δ_c is merely a symbol to represent the terms. The derivatives in the above equation may be approximated by differences if solutions to the momentum equation are available for closely spaced Reynolds' numbers about a central Re. Using this approach, the momentum equation is first solved assuming Δ_c to be zero for three Reynolds' numbers ($\text{Re}_3 = \text{Re}_2 + \Delta\text{Re}$, Re_2, $\text{Re}_1 = \text{Re}_2 - \Delta\text{Re}$) and the derivatives are approximated by

$$\left(\frac{\partial f'}{\partial \text{Re}}\right) = \left[\frac{f_3' - f_1'}{\text{Re}_3 - \text{Re}_1}\right]_\eta \tag{3-2a}$$

and

$$\left(\frac{\partial f}{\partial \text{Re}}\right)_\eta = \left[\frac{f_3 - f_1}{\text{Re}_3 - \text{Re}_1}\right] \tag{3-2b}$$

Thus, Equation 3-1 becomes

$$\Delta_{c_2} = \frac{2\text{Re}_2 \left[f_2'\left[\frac{f_3' - f_1'}{\text{Re}_3 - \text{Re}_1}\right] - f_2''\left[\frac{f_3 - f_1}{\text{Re}_3 - \text{Re}_1}\right]\right]_\eta}{(1 + \varepsilon/\nu)} \tag{3-3}$$

where the subscript "2" signifies that the estimation applies to the central Re. It should be noted that all values in the above equation are at constant η.

The streamwise terms are negligible in the inner region of the boundary layer (η less than η at the transition point) for reasons which will be discussed in Chapter IV. However, for the outer region the ξ-derivatives are very significant. Although Equation 3-3 only gives a first order approximation of Δ_c, a more accurate estimate can be obtained if the following procedure is used:

1.) Ignore streamwise terms, solve momentum equation for series of three Reynolds' numbers with all other parameters constant.
2.) Calculate Δ_c using Equation 3-3.
3.) Solve momentum equation again for central Re using:
$$[f''' = f''' + \Delta_c]_\eta . \qquad (3\text{-}4)$$
4.) Obtain least squares fit of Δ_c as a function of η.
5.) Repeat steps 1 through 4 (except in step 1 where the correction term is used rather than assuming it zero) until f''_o is within 95% of the previous value.

The above method is also presented in Figure 3-1. This method is much better than it first appears, since only one correction for the streamwise terms is required for all cases where Re is greater than 10^5 and for most cases where Re is less than 10^5.

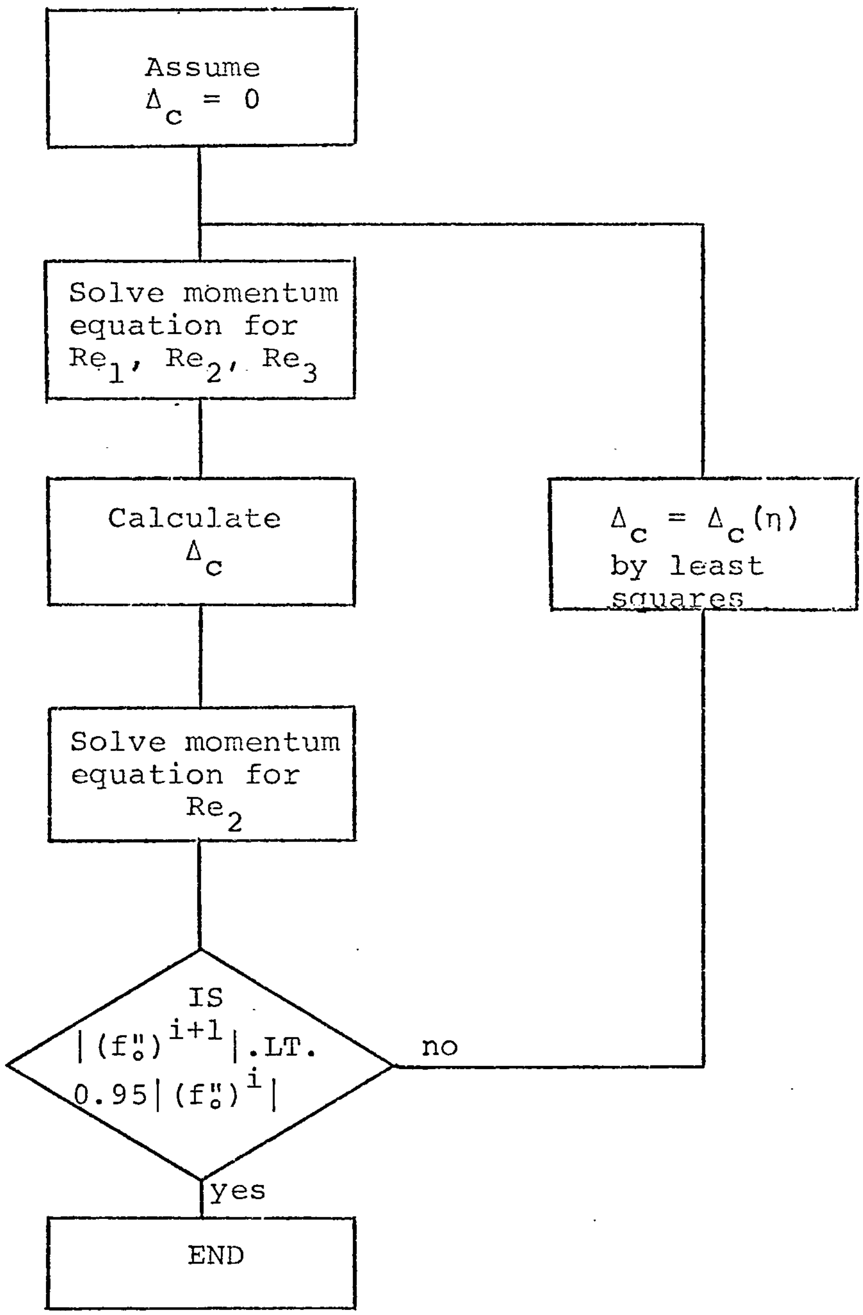

Figure 3-1

Correction for Streamwise Terms

<u>Convergence Technique for f''_o and η_δ</u>

In order to integrate the momentum equation (Equation 2-26), one must first assume values for f''_o and η_δ. Thus, some technique is needed to converge upon the proper values of these parameters, that is, assume f''_o and η_δ, integrate the momentum equation, update f''_o and η_δ and integrate again, until the f''_o and η_δ are found which satisfy the boundary conditions as given by Equation 2-27.

However, before discussing the convergence technique, the convergence criterion should be established, that is, what condition should be used to define the edge of the boundary layer. According to the boundary conditions (Equation 2-27) for the momentum equation, as η approaches infinity f' goes to zero. However, as in all numerical methods involving asymptotic boundary conditions, the boundary conditions are never reached exactly. Therefore, some specified limits are required.

Since f' is used as a boundary condition in the convergence technique for f''_o and η_δ , f'' is used to define the edge of the boundary layer.

As one would expect, large variations in the boundary layer thickness (η_δ) are found for various specified cut-off limits, due to the asymptotic nature of f'' in the vicinity of the edge of the boundary layer. The only parts of the momentum equation which are affected by these variations in η_δ are those terms involving the eddy viscosity. Hence, the cut-off conditions which gave the best overall results were chosen.

An influence function technique is used to update f''_o and η_δ in the convergence routine. According to Meissinger (11), if the problem solution $f(\eta,\alpha)$ and the parameter influence coefficient $\frac{\partial f(\eta,\alpha)}{\partial\alpha}$ are known for a particular point where $\alpha = \alpha_o$, then it is possible to make a first order prediction of the system behavior at a neighboring point having the new parameter value $\alpha_1 = \alpha_o + \Delta\alpha$.

Meissinger's influence function technique for the turbulent boundary layer momentum equation is presented in Appendix B. However, as an example to demonstrate the method, the influence function technique for the laminar boundary layer momentum equation is shown here. The transformed equation for laminar flow on a flat plate is (16)

$$ff'' + 2f''' = 0 \tag{3-5}$$

In this example the prime denotes differentiation with respect to η as before. The boundary conditions are the same as for the turbulent boundary layer (Equation 2-27) and will be repeated for clarity

$$\text{at } \eta = 0 \begin{cases} f = 0 \\ f' = 0 \end{cases} \qquad \text{as } \eta \to \infty \begin{cases} f' \to 1.0 \\ f'' \to 0 \end{cases} \tag{3-6}$$

Again, as in the case of the turbulent boundary layer, f''_o must be found. For convenience α will be used for f''_o in this development. Thus

$$\alpha = \left[\frac{d^2f}{d\eta^2}\right]_{\eta=0} = f''_o \tag{3-7}$$

Equation 3-5 is differentiated with respect to the influence parameter α to obtain

$$f\frac{d}{d\alpha}\left[\frac{d^2 f}{\partial\eta^2}\right] + \frac{d^2 f}{d\eta^2}\frac{d}{d\alpha}(f) + 2\frac{d}{d\alpha}\left[\frac{d^3 f}{d\eta^3}\right] = 0 . \tag{3-8}$$

The order of differentiation is not material, therefore, Equation 3-8 can be written as

$$f\frac{d^2}{d\eta^2}\left[\frac{df}{d\alpha}\right] + \frac{d^2 f}{d\eta^2}\frac{df}{d\alpha} + 2\frac{d^3}{d\eta^3}\left[\frac{df}{d\alpha}\right] = 0 . \tag{3-9}$$

Using

$$U = \frac{df}{d\alpha} \tag{3-10}$$

in the above equation yields

$$fU'' + f'''U + 2U''' = 0 \tag{3-11}$$

where the prime denotes differentiation with respect to η as usual. The boundary conditions for Equation 3-11 are derived as follows:

$$(U)_{\eta=0} = \left[\frac{df}{d\alpha}\right]_{\eta=0} = \frac{d}{d\alpha}(f)_{\eta=0} = 0 \tag{3-12a}$$

$$\left[\frac{dU}{d\eta}\right]_{\eta=0} = \frac{d}{d\eta}\left[\frac{df}{d\alpha}\right]_{\eta=0} = \frac{d}{d\alpha}\left[\frac{df}{d\eta}\right]_{\eta=0} = 0$$

$$= \frac{d\left[\frac{df}{d\eta}\right]_{\eta=0}}{d\left[\frac{d^2f}{d\eta^2}\right]_{\eta=0}} = \frac{d(0)}{d\left[\frac{d^2f}{d\eta^2}\right]_{\eta=0}} = 0 \qquad \text{(3-12b)}$$

$$\left[\frac{d^2U}{d\eta^2}\right] = \frac{d^2}{d\eta^2}\left[\frac{df}{d\alpha}\right]_{\eta=0} = \frac{d\alpha}{d\alpha} = 1 \; . \qquad \text{(3-12c)}$$

These boundary conditions also apply to the turbulent boundary layer. Equation 3-12 specifies all boundary conditions necessary for the direct solution of Equation 3-11 once f and f" are known. After assuming f''_o and η_δ, Equations 3-5 and 3-11 may be solved simultaneously.

The influence function which produces successive estimates of α (or f''_o) is developed as follows: It is obvious that

$$(f')_{\eta=\infty} = g\left[(f'')_{\eta=0}\right] = g(\alpha) \qquad \text{(3-13)}$$

where g denotes a function. Expanding Equation 3-13 in a Taylor series and terminating after the second term gives:

$$(f'_\infty)^{i+1} = (f'_\infty)^i + \frac{d}{d\alpha}(f'_\infty)^i \Delta\alpha \ . \tag{3-14}$$

After using Equation 3-10 and recognizing that

$$(f'_\infty)^{i+1} = 1.0 \tag{3-15}$$

when the proper f''_o (or α) is found, one obtains

$$(f'_\infty)^i + (U'_\infty)^i \Delta\alpha = 1.0 \ . \tag{3-16}$$

Upon rearranging, the influence function in its final form is acquired

$$(f''_o)^{i+1} = \frac{1.0 - (f'_\infty)^i}{(U'_\infty)^i} + (f''_o)^i \ . \tag{3-17}$$

Thus, the new value for f''_o is given by the old value plus a correction term.

The convergence routine may now be expressed as follows:

1.) Assume values for f''_o and η_δ (the value of η at the point where f" becomes less than 0.001 is used for η_δ.).
2.) Converge on a f''_o for the assumed η_δ.
3.) Repeat step 2 until $(\eta_\delta)^{i+1} = (\eta_\delta)^i$ and $(f''_o)^{i+1} = (f''_o)^i$ within specified limits.

The convergence method is more easily comprehended in the form of a simple flow diagram as shown in Figure 3-2.

Establish Inner and Outer Regions of Boundary Layer

Once a convergence technique for η_δ and f''_o has been found, the transition point defining the end of the inner region and the beginning of the outer region may be determined. The transition point is generally expressed as a fraction of the boundary layer thickness.

As discussed in Chapter II, the inner and outer regions are established by assuming a transition point and using the value of $(\varepsilon)_i$ at the assumed transition point for $(\varepsilon)_o$. Then the momentum thickness is calculated by using Clauser's equation for the eddy viscosity in the outer region (Equation 2-20). This momentum thickness will be denoted by δ^*_c. If δ^*_c is larger than δ^* (as calculated by integration of Equation 2-32), the assumed transition point is too large. When the two values of the momentum thickness are equal the transition point has been located. This procedure is demonstrated in diagram form in Figure 3-3.

When the aforementioned method was used, it was noted that for any particular value of the dimensionless velocity gradient term, λ, the transition point is essentially constant. These results suggest a universal curve of transition point as a function of λ as shown in Figure 3-4. Furthermore, the curve of transition point as a function of λ was found to be independent of Reynolds' number within the limits shown in Figure 3-4. Therefore, once the curve has been established for the range of pressure gradients of interest, the transition point determination may be dropped.

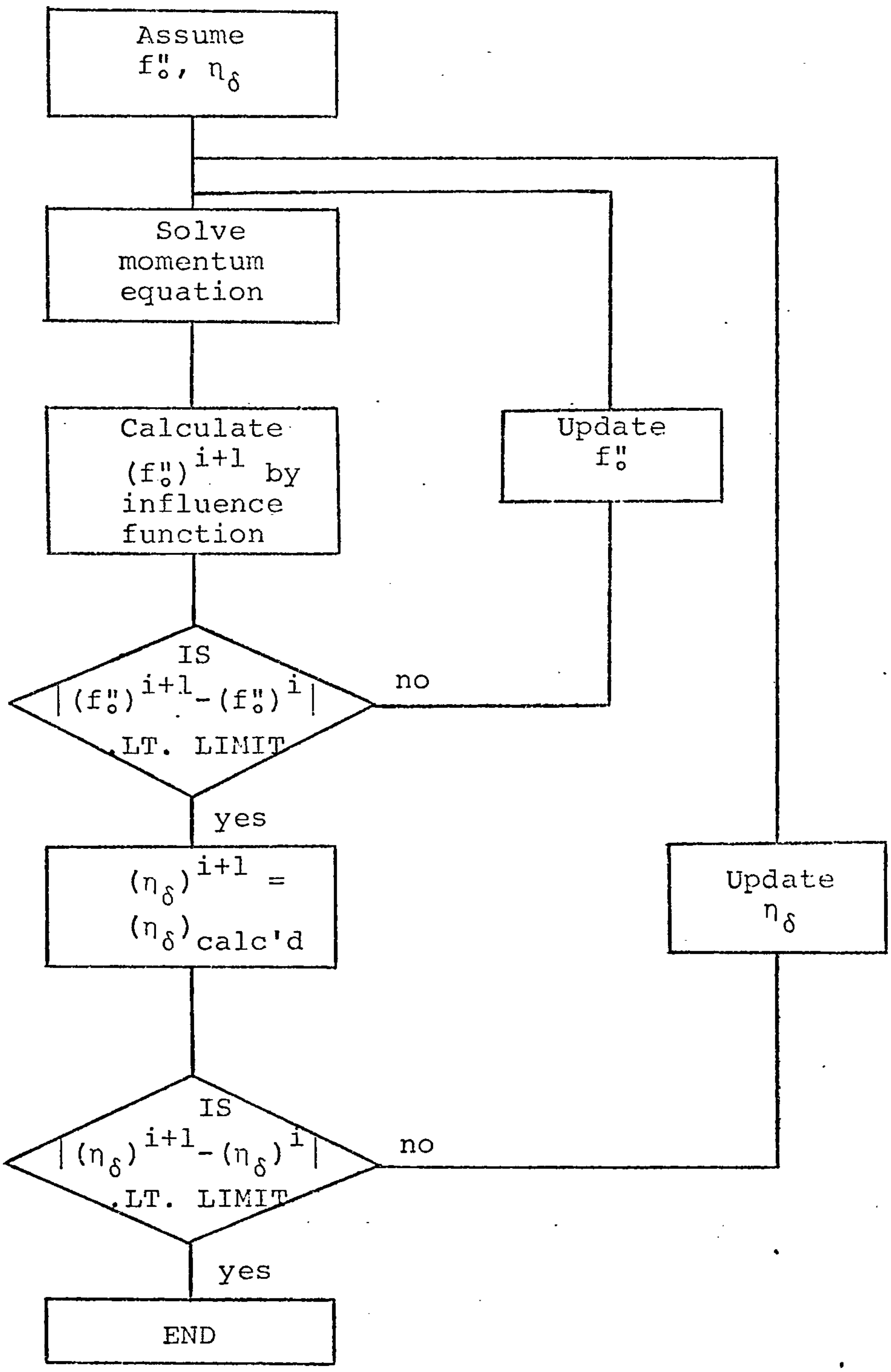

Figure 3-2

Convergence Technique for f_o'' and η_δ

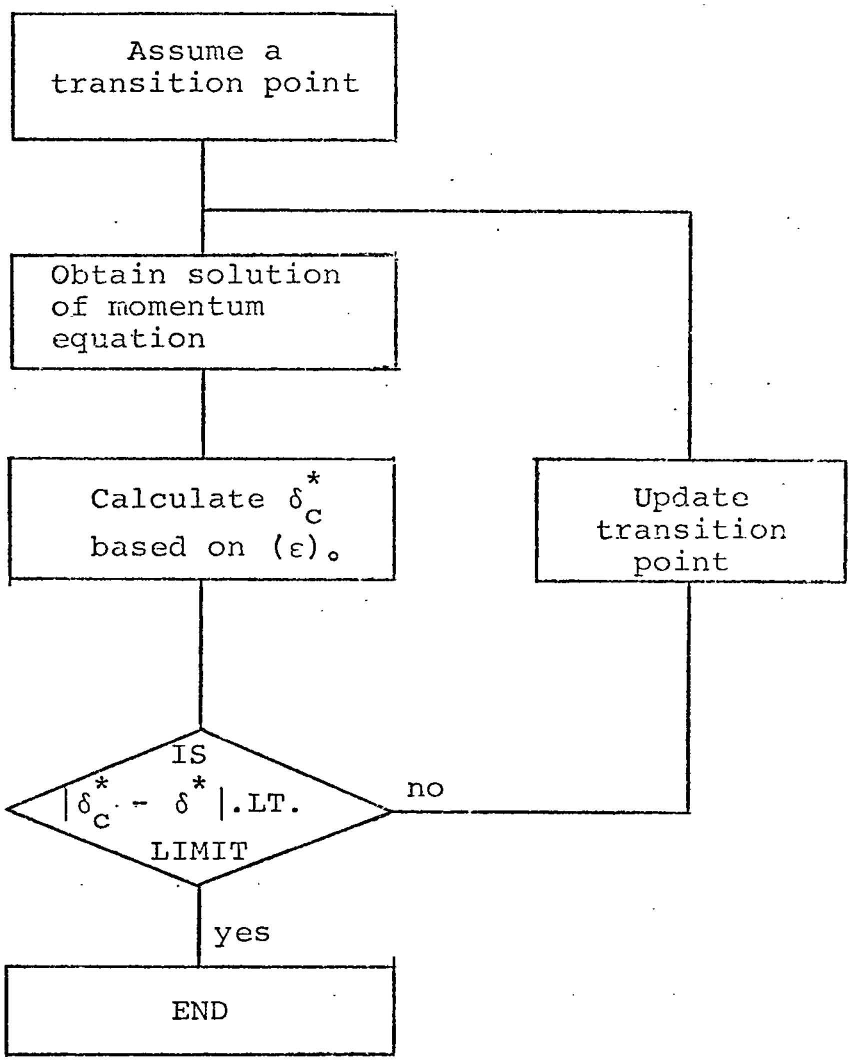

Figure 3-3

Determination of Transition Point

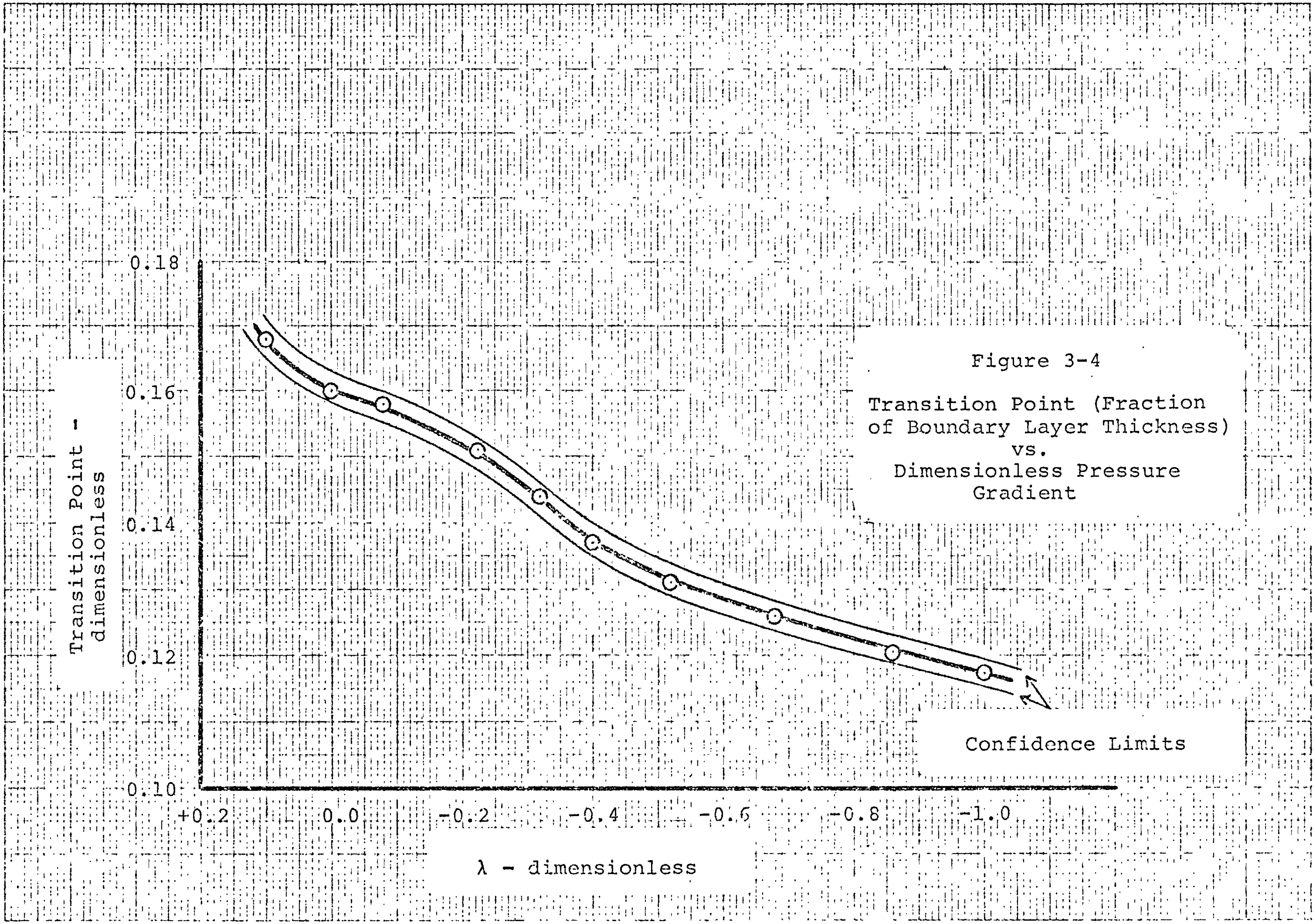

Figure 3-4

Transition Point (Fraction of Boundary Layer Thickness) vs. Dimensionless Pressure Gradient

Numerical Techniques

The momentum equation is integrated by using the Runge-Kutta integration routine in IBM's Continuous Systems Modeling Program (CSMP) (20,21). The main program is shown in Appendix A along with definitions of symbols used. An IBM 360/Model 44 Computer was utilized.

CSMP has many features which are particularly useful in solving two point boundary value problems. These include an applications-oriented language, simplified user-oriented input and output, and more specifically, an integration step size which may be easily changed as needed for the various regions of the solution.

Summary

A brief summary of the method of solution is:

1.) Solve momentum equation by Runge-Kutta integration in CSMP.

2.) Converge on f''_o and η_δ using Meissinger's influence function technique.

3.) Correct for streamwise terms.

4.) Establish inner and outer regions for each value of λ as needed.

One of the major advantages of this method is that a solution may be obtained at any point along the boundary layer without solving the entire boundary layer.

Chapter IV

Discussion of Results and Comparison to Experiment

As stated in Chapter III, the streamwise terms in the momentum equation were found to be not negligible in the outer region. This fact is demonstrated in Figure 4-1 and Table 4-1. In Figure 4-1, the velocity profile (Re = 1.0×10^7, $\lambda = 0.0$) has been plotted in terms of the dimensionless coordinates u/u_o and η for calculations where the zeroth (no correction) and first approximation of the streamwise terms were used. The affect of streamwise terms on the skin friction coefficient, the momentum and displacement thicknesses, and the calculated boundary layer thickness is shown in Table 4-1. In order to show that successive approximations of the streamwise terms will approach a constant value for each η, values of Δ_c, an approximation for the streamwise terms, for the first five estimations have been plotted for the above mentioned conditions in Figure 4-2. Since the integration process tends to reduce errors significantly and since Δ_c is a correction in f''', good results can be expected with only a rough approximation of Δ_c. For all cases encountered in this study with Reynold's numbers above 2×10^5 only one correction was needed for the streamwise terms.

Although the streamwise terms were of considerable importance in the outer region of the boundary layer, they were negligible in the inner region. It can be seen from Equation 3-1 that the streamwise terms must be zero at the

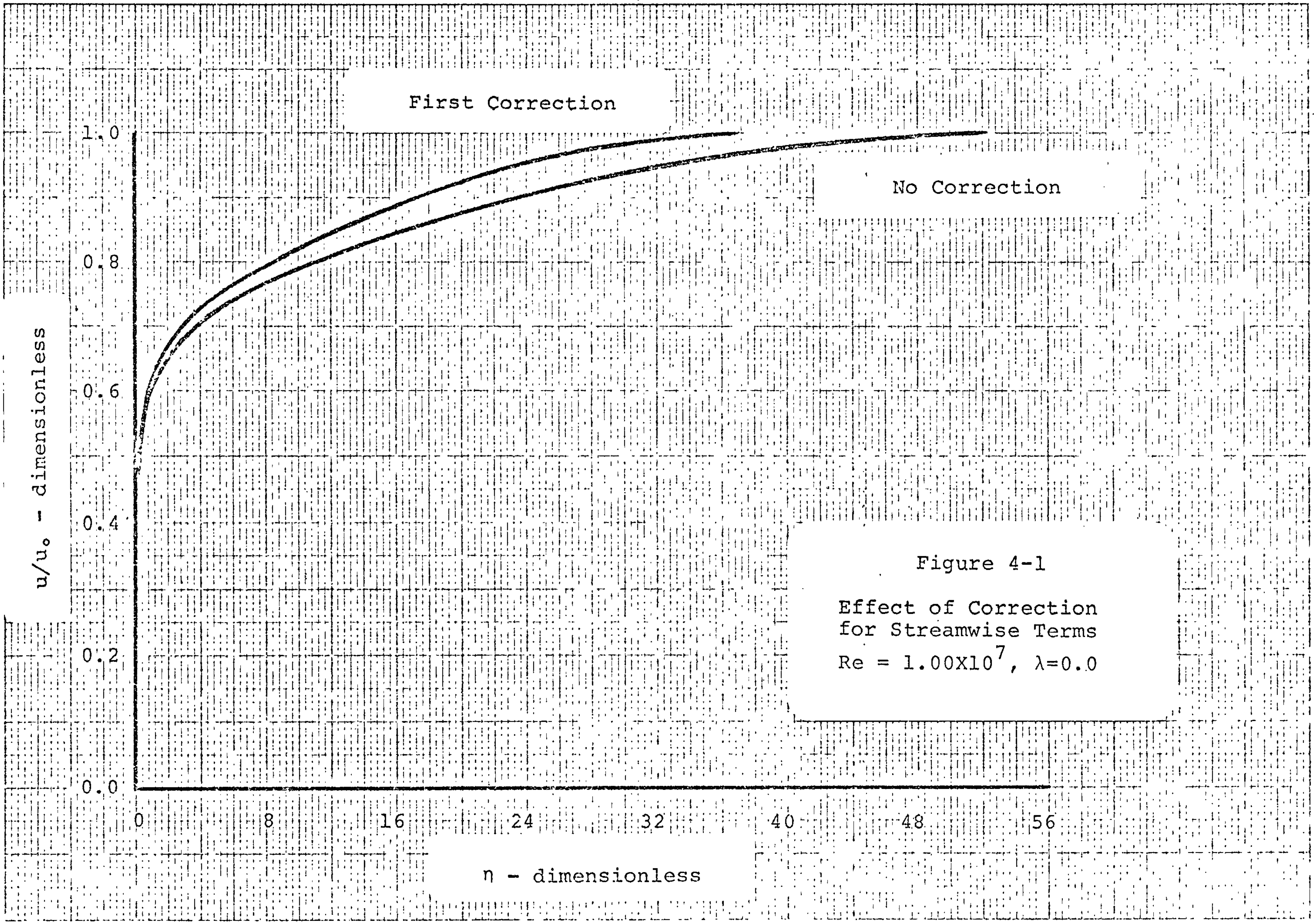

Figure 4-1

Effect of Correction for Streamwise Terms

Re = 1.00×10^7, $\lambda = 0.0$

Table 4-1

Affect of Successive Approximations of Streamwise Terms on Boundary Layer Parameters

Approximation	$c_f X10^{2}$ [1]	δ^*,in.	θ,in.	H	η_δ	u_o^+
0 [2]	0.231	0.075	0.058	1.29	52.0	29.4
1	0.242	0.055	0.042	1.30	37.0	28.8
2	0.245	0.058	0.045	1.28	43.8	28.6
3	0.240	0.058	0.044	1.30	39.8	28.9
4	0.244	0.057	0.044	1.29	42.0	28.6
5	0.242	0.057	0.044	1.29	40.0	28.7

(1) All parameters are dimensionless unless otherwise noted.

(2) No correction for streamwise terms.

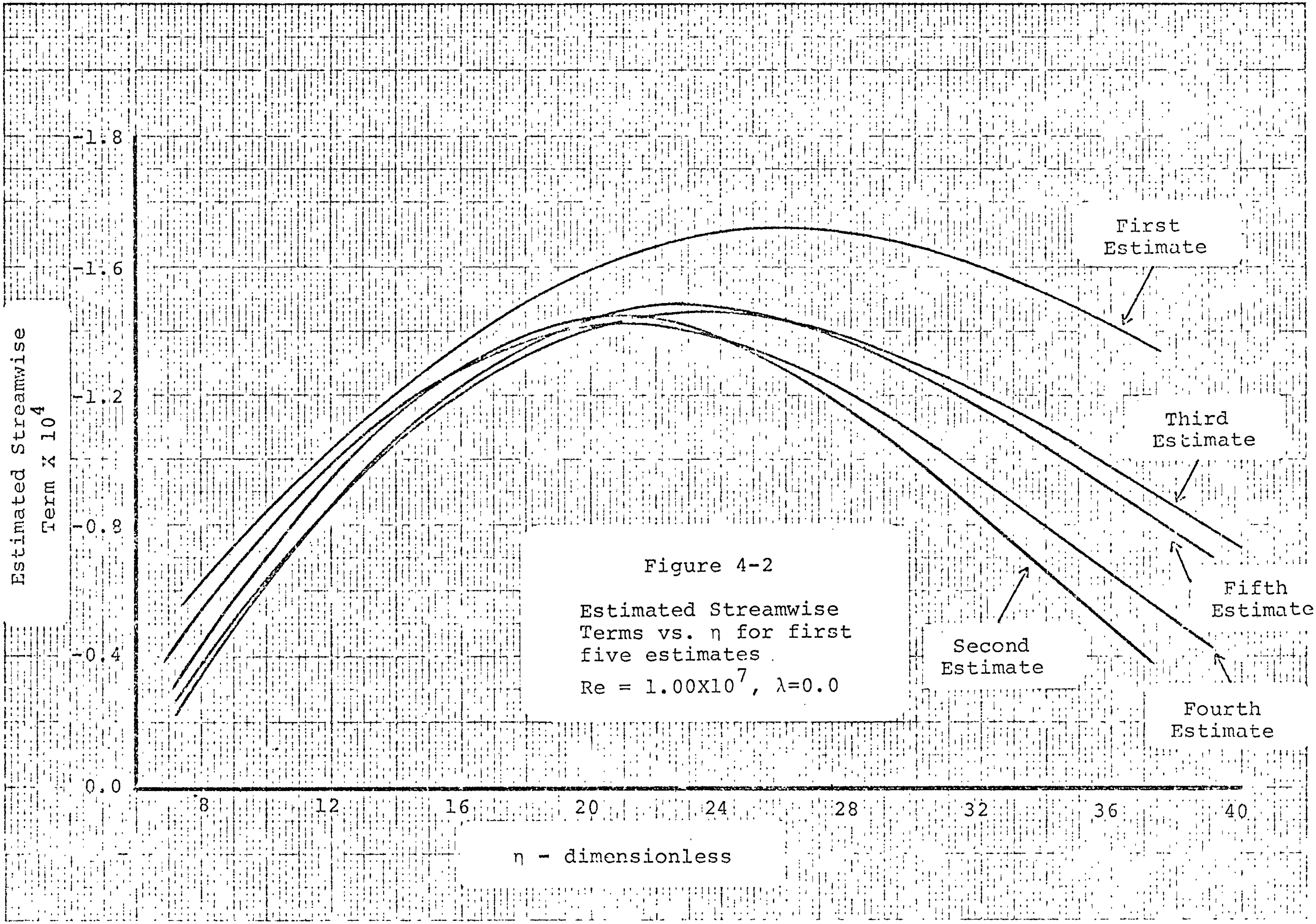

Figure 4-2

Estimated Streamwise Terms vs. η for first five estimates

Re = 1.00×10^7, λ=0.0

wall ($\eta = 0$) since f and f' are zero at this point. Even though the streamwise terms are smaller in absolute value in the inner region, the primary reason that they are negligible in this region is that the absolute value of f''' is much larger in the inner region than in the outer region. Therefore, in the inner region the value of the streamwise terms are very small relative to f''' and have no appreciable effect on the results.

Although good agreement with the data was obtained for favorable and zero pressure gradients as will be discussed later, completely unacceptable results were obtained for adverse pressure gradients (positive λ's). As stated in Schlichting (16), the parameters f', f", and f''' should have general distributions of the type shown in Figures 4-3 and 4-4 for favorable and adverse pressure gradients, respectively. The parameter f" which is directly related to the shear stress is seen to decrease monotonically over the entire boundary layer for zero and favorable pressure gradients. On the other hand, for adverse pressure gradients, f" is seen to increase from some initial value at the wall to a maximum at some point in the boundary layer then decrease to zero at the free stream. The above behavior of f" has been verified by experiment and is well established. In the present study the shear stress for all adverse pressure gradient cases (except those with small λ's, say less than +0.1) was found to decrease monotonically from the wall in the inner region, then, when the transition point separating the inner and outer regions was reached, the shear stress was observed to increase for a period as shown in Figure 4-4b. Accordingly, f''' which is directly proportional to the derivative of the shear stress was found to vary as

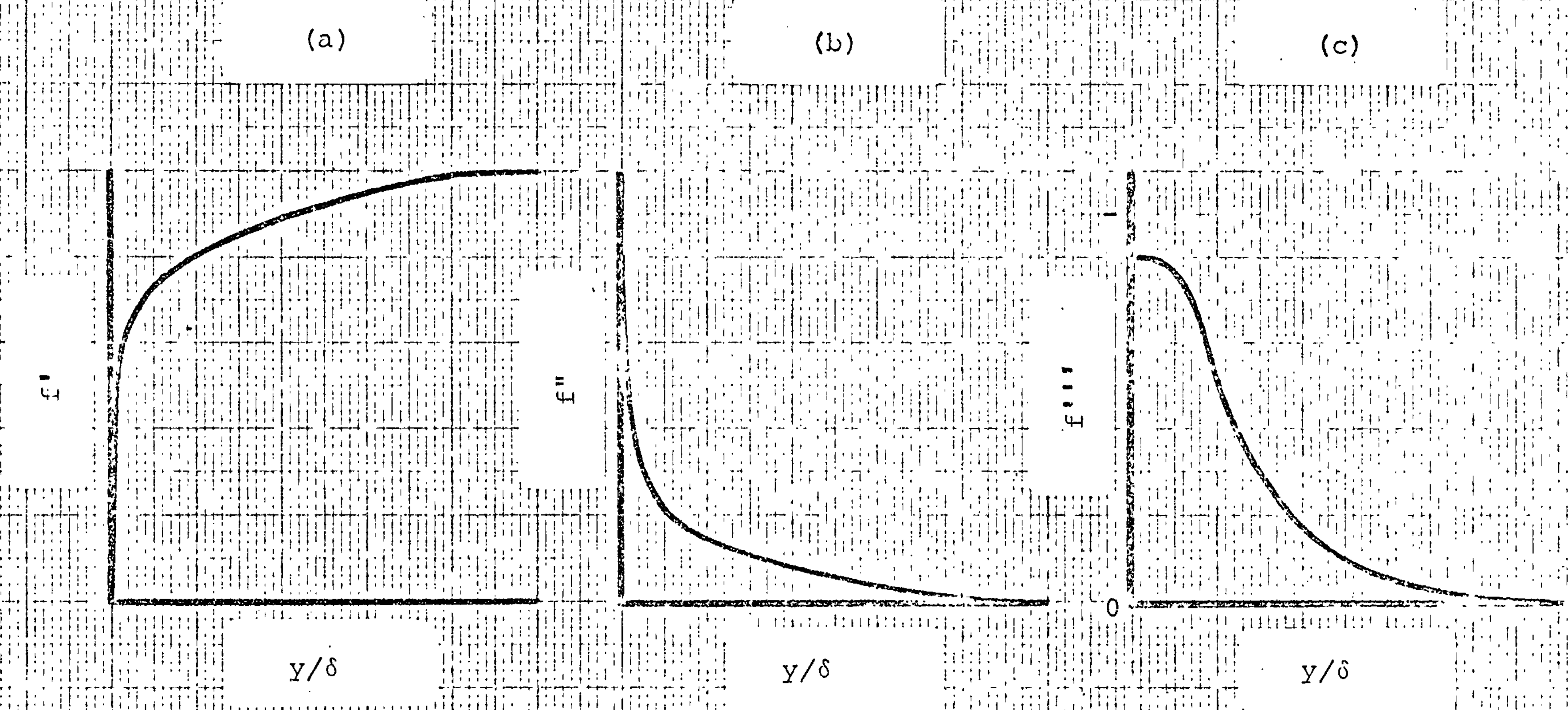

Figure 4-3

Distributions in a Boundary Layer with Favorable Pressure Gradient from Schlichting (16)

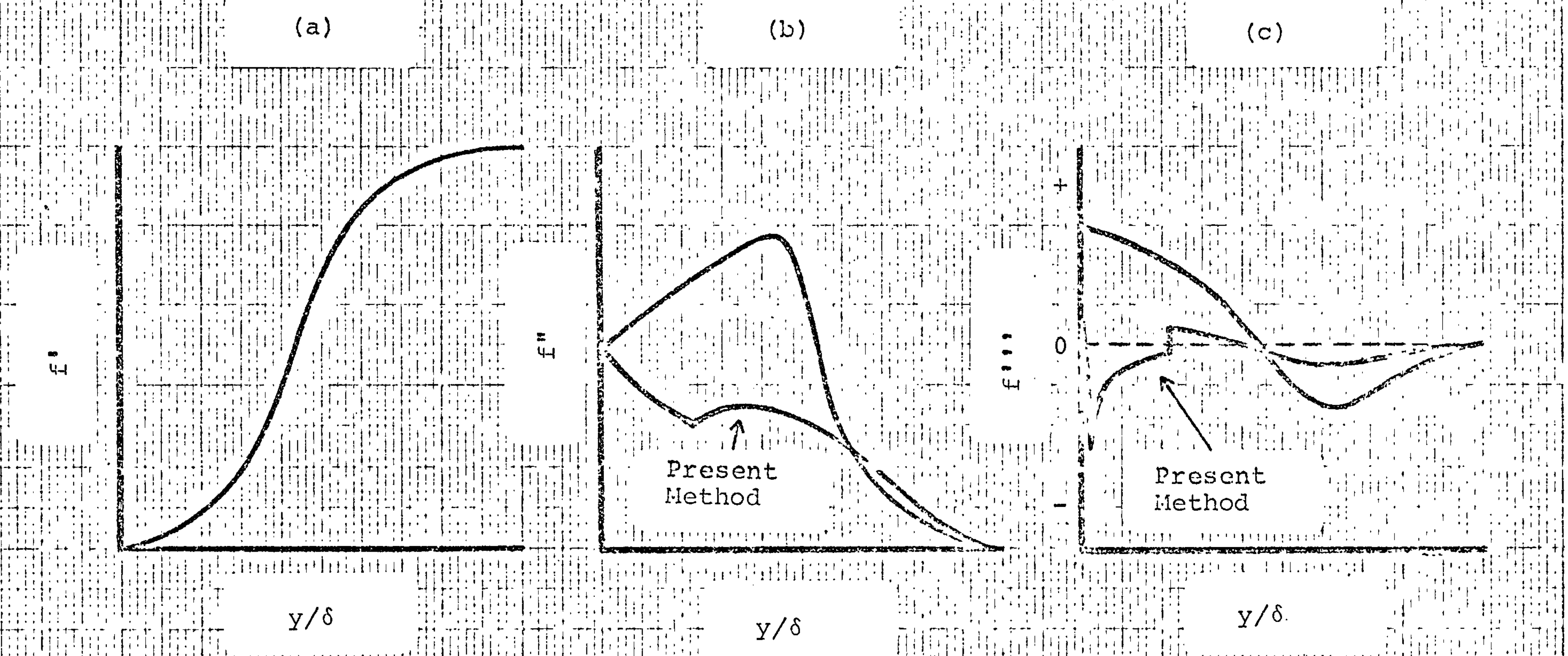

Figure 4-4

Distributions in a Boundary Layer with Adverse Pressure Gradient from Schlichting (16) unless otherwise noted shown in Figure 4-4c.

After careful study of Figure 4-4 and Equations 2-15 and 2-26, it was concluded that the eddy viscosity distribution was not representative of the flow for adverse pressure gradients. In particular, highly artificial conditions were observed at the transition point. These conditions suggested that the transition of the eddy viscosity from the inner region to the outer region was not representative at all. Furthermore, "smoothing" the eddy viscosity distribution in the neighborhood of the transition point produced no encouraging results.

In addition, for zero and favorable pressure gradients the eddy viscosity was not representative of the flow for certain combinations of Reynolds' number and turbulence damping factor "a". For values of "a" above approximately 75 the numerical value of ϕ in the eddy viscosity equation (Equation 2-22) becomes negative for Reynolds' numbers below a particular value (depending upon the values of "a" and λ). From Equation 2-22 it can be seen that, when ϕ is negative, the exponential term in the eddy viscosity increases with η instead of decreasing with η which could not possibly be the case.

Results

Calculated velocity profiles in terms of u^+ and y^+ are shown in Figures 4-5, 4-6, and 4-7 for Reynolds' numbers of 1.0×10^5 and 1.0×10^7 and λ's of 0, -0.5, and -1.0, respectively. Local skin friction coefficients were calculated over a range of Reynolds' numbers for the following cases:

1.) No pressure gradient ($\lambda = 0$)

  a.) a = 1

  b.) a = 50

2.) Favorable pressure gradient ($\lambda = -0.5$)

a.) a = 1

b.) a = 50

3.) Favorable pressure gradient ($\lambda = -1.0$)

a.) a = 1

b.) a = 50

The results are presented in Figures 4-8, 4-9, and 4-10, respectively. The constant "a" is a turbulence damping factor. A value of 1.0 represents fully developed turbulence. The average skin friction coefficient could be calculated for zero pressure gradients only and is shown in Figure 4-11.

Comparison of Calculated and Experimental Results

Since no exact solutions of the turbulent boundary layer equations are possible at the present, the primary basis for an evaluation of any prediction method is the comparison with experimental data. In order to evaluate the present method, the results were compared to three flows under various conditions.

The local and average skin friction coefficients for zero pressure gradients are compared to experimental data in Figures 4-12 and 4-13, respectively. The Smith and Walker (19) data was taken for an incompressible turbulent boundary layer along a smooth, flat plate having zero pressure gradient. The local surface-shear stress was measured by a floating - element - type device similar to that used by Dhawon (5). The average skin friction coefficient was computed using the momentum thickness obtained from integration of the velocity profiles. The local skin friction coefficient as calculated by the present method agrees very closely with the data especially after considering that the data had a scatter of about ±1%. The results for c_{favg} were about 5% above the data. However, Smith and Walker state that the experimental c_{favg} are slightly lower than expected.

The c_{favg} data from Schlichting (16, Figure 21-2, page 538) were taken by several investigators. The data points in Figure 4-13 represent the scatter of all the various data from Schlichting. In general, the calculated values are within the scatter of the experimental data.

No experimental data could be located for favorable pressure gradient cases.

Flat Plate Flow with Zero Pressure Gradient:

The zero pressure gradient flow of Smith and Walker (19) which was used for comparison with skin friction coefficients is also used here. The experimental investigators concluded that the virtual origin of the turbulence was at x = 0 for all practical purposes. Figures 4-14, 4-15, 4-16, and 4-17 show the calculated and experimental velocity profiles in terms of the dimensionless coordinates u^+ vs. y^+ and u/u_o vs. η for Reynolds' numbers of 3.33×10^6 and 1.0×10^7, respectively. Since there was no pressure gradient, λ was, of course, zero. A maximum deviation from the experimental data of 2.0% for Re = 3.33×10^6 and of 1.5% for Re = 1.0×10^7 was observed. However for the latter case the first data point appears to be unrepresentative as can be seen in Figure 4-16 and should be disregarded. The local skin friction coefficient, displacement thickness, momentum thickness, and shape parameter (H) are compared to the data in Table 4-2. Excellent agreement (within 3.0%) was found for c_f in both cases. The displacement thickness and the momentum thickness were found to be almost 8% above the experimental values.

Equilibrium Flow with Favorable Pressure Gradient:

Equilibrium boundary layers are characterized by

$$E = \frac{\delta^*}{\tau_w} \frac{dP}{dx} \tag{4-1}$$

as first suggested by Clauser (3). The nondimensional velocity defect distribution is invarient along the direction of flow for equilibrium boundary layers. Herring and Norbury experimentally studied two equilibrium flows with values for E of -0.35 and -0.53. The former flow was used for comparison. In order to determine the virtual origin of the flow, Smith and Cebeci (18) used the velocity distribution (obtained by trial and error) shown in Figure 4-18 to match the momentum thickness at x = 2 feet, the first streamwise point where data was taken. Due to the virtual origin, the experimental lengths along the wall are translated 4.37 feet.

Calculated and experimental velocity profiles at x = 3 feet and 5 feet in terms of u^+ vs. y^+ and u/u_o vs. η are shown in Figures 4-19, 4-20, 4-21, and 4-22, respectively, while the other boundary layer parameters (c_f, δ^*, θ and H) are compared in Table 4-3. The dimensionless pressure gradient term, λ, was -0.866 for both cases. Although the agreement in u^+ for the x = 3 feet cases was excellent (within 0.5%) for y^+ above 90, the experimental values of u^+ rose above the logarithmic line for y^+ below 90 and the calculated values were within only 10% of the experimental data. On the other hand, for x = 5 feet cases, the velocity profiles agreed to within 2% except for the first data point from the wall. In many cases, the first data point may be unrepresentative due to the size of the probe and the nearness of the wall. The skin friction coefficient agreed to within 4% for both cases while the displacement and momentum thicknesses were below the experimental values by 6% for x = 3 feet and 7% for x = 5 feet. Thus, the overall agreement between the calculations and experiment was good.

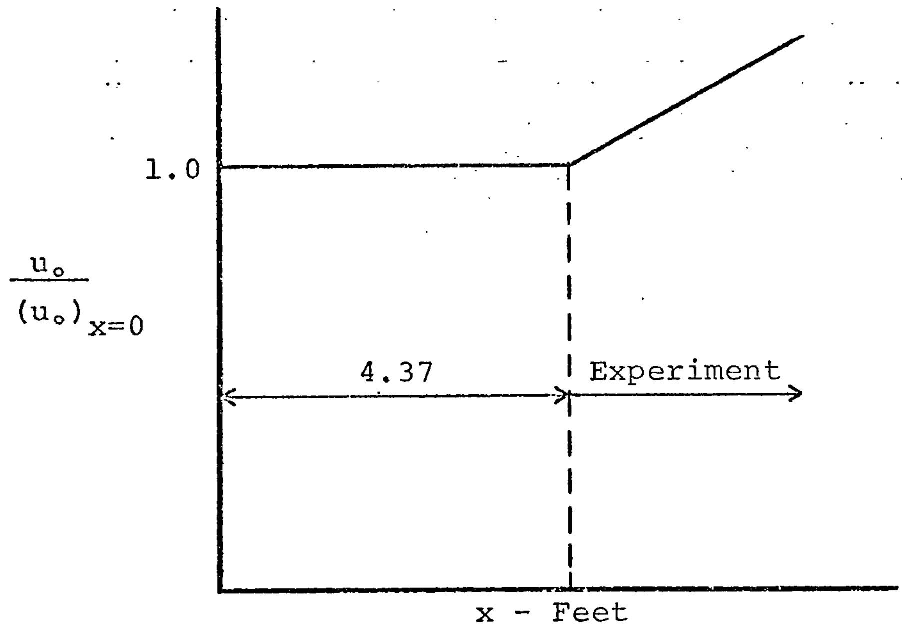

Figure 4-18

Velocity Profile Used to Match the Momentum Thickness at x = 2 feet (Herring and Norbury)

Flow with Favorable Pressure Gradient on an Aerofoil-like Body:

Schubauer and Klebanoff (17) experimentally investigated a turbulent boundary layer along an aerofoil-like body as shown in Figure 4-23. The flow was characterized by a varying favorable pressure gradient for the first 17.5 feet. Velocity profiles in terms of u^+ vs. y^+ and u/u_o vs. η are shown for x = 5.5, 6.5, 10.5, 17.5 feet in Figures 4-24 through 4-31, respectively. The corresponding dimensionless pressure gradient term, λ, which was used, is -0.400, -0.225, -0.077, and zero, respectively. Disregarding the first experimental point, the velocity profiles agreed to within 4%. The other boundary layer parameters are presented in Table 4-4 along with experimental values. Although the skin friction coefficients agreed to within 3%, the displacement and momentum thicknesses agreed within a 5 to 15% range. However, one must recognize that this is not equilibrium flow.

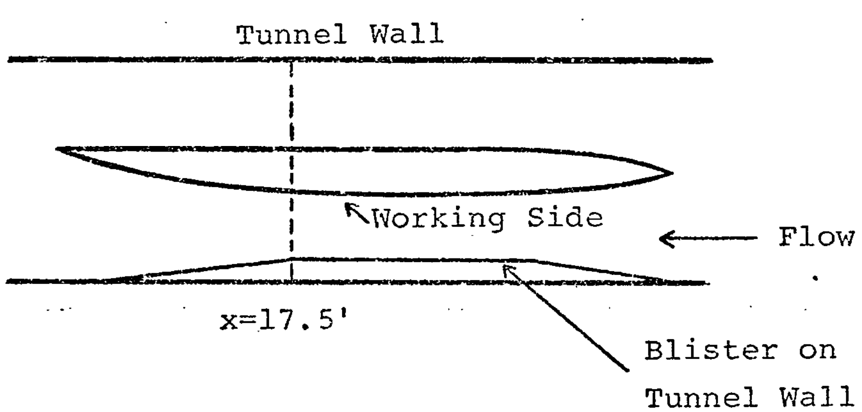

Figure 4-23

Boundary Layer Wall Used by Schubauer & Klebanoff

Results Using Alternate Eddy Viscosity Distribution

As discussed in Chapter II, an alternate eddy viscosity formulation was considered. This distribution used the same eddy viscosity equation as the previous method for the inner region. However, the eddy viscosity in the outer region was modified by Klebanoff's intermittency factor, and, in addition, the transition point defining the inner and outer regions was assumed constant at 0.16.

For this distribution, the eddy viscosity in the outer region varies directly with the intermittency factor (γ), that is,

$$(\varepsilon/\nu)_{\circ\gamma} = \gamma(\varepsilon/\nu)_{0.16} \qquad (4\text{-}2)$$

However, the derivative of $(\varepsilon/\nu)_{\circ\gamma}$ was assumed zero.

This method is also different from the previous method in that the streamwise terms were assumed zero. When a correction for the streamwise terms was used the results agreed very poorly with the data. In the case where the derivative of the eddy viscosity in the outer region was used, corrections for the streamwise terms did improve the results slightly.

In order to avoid confusion, the results from this method are presented in Appendix C. Velocity profiles are compared with the Re = 1.0 X 10^7 case of Smith and Walker and with the Re = 5.23 X 10^6 case of Schubauer and Klebanoff in Figures C-1 and C-2, respectively. The other boundary layer parameters for these two cases are compared in Table C-1. In general, the results from this method are slightly inferior to the previous method.

Chapter V

Summary of Results and Recommendations

The turbulent boundary layer momentum equation was solved by using a similarity transformation to convert the partial differential equation into a more manipulative equation which contained a term involving streamwise derivatives. The Runge-Kutta integration routine in IBM's Continuous Systems Modeling Program was used to integrate the momentum equation. Since the streamwise terms were found not to be negligible, a successful method was devised to estimate these terms.

A modification of the Gill and Sher eddy viscosity distribution was shown to apply for zero and favorable pressure gradient cases. However, for adverse pressure gradients, the eddy viscosity distribution was not representative of the flow.

Good agreement was observed for the local and average skin friction coefficients and the velocity profiles when compared to experimental data. Except for one boundary layer involving nonequilibrium flow, good results were obtained for the displacement and momentum thickness.

Furthermore, for any given boundary layer, the only input information required in the present method was the approach velocity and the streamwise pressure gradient.

Obviously, the normal extension of this study would be to obtain solutions for the adverse pressure gradient cases or, more precisely, en eddy viscosity distribution which would apply to these cases. The new eddy viscosity distribution should be formulated such that it would be representative of the unusual conditions just prior to separation of the boundary layer from the wall.

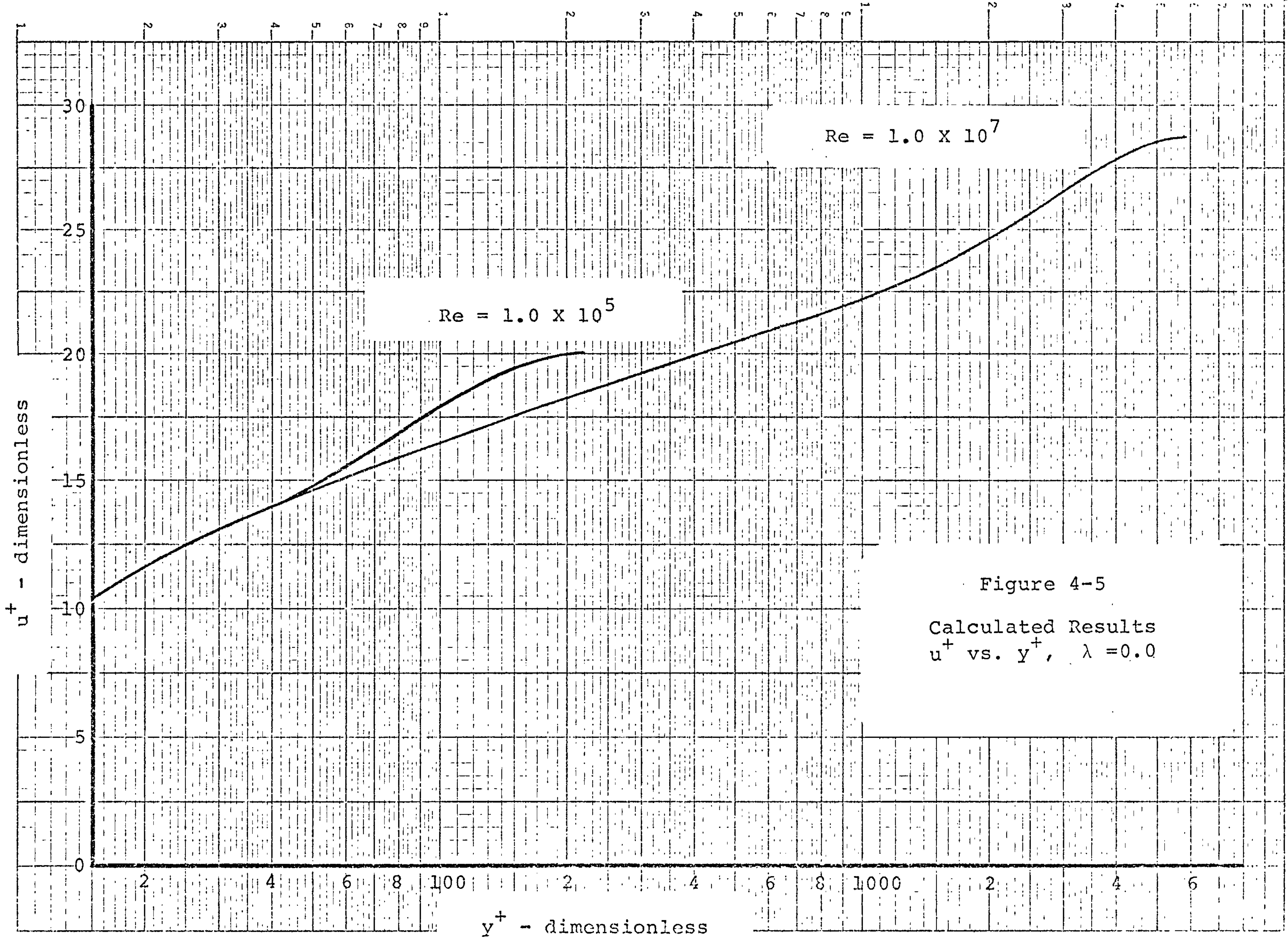

Figure 4-5

Calculated Results
u^+ vs. y^+, λ =0.0

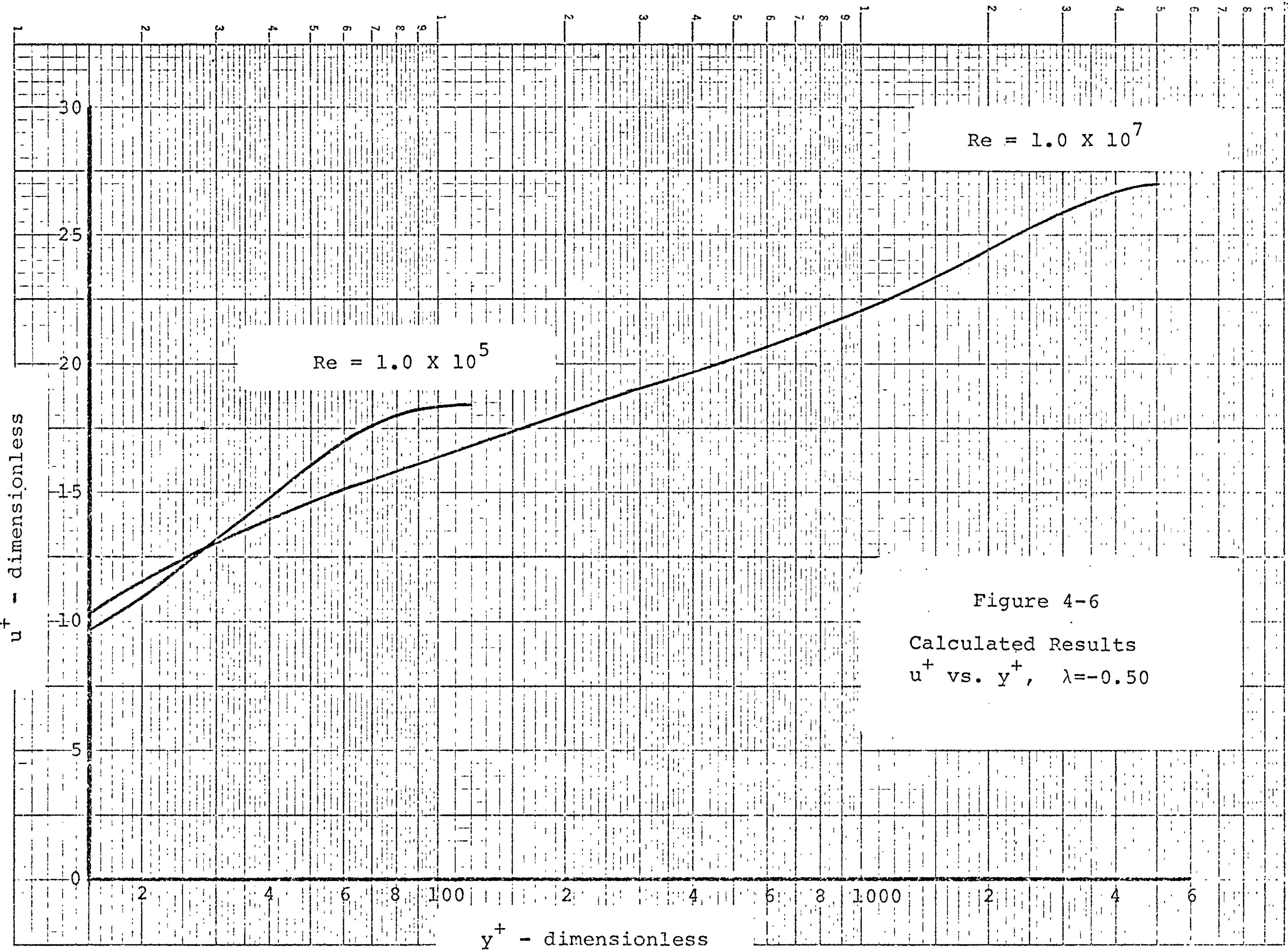

Figure 4-6

Calculated Results
u^+ vs. y^+, λ=-0.50

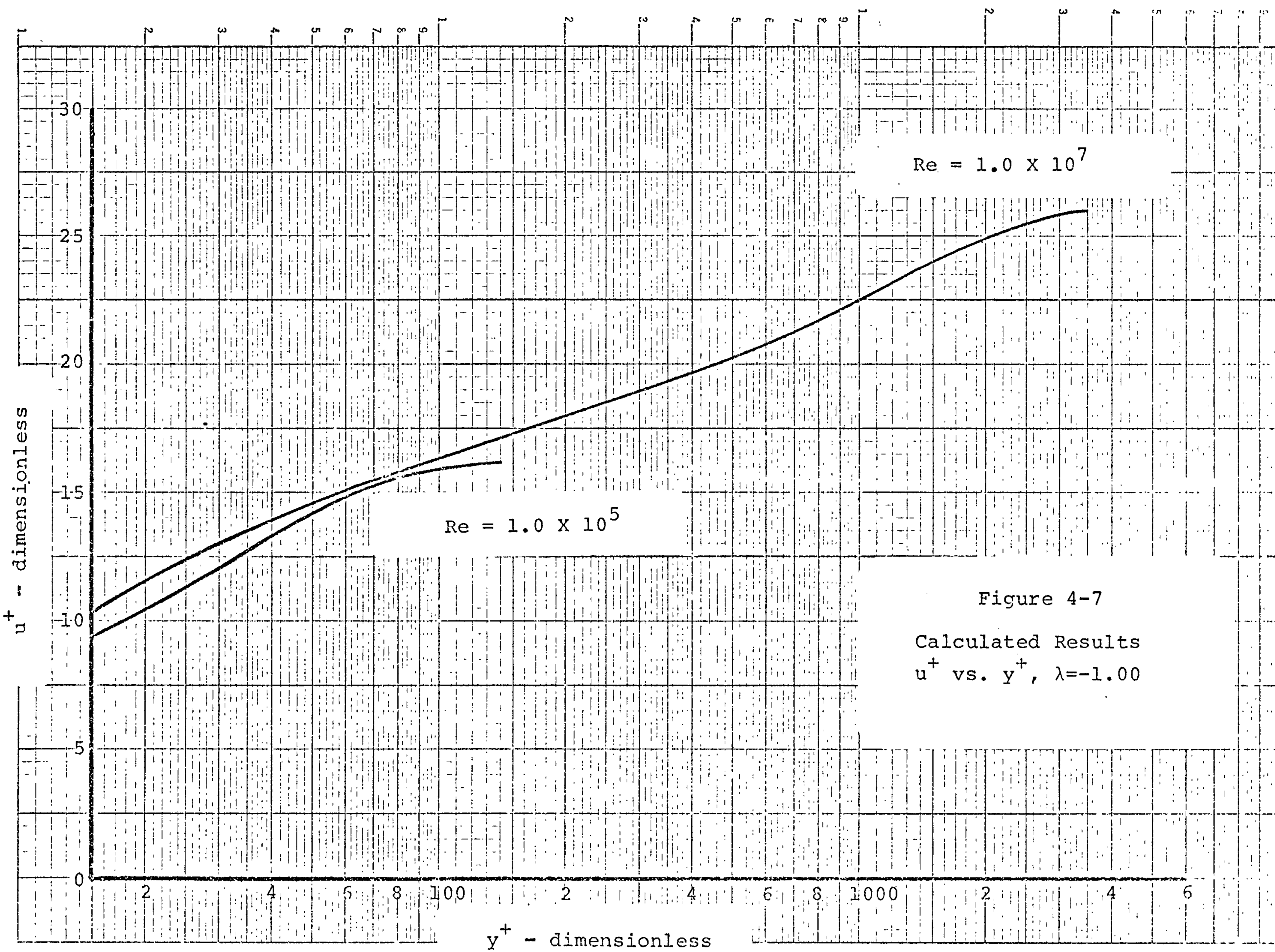

Figure 4-7

Calculated Results
u^+ vs. y^+, $\lambda=-1.00$

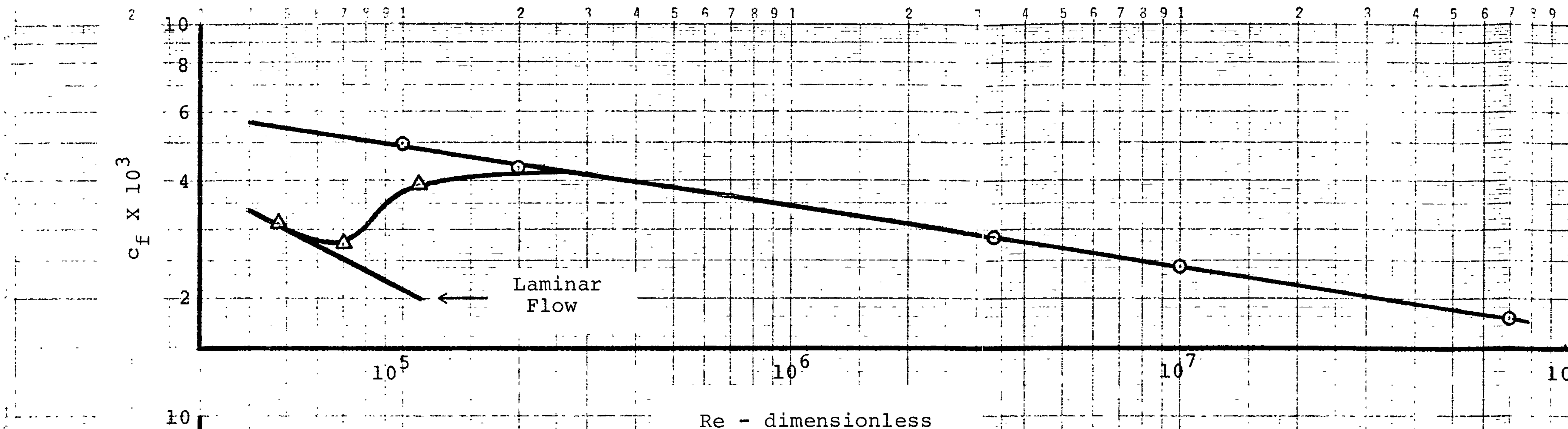

Figure 4-8

Calculated Results

c_f vs. Re, λ=0.00

⊙ a=1.0 △ a=50.0

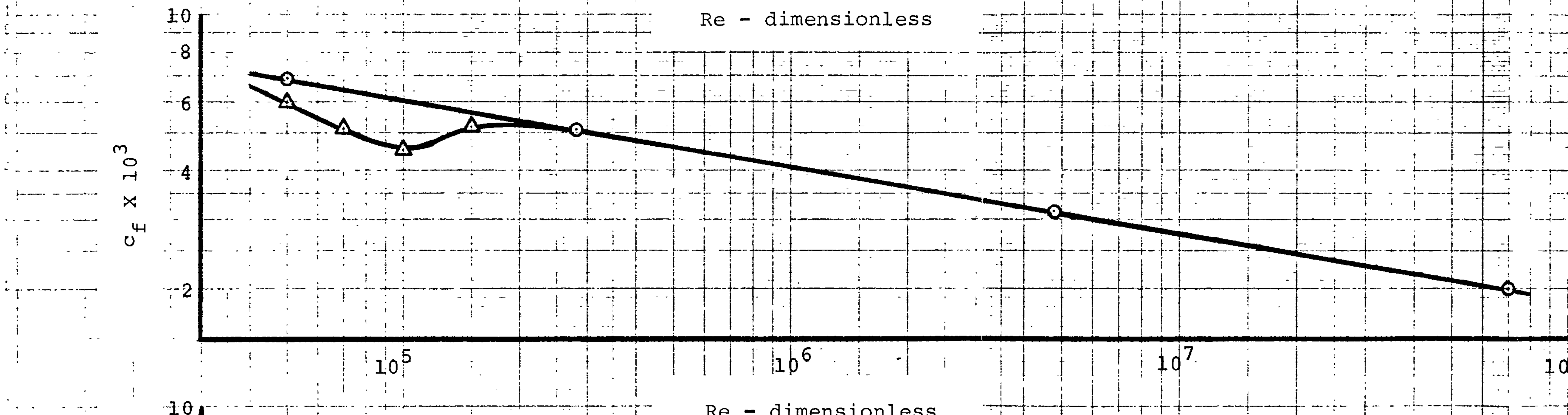

Figure 4-9

Calculated Results

c_f vs. Re, λ=-0.50

⊙ a=1.0, △ a=50.0

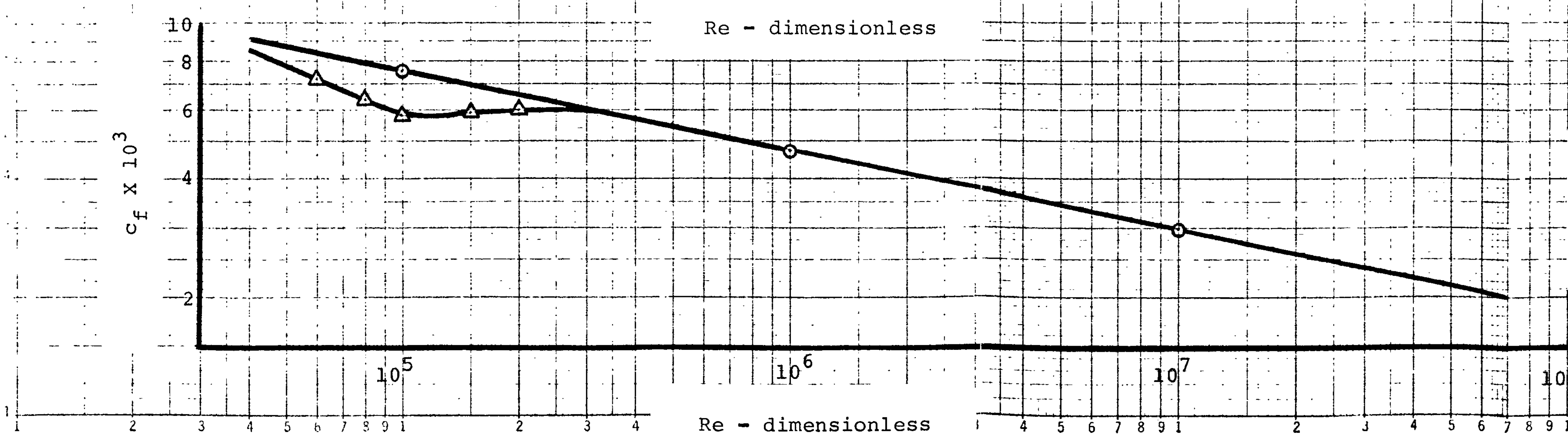

Figure 4-10

Calculated Results

c_f vs. Re, λ=-1.00

⊙ a=1.0, △ a=50.0

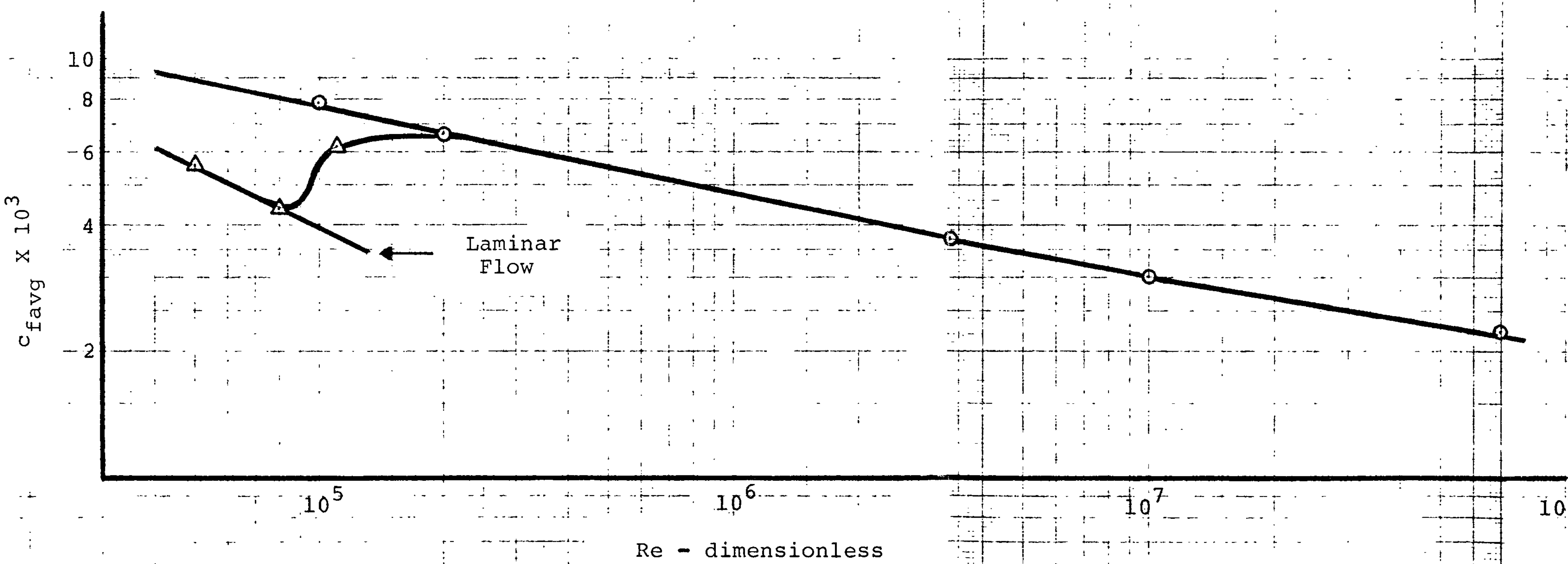

Figure 4-11

Calculated Results

c_{favg} vs. Re, λ=0.0

⊙ a=1.0, △ a=50.0

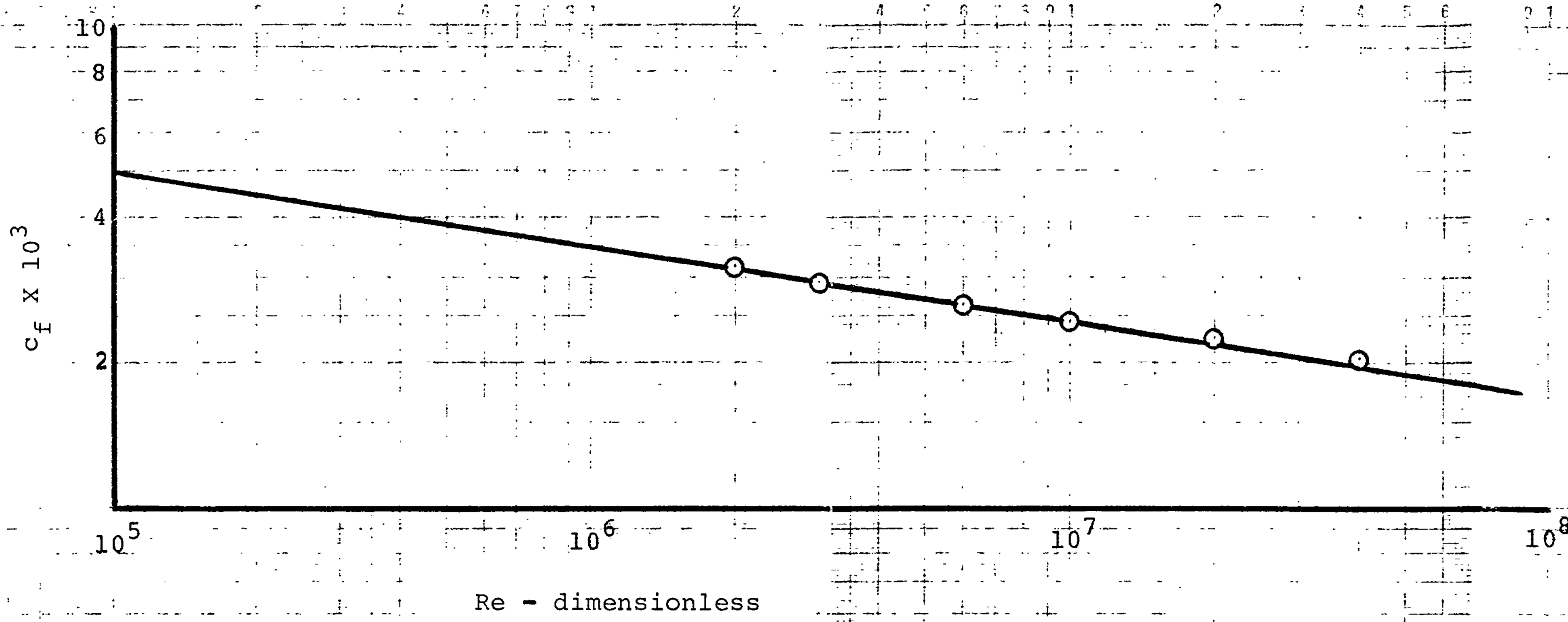

Figure 4-12

c_f vs. Re

λ=0.0, a=1.0

O Smith & Walker
— Present Method

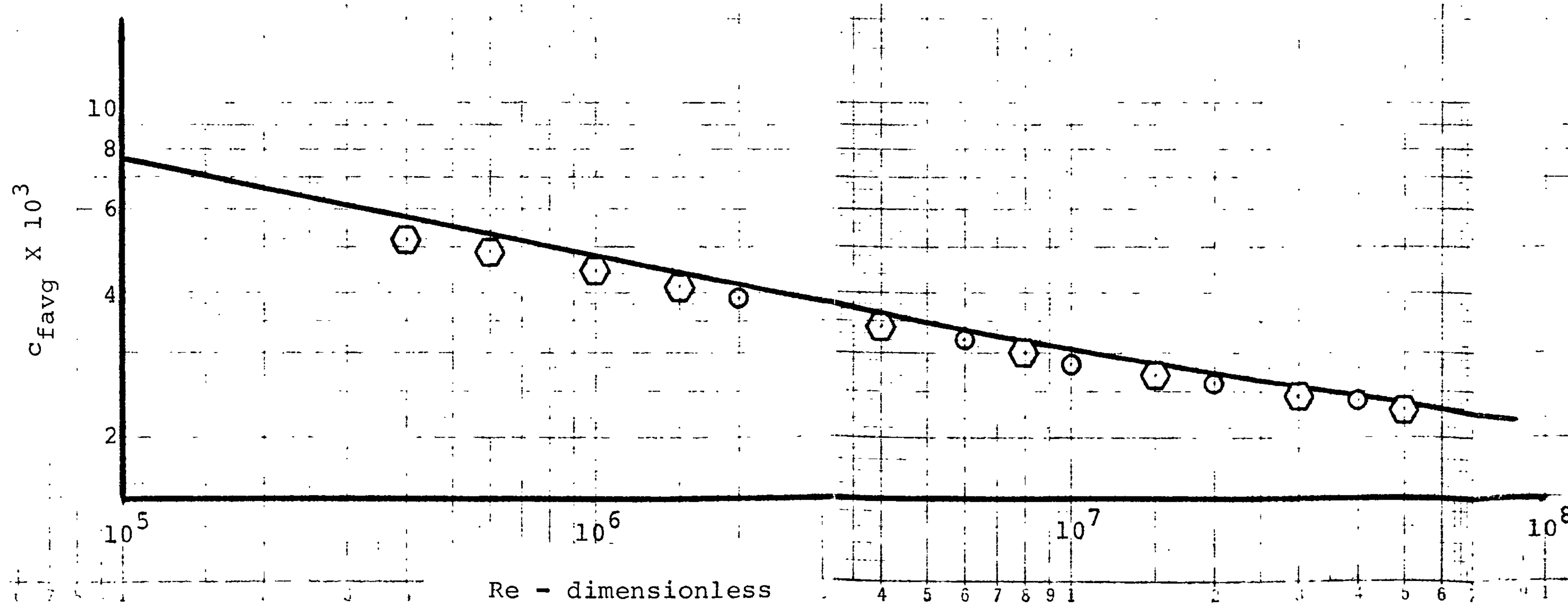

Figure 4-13

c_{favg} vs. Re

λ=0.0, a=1.0

O Smith & Walker
⬡ Schlichting
— Present Method

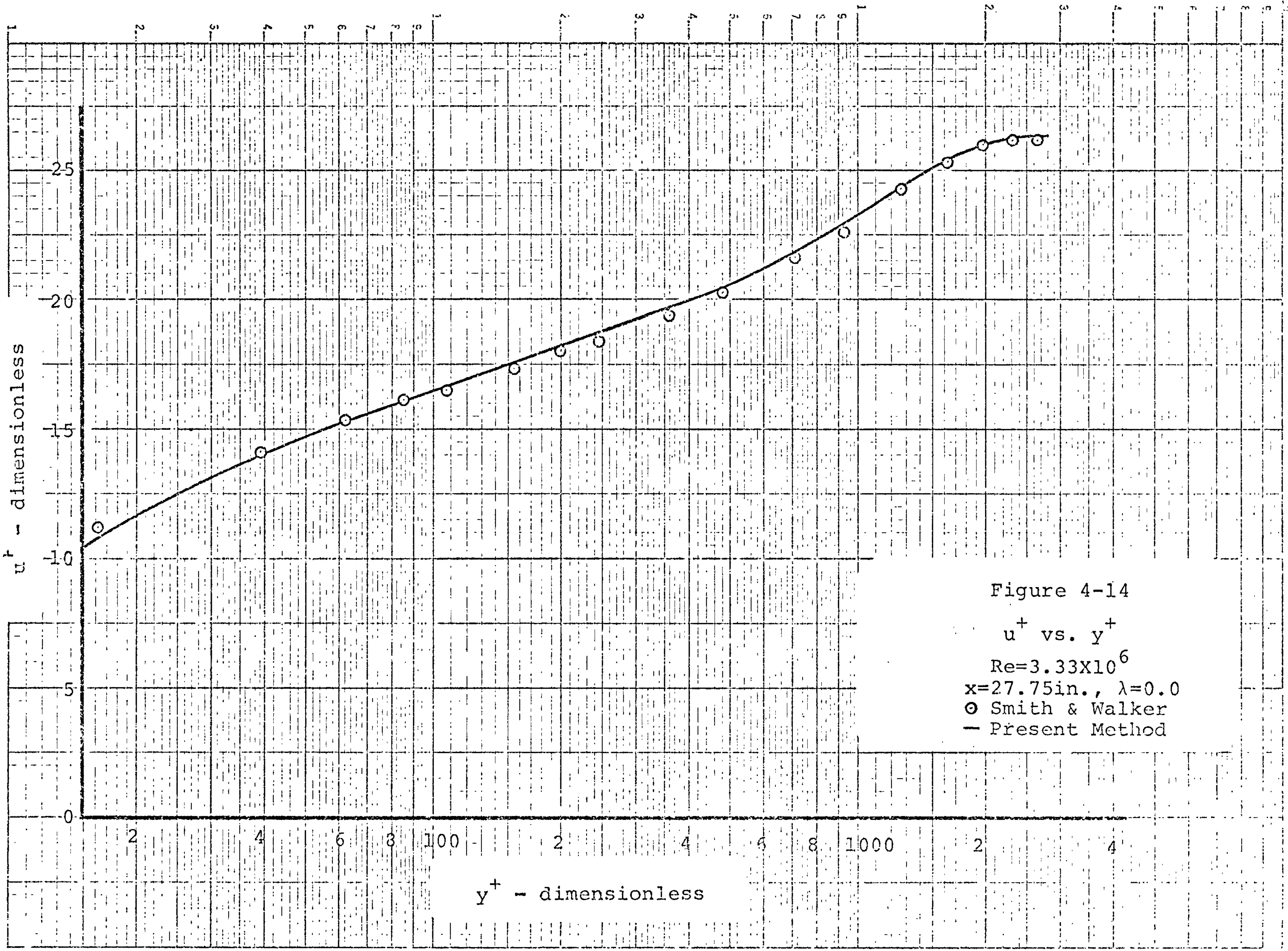

Figure 4-14

u^+ vs. y^+

$Re=3.33X10^6$

$x=27.75in., \lambda=0.0$

⊙ Smith & Walker

— Present Method

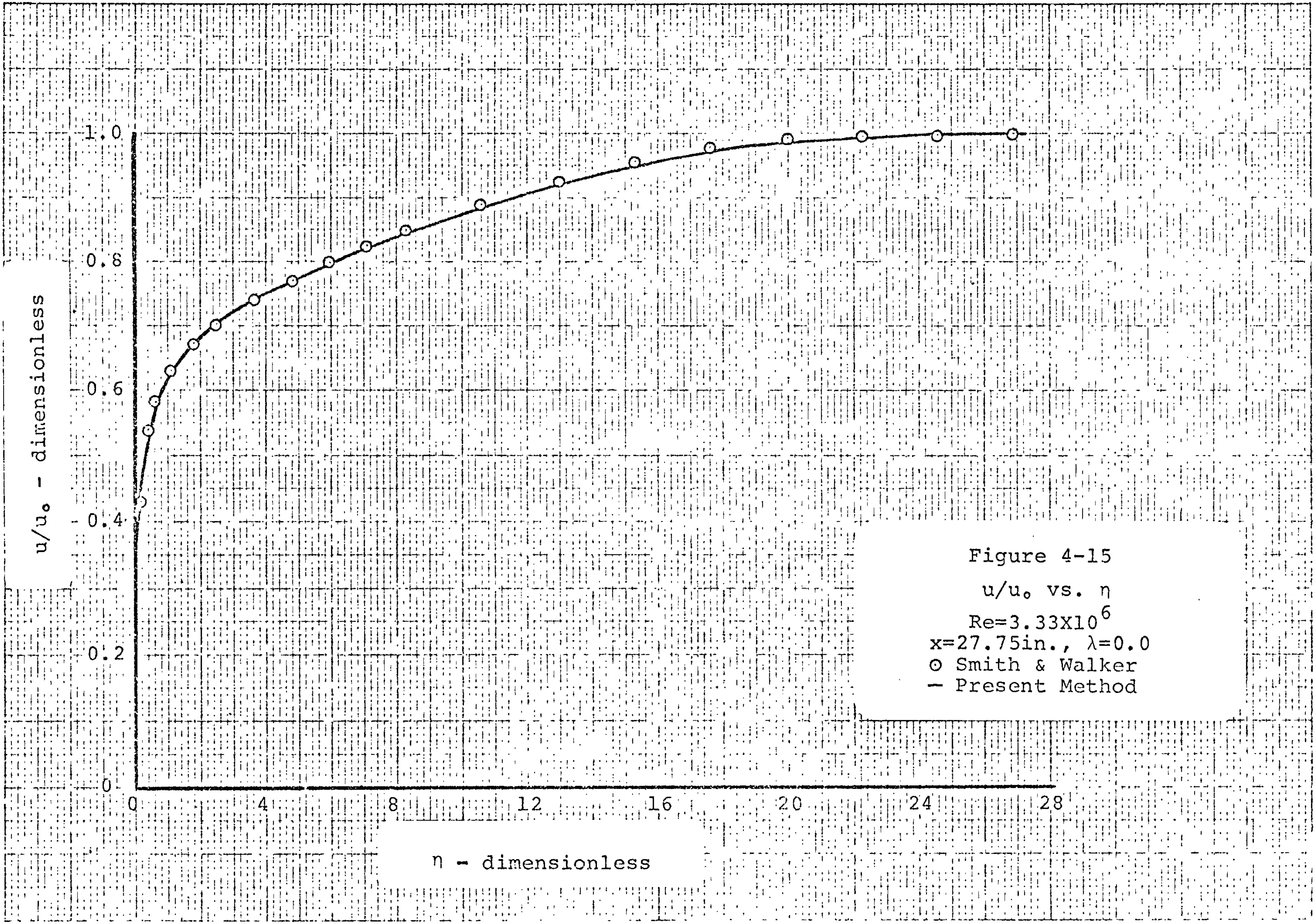

Figure 4-15
u/u_o vs. η
$Re=3.33X10^6$
$x=27.75$in., $\lambda=0.0$
⊙ Smith & Walker
— Present Method

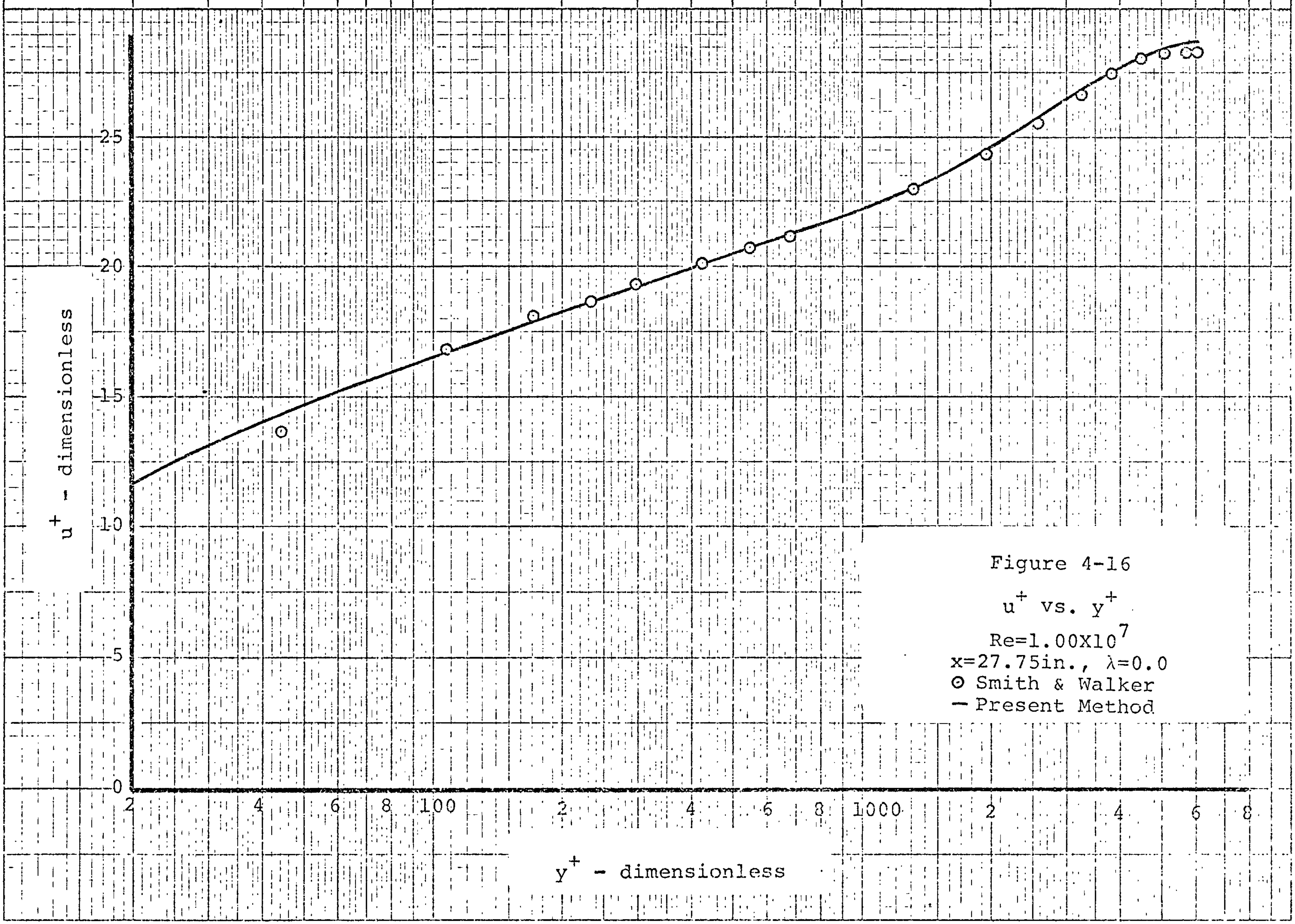

Figure 4-16

u^+ vs. y^+

Re=1.00X10^7

x=27.75in., λ=0.0

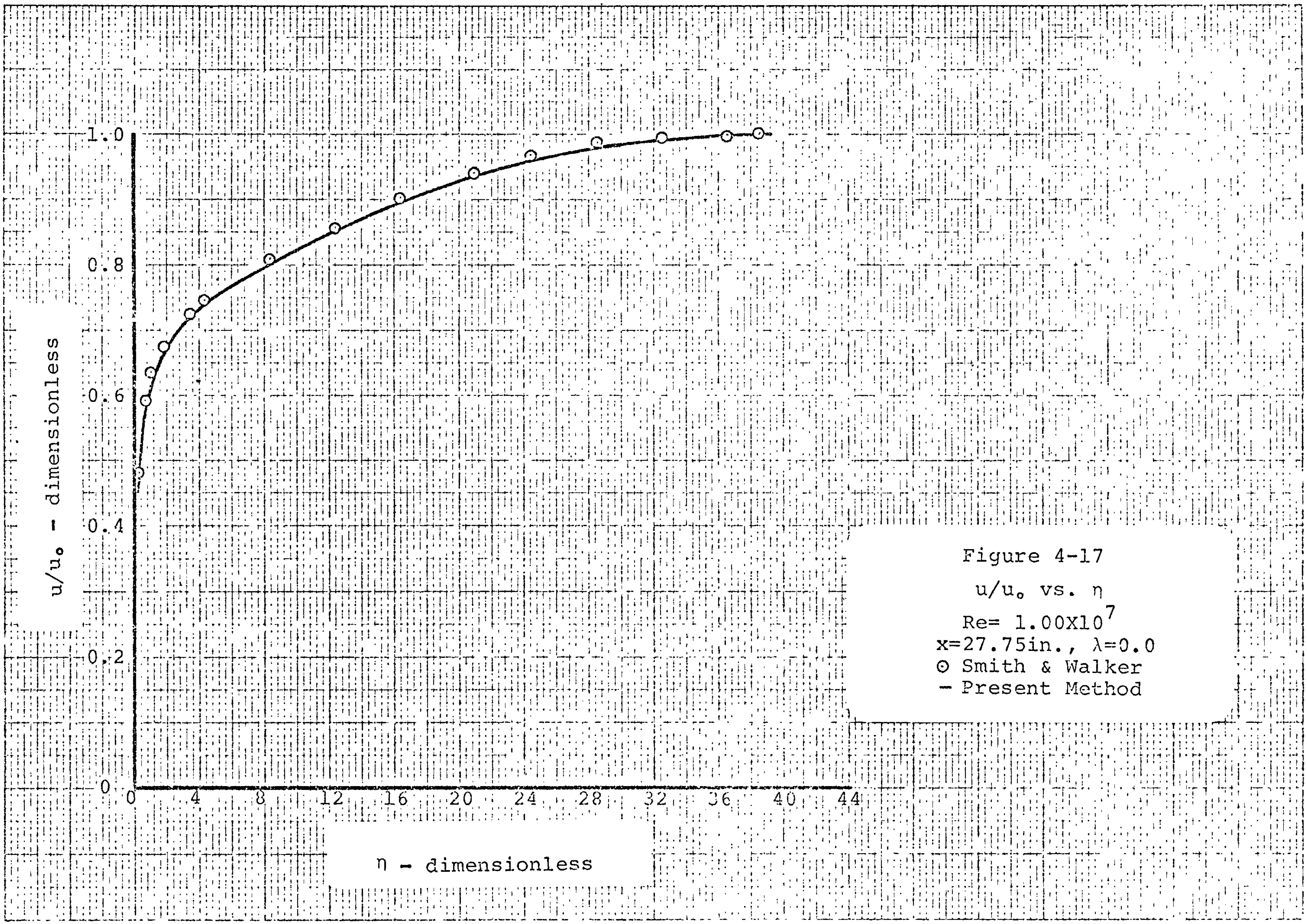

Figure 4-17

u/u_o vs. η

Re= 1.00×10^7

x=27.75in., λ=0.0

⊙ Smith & Walker

— Present Method

See page 50 for Figure 4-18.

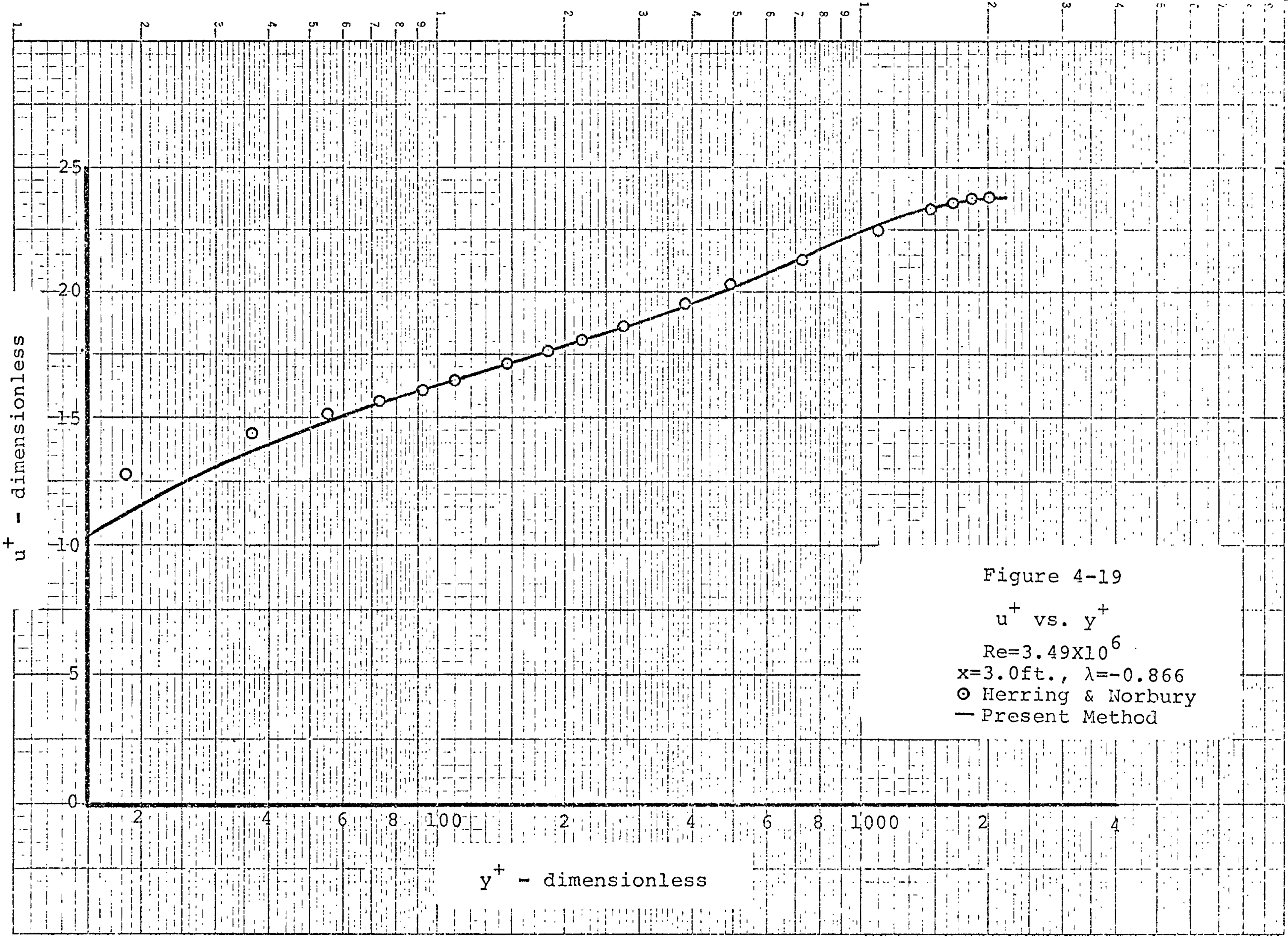

Figure 4-19

u^+ vs. y^+

$Re=3.49X10^6$

$x=3.0$ft., $\lambda=-0.866$

⊙ Herring & Norbury

— Present Method

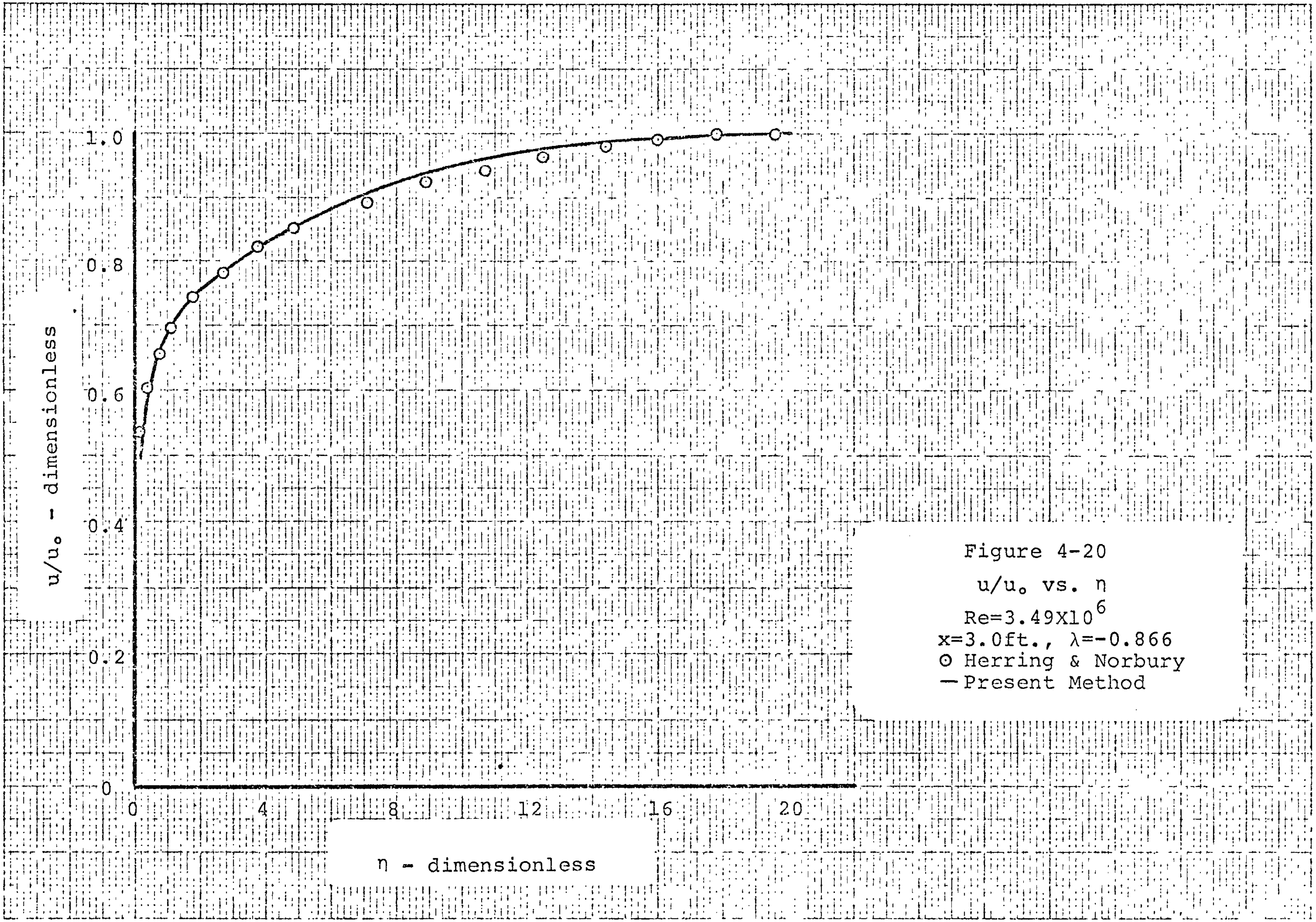

Figure 4-20

$u/u_\circ$ vs. η

$Re=3.49 \times 10^6$

$x=3.0$ft., $\lambda=-0.866$

⊙ Herring & Norbury

— Present Method

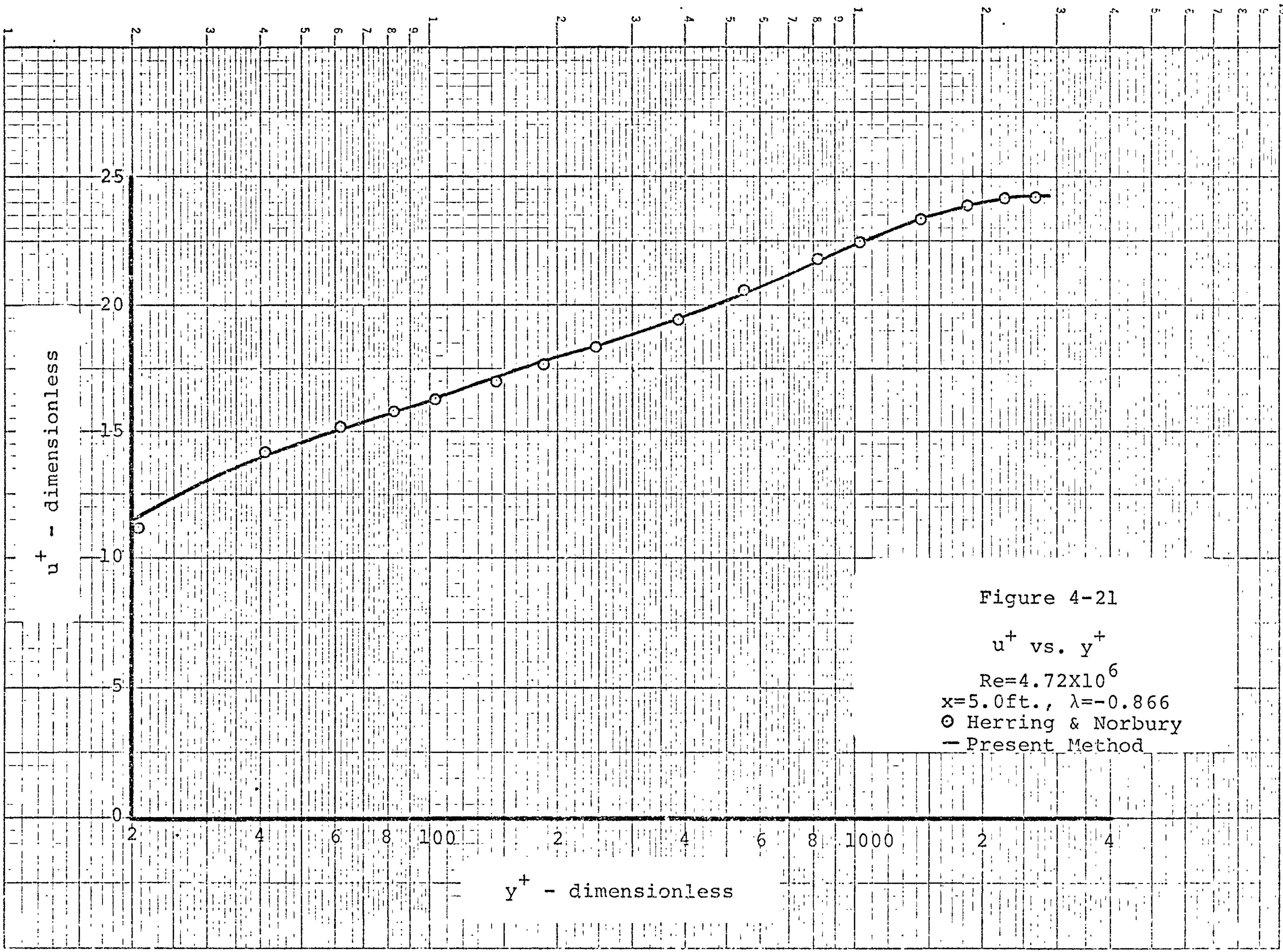

Figure 4-21

u^+ vs. y^+

$Re=4.72X10^6$

$x=5.0ft.$, $\lambda=-0.866$

⊙ Herring & Norbury

— Present Method

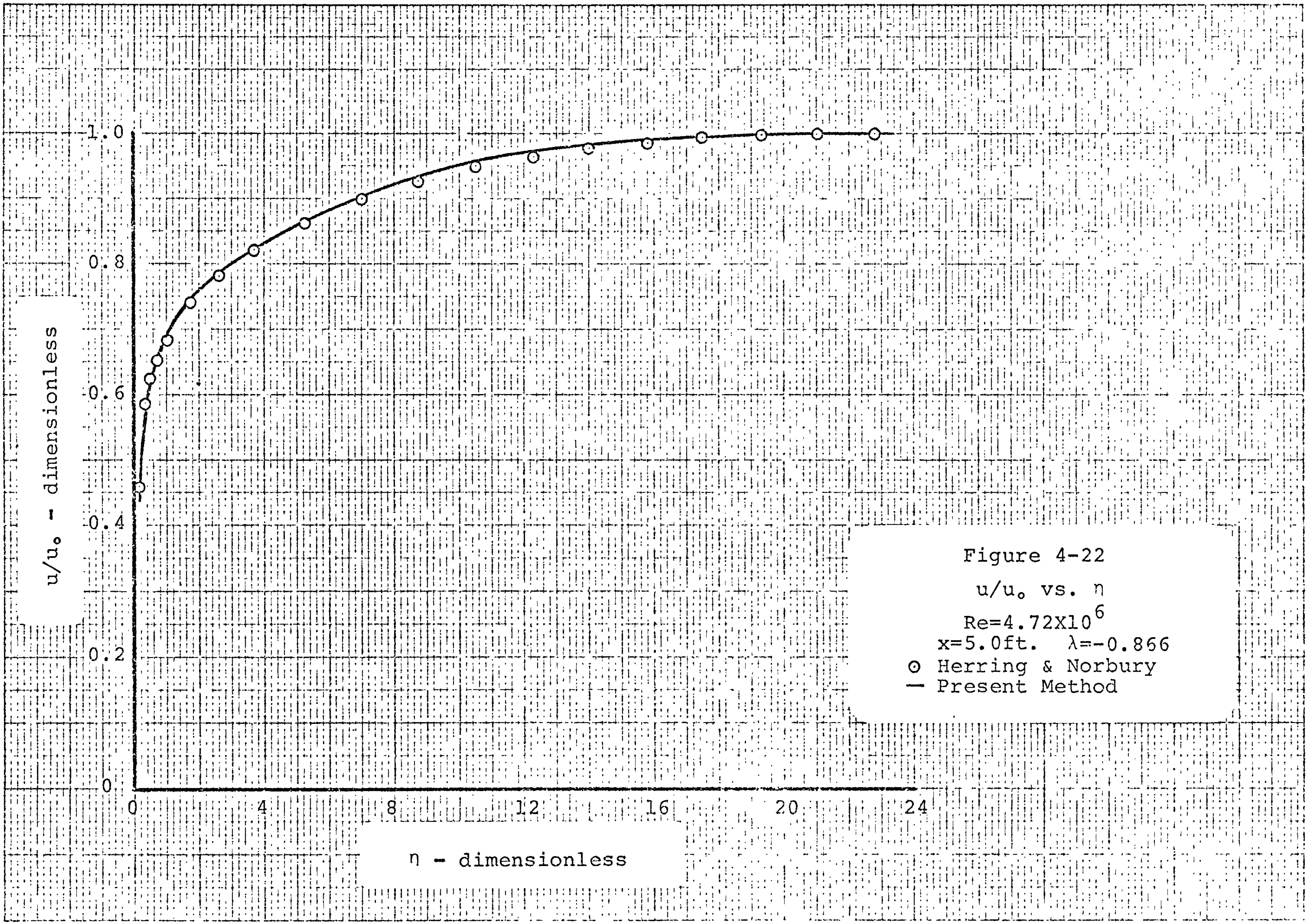

Figure 4-22

$u/u_\circ$ vs. η

$Re=4.72X10^6$

$x=5.0ft.$ $\lambda=-0.866$

See page 51 for Figure 4-23.

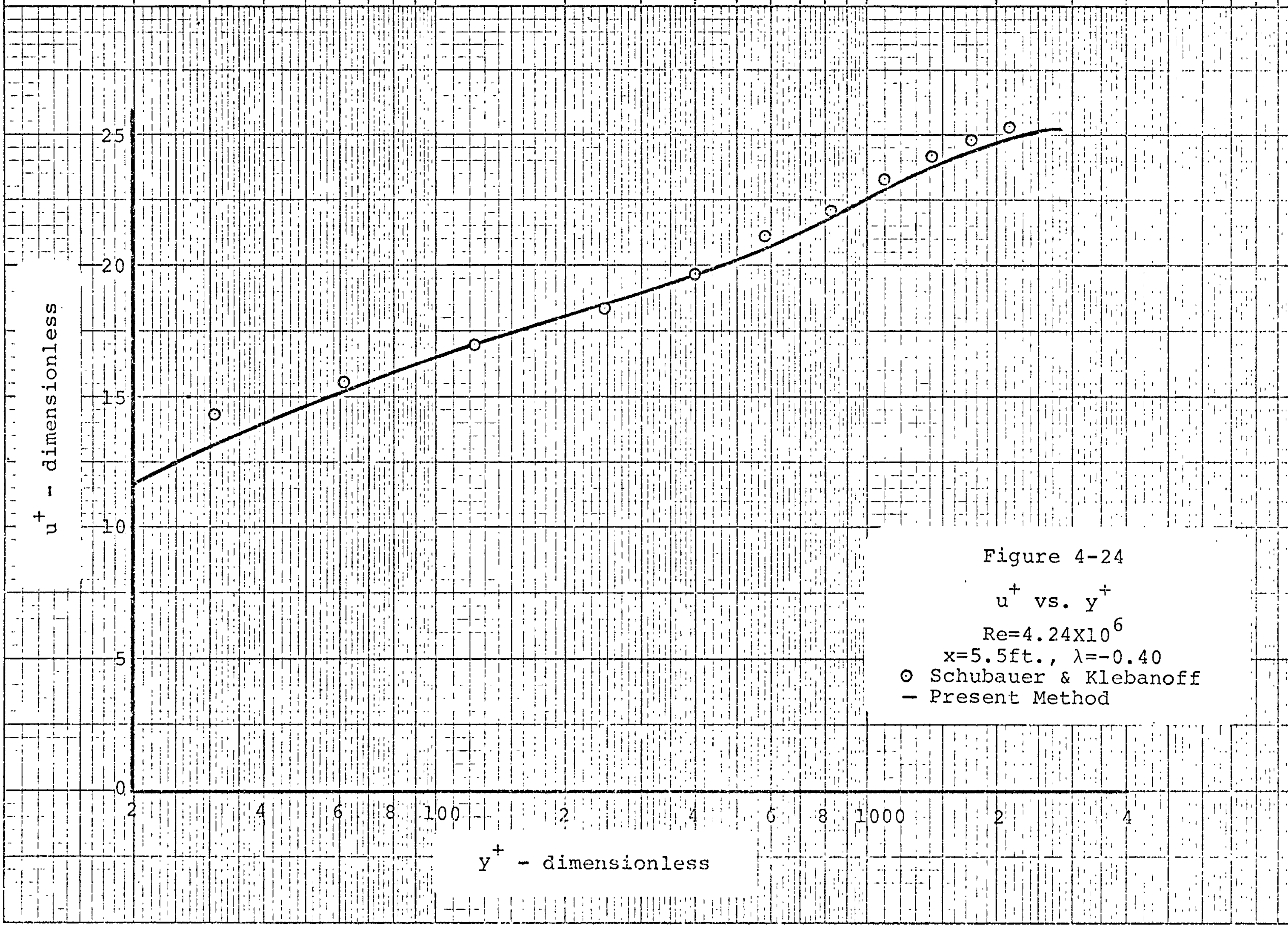

Figure 4-24

u^+ vs. y^+

Re=4.24X10^6

x=5.5ft., λ=-0.40

⊙ Schubauer & Klebanoff

— Present Method

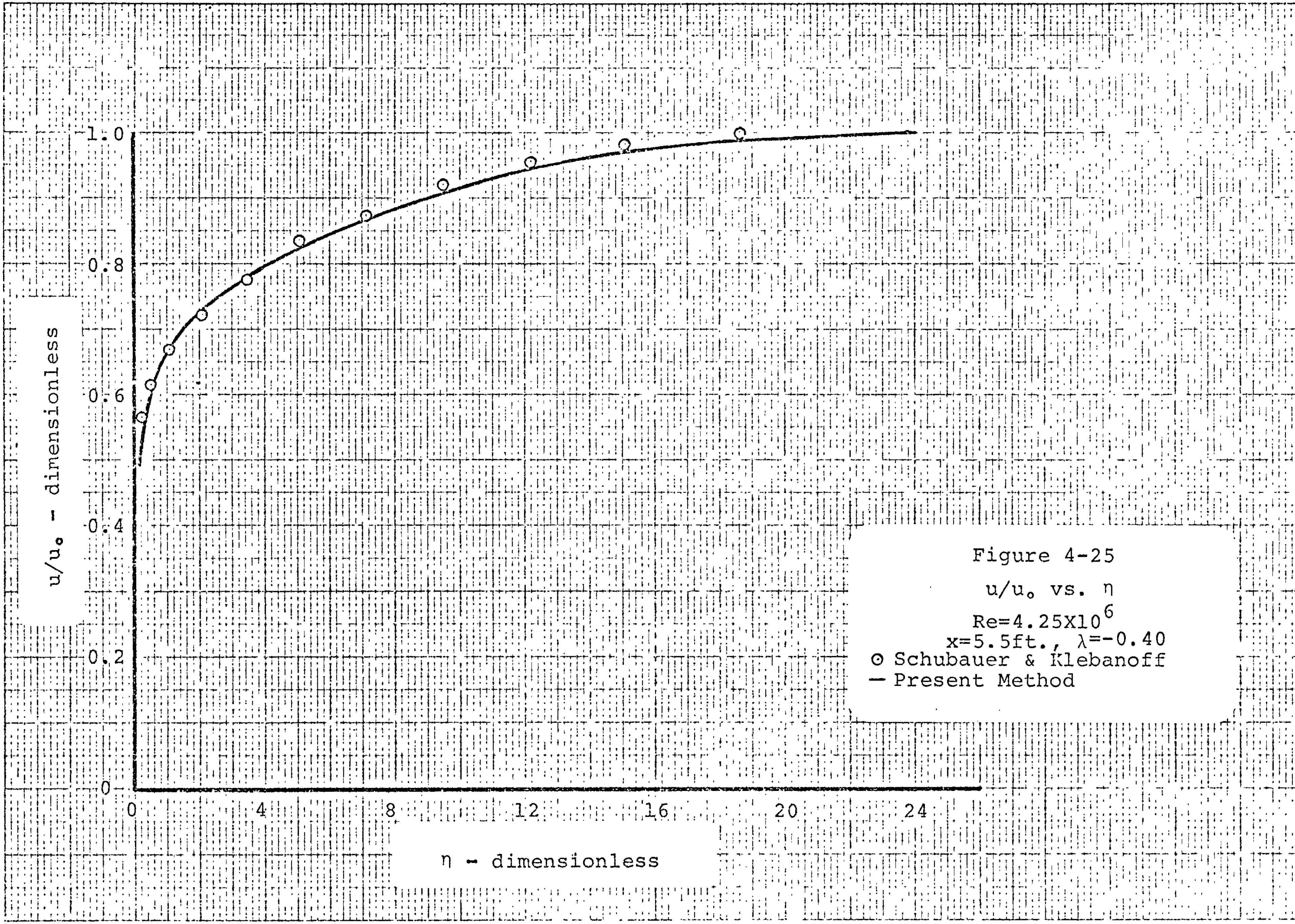

Figure 4-25

u/u_o vs. η

$Re=4.25X10^6$

$x=5.5ft.$, $\lambda=-0.40$

⊙ Schubauer & Klebanoff

— Present Method

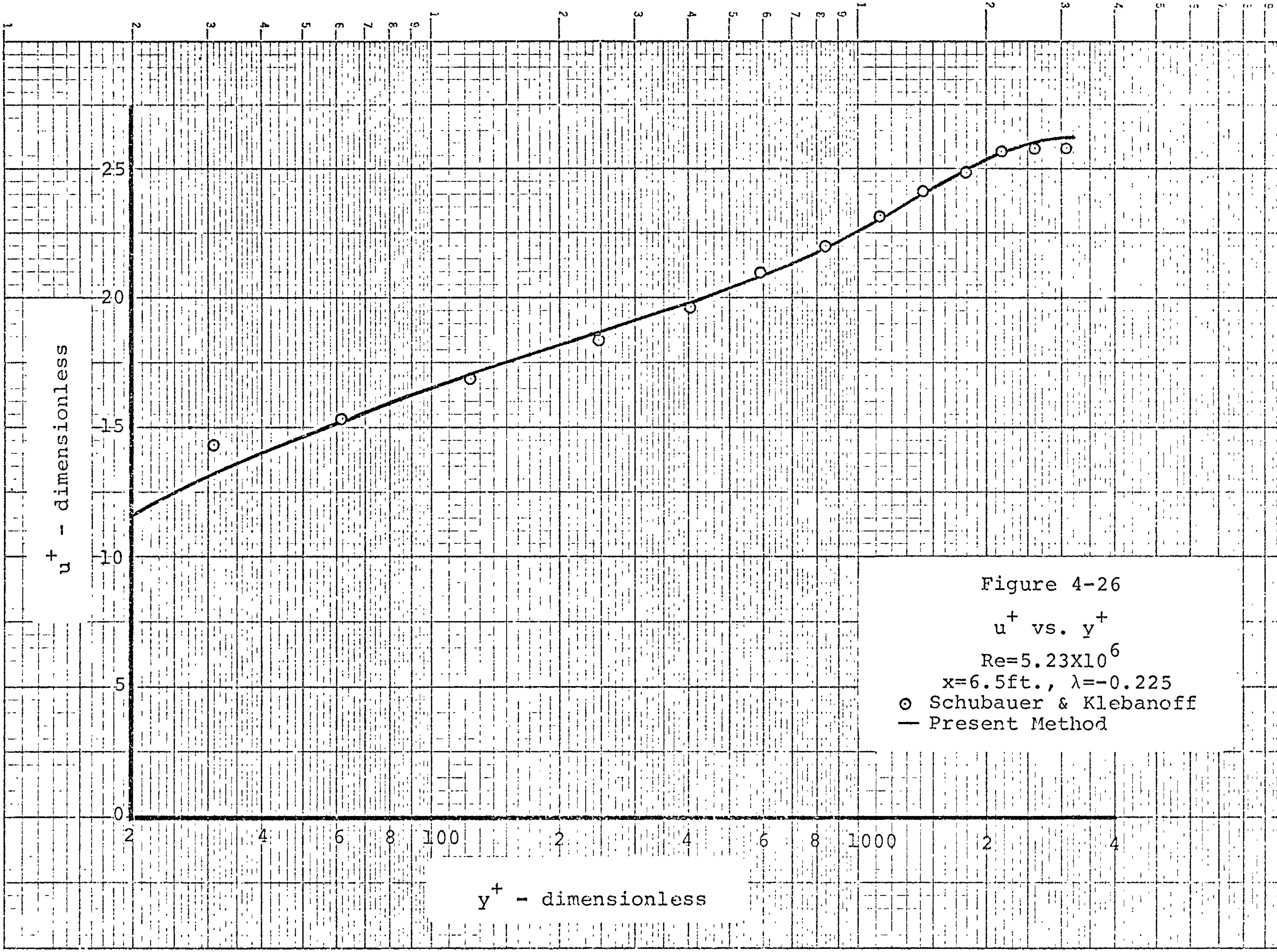

Figure 4-26

u^+ vs. y^+

Re=5.23X10^6

x=6.5ft., λ=-0.225

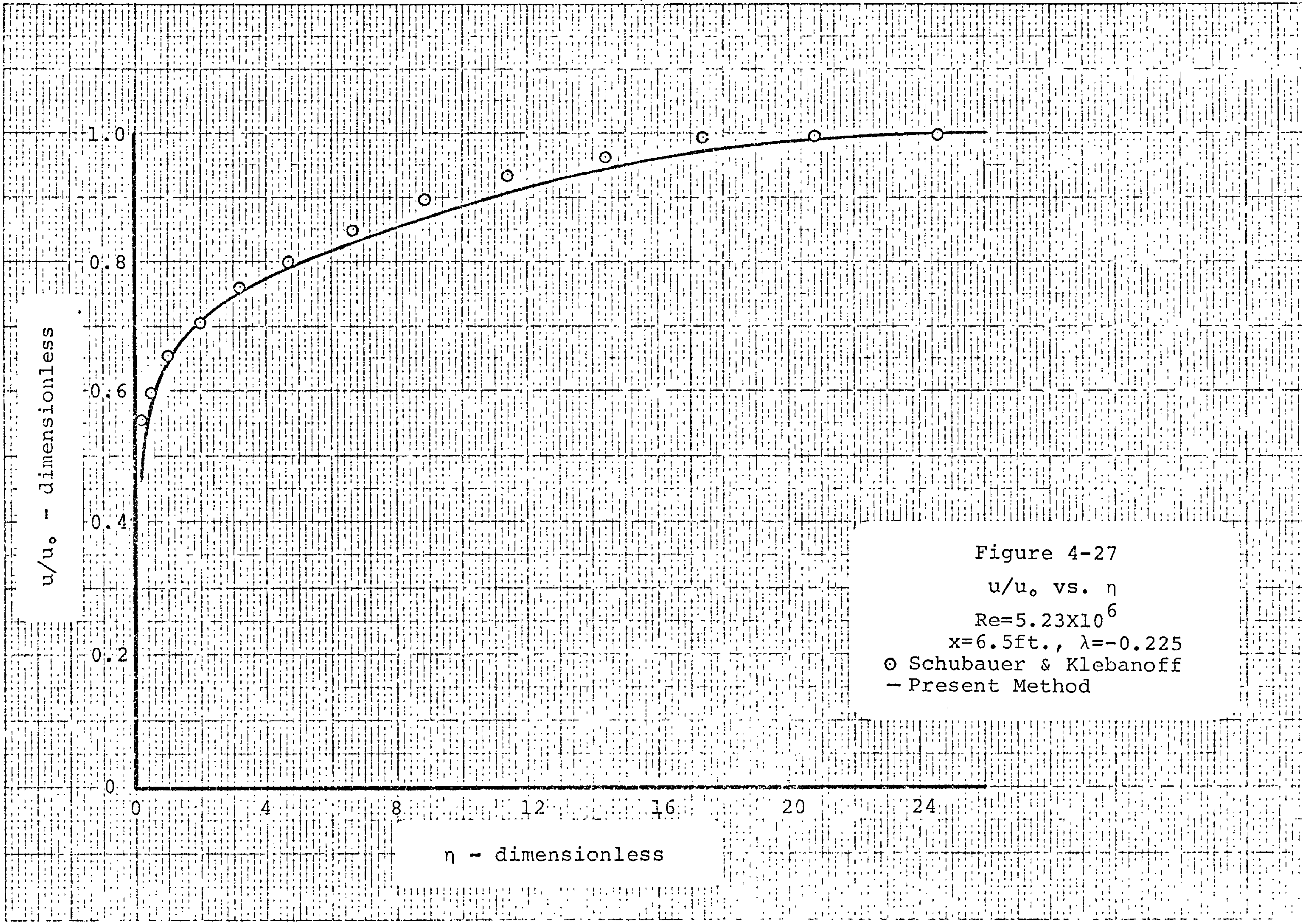

Figure 4-27

$u/u_\circ$ vs. η

$Re=5.23X10^6$

$x=6.5ft.$, $\lambda=-0.225$

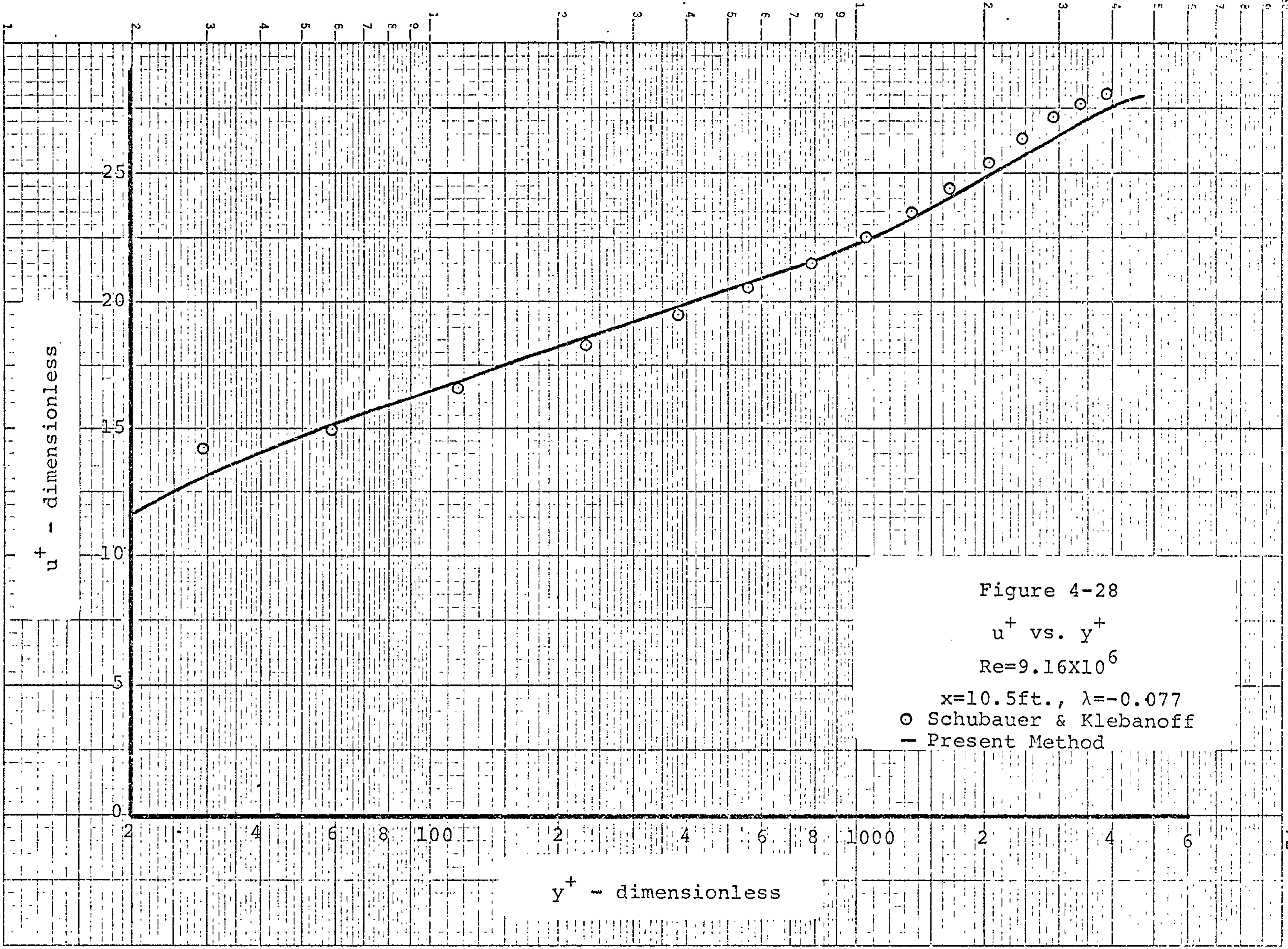

Figure 4-28

u^+ vs. y^+

$Re=9.16X10^6$

$x=10.5ft., \lambda=-0.077$

⊙ Schubauer & Klebanoff

— Present Method

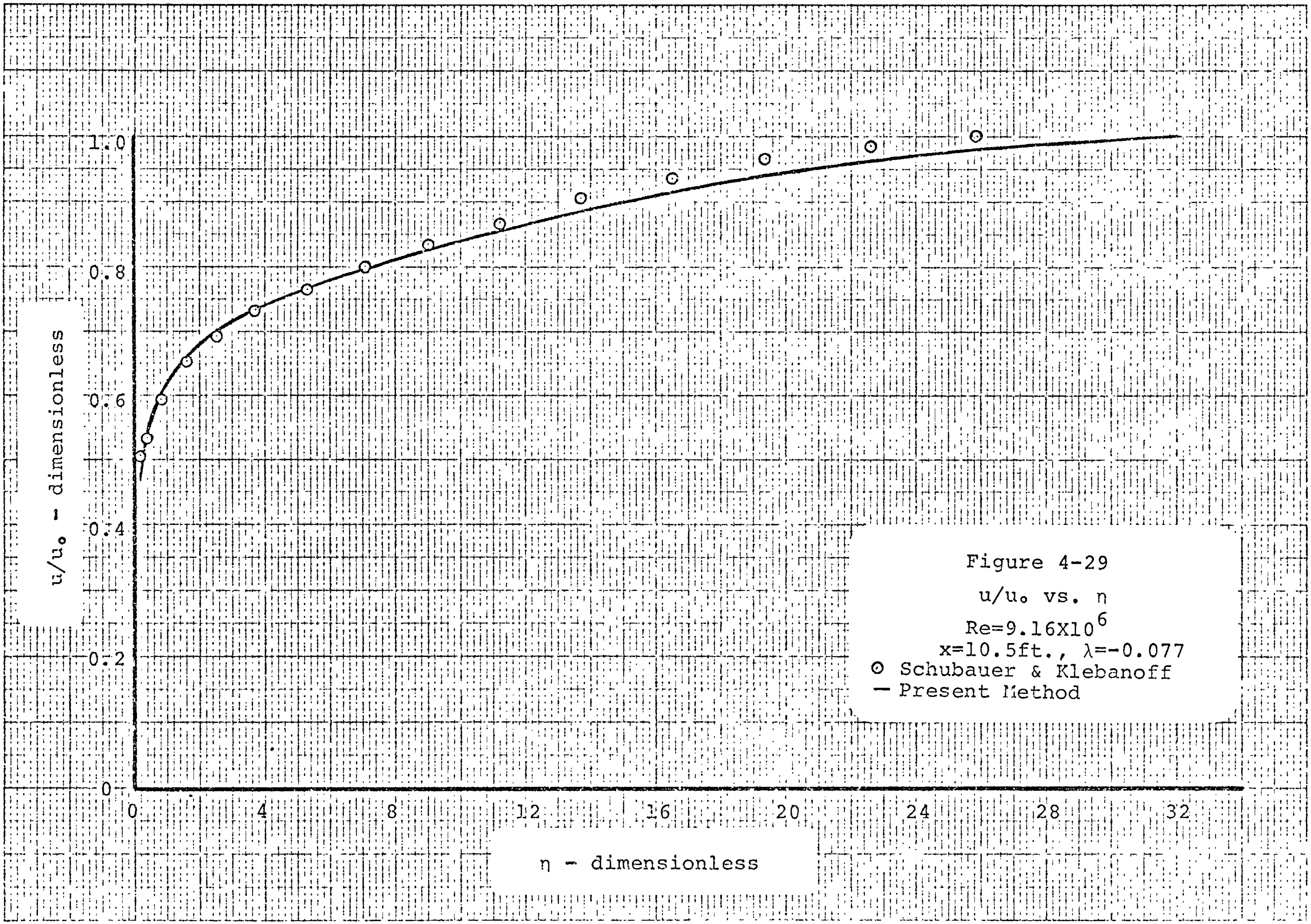

Figure 4-29

u/u_0 vs. η

$Re=9.16X10^6$

$x=10.5ft.$, $\lambda=-0.077$

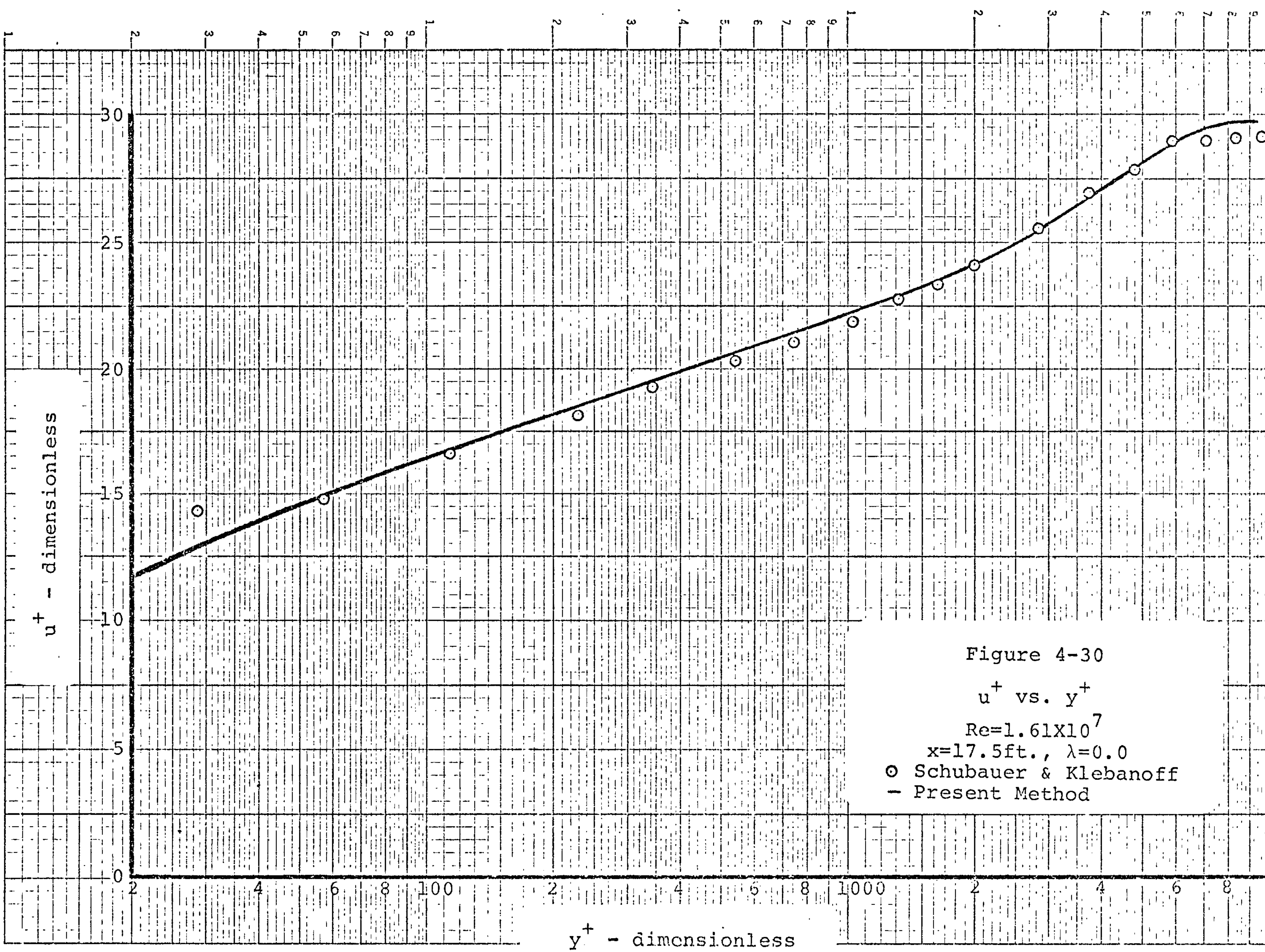

Figure 4-30

u^+ vs. y^+

$Re=1.61X10^7$

$x=17.5ft.$, $\lambda=0.0$

⊙ Schubauer & Klebanoff

— Present Method

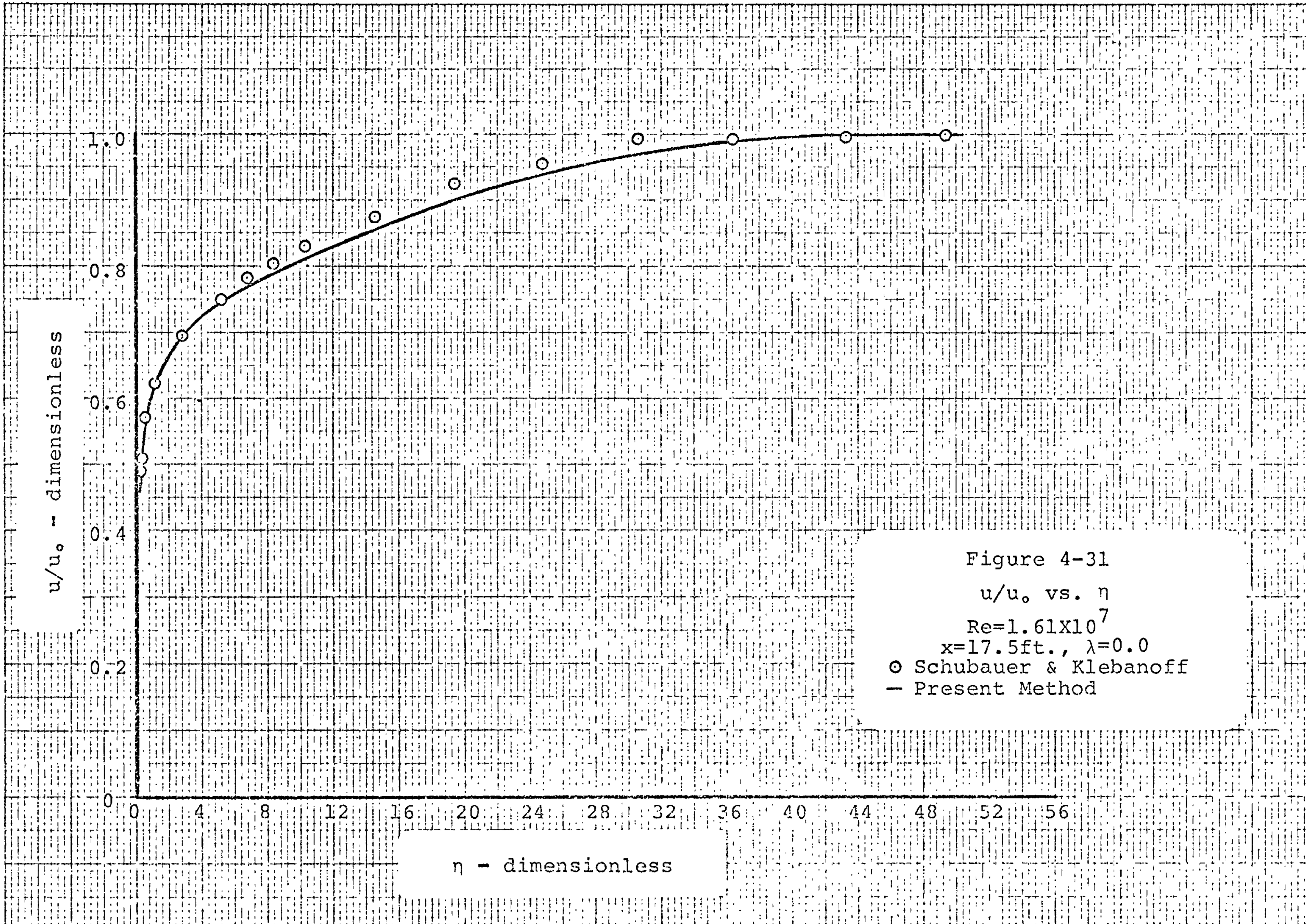

Figure 4-31

u/u_o vs. η

$Re=1.61X10^7$

$x=17.5ft., \lambda=0.0$

Table 4-2

Comparison of Experiment and Calculated Boundary Layer Parameters

SMITH AND WALKER

	Re[1]	λ	$c_f X10^2$	δ^*,in.	θ,in.	H
Experimental	$3.33X10^6$	0.000	0.293	0.066	0.0480	1.37
Calculated	$3.33X10^6$	0.000	0.288	0.070	0.0522	1.34
Experimental	$1.00X10^7$	0.000	0.249	0.052	0.0390	1.33
Calculated	$1.00X10^7$	0.000	0.242	0.055	0.0422	1.30

(1) All parameters are dimensionless unless otherwise noted.

Table 4-3

Comparison of Experimental and Calculated Boundary Layer Parameters

HERRING AND NORBURY

	$Re^{(1)}$	λ	$c_f X10^2$	δ^*,in.	θ,in.	H
Experimental	$4.72X10^6$	-0.866	0.355	0.111	0.086	1.29
Calculated	$4.72X10^6$	-0.866	0.341	0.105	0.081	1.30
Experimental	$3.49X10^6$	-0.866	0.358	0.111	0.086	1.29
Calculated	$3.49X10^6$	-0.866	0.351	0.104	0.079	1.31

(1) All parameters are dimensionless unless otherwise noted.

Table 4-4

Comparison of Experimental and Calculated Boundary Layer Parameters

SCHUBAUER AND KLEBANOFF

	$Re^{(1)}$	λ	$c_f X10^2$	δ^*,in.	θ,in.	H
Experimental	$4.25X10^6$	-0.400	0.315	0.087	0.065	1.35
Calculated	$4.25X10^6$	-0.400	0.314	0.092	0.071	1.30
Experimental	$5.23X\ 10^6$	-0.225	0.294	0.101	0.076	1.33
Calculated	$5.23X10^6$	-0.225	0.287	0.116	0.089	1.32
Experimental	$9.16X10^6$	-0.077	0.253	0.180	0.135	1.33
Calculated	$9.16X10^6$	-0.077	0.253	0.204	0.157	1.30
Experimental	$1.61X10^7$	0.000	0.230	0.310	0.230	1.28
Calculated	$1.61X10^7$	0.000	0.225	0.346	0.268	1.29

(1) All parameters are dimensionless unless otherwise noted.

Bibliography

1.) Blasius, H., Grenzschlichen in Flussegkeiten mit Kleiner Reibung. Z. Math. u. Phys. 56,1.

2.) Chao, B. T.,Advanced Heat Transfer., University of Illinois Press, Chicago, 1969, pp. 54-56.

3.) Clauser, F. H., "The Trubulent Boundary Layer," Advances in Applied Mechanics, Volume 4, Academic Press, N. Y., 1956.

4.) Coles, D. E. and Hirst, E. A.,et. al. Computation of Turbulent Boundary Layers - 1968 AFOSR-IFP-Stanford Conference

5.) Dhawan, Satish, "Direct Measurements of Skin Friction" NACA Rep. 1121, 1953.

6.) Gill, W. N. and Sher, M., A Modification of the Momentum Transfer Hypothesis., AIChE Journal Vol. 7, page 61, 1961.

7.) Herring, H. J. and Norbury, J. F., Some Experiments on Equilibrium Turbulent Boundary Layers In Favorable Pressure Gradients, Journal of Fluid Mechanics, Vol. 27, Part 3, 1967, pp. 541-549.

8.) Hinze, J. O., Turbulence, McGraw-Hill, N. Y., 1961.

9.) Klebanoff, P. S., "Characteristics of Turbulence in a Boundary Layer with Zero Pressure Gradient", NACA TN 3178, July, 1958.

10.) Meksyn, D., Laminar Boundary Theory, Pergamon Press, N. Y., 1961, pp. 47-51.

11.) Meissinger, H. F., "The Use of Parameter Influence Coefficients in Computer Analysis of Dynamic Systems" Simulation, August, 1964.

12.) Padilha, Jose C. B., "Similarity Solutions of the Boundary Layer Equation for Laminar Film - Boiling and Turbulent Single Phase Flow", Masters Thesis, University of Houston, June, 1964.

13.) Prandtl, L., Uber Flussigkeitsbewegung Ber Schr Kleiner Reibung, Proceedings of the Third International Math Rongr, Heidelberg, 1904, or Boundary Layer Theory, Schlichting.

14.) Reynolds, W. C., "A Morphology of the Prediction Methods," Computation of the Turbulent Boundary Layers, 1968, AFOSR-IFP-Stanford Conference Vol. 1.

15.) Rotta, J. C., "Turbulent Boundary Layers In Incompressible Flow", Progress in Aeronautical Sciences, Vol. 2, Macmillan, N. Y., 1962.

16.) Schlichting, H., Boundary Layer Theory., McGraw-Hill, N. Y., 1960.

17.) Schubauer, G. B. and Klebanoff, P. S., NACA Report No. 1030, "Investigation of Separation of the Turbulent Boundary Layer", 1951.

18.) Smith, A. M. O. and Cebeci, T. D., "Numerical Solution of the Turbulent Boundary Layer Equation", Douglas Aircraft Co., Report No. 33735, May, 1967.

19.) Smith, D. W. and Walker, J. H., "Skin Friction Measurements In Incompressible Flow", NACA TN 4231, 1958.

20.) System/360 Continuous Systems Modeling Program (360A-CX-16X) User's Manual, I. B. M. Corp., 1967.

21.) System/360 Continuous Systems Modeling Program (360A-CX-16X) Systems Manual, I. B. M. Corp., 1967.

22.) Telles, A. S., "Application of the Similarity Method to Some Cases of Turbulent Boundary Layer Flow", Masters Thesis, University of Houston, 1963.

23.) Telles, A. S. and Dukler, A. E., "Similarity Types of Solutions of the Turbulent Boundary Layer Equations for Momentum and Energy", AIChE Journal, May, 1968, p. 440.

Appendix

Appendix A

Program for Turbulent Boundary Layer Calculations

The program used in solving the momentum equation is presented following this page. A definition of the symbols used in the program is given in Table A-1. Contrary to a Fortran IV Program, the input data statements are at the beginning of the program in CSMP.

When more than one estimation of the streamwise terms is needed, ERRORK (the estimated value for the streamwise terms) from the first run is expressed in equation form as a function of η by using a separate least squares program. Then ERRORK is used in the boundary layer program in equation form as ERROR1. This procedure may be repeated as many times as needed.

Before running the program, attention should be given to the values of the following parameters in the program:

(1) RE, (2) DELRE, (3) FPPO, (4) LAMDA, (5) FIN1, (6) DELT1, (7) DELT2, (8) PRDEL1, (9) PRDEL2, (10) OUTDL1, (11) OUTDL2, (12) TRANSP, (13) A

Program for Turbulent Boundary Layer Calculations

```
LABEL    TURBULENT BOUNDARY LAYER
*
/        DIMENSION F2P(3,200),F1P(3,200),FOP(3,200),EPNU(3,200)
/        DIMENSION ERROR (200)
*
*        DATA INPUT AND INITIAL CONDITIONS
FIXED    KOUNT,KOUNT2,KOUNT4,KOUNT3,I,J,K,N,L,J4,J16
INCON    KOUNT=0, KOUNT2=0,KOUNT3=0,KOUNT4=0,J=1,K=1,I=1,L=0,J4=3,J16=0
PARAM    KC=0.4, A= 1.0, B=25.0, ETAO=0.0, DISPO=0.0,...
         FPO=0.0, FO=0.0, WPPO=1.0, WPO=0.0, MOMO=0.0, WO=0.0,...
         DELT=0.01, FINTIM=0.50, PRDEL1=0.02, OUTDL1=0.02,...
         EDL1=0.0, EDL2=0.0, PRDEL2=0.5, OUTDL2=0.5, DELT1=0.01, DELT2=0.25,...
         LAMDA= 0.000, FPPO=5.700,FPPOO=5.700,TRANSP=0.16,...
         ETADEL=38.250, RE=1.20E7,FIN1=39.00,DELRE=0.2E7,
*
         ETA=TIME+ETAO
         Y=COMPAR(ETA/ETADEL,TRANSP)
         BETA= 2.0*KC**2*RE**0.5*2.0**0.50
         PHI= (2.0**0.25*RE**0.25*FPPOO**0.5*ETADEL-A)/B
         PHIR1=PHI*ETA/ETADEL
         PHIR=ZHOLD((130.0-PHIR1),PHIR1)
         EX=EXP(-PHIR)
```

```
      PHIRLO=ZHOLD((130-PHIR1),PHIR1)
      EXLO=EXP(-PHIRLO)
      BRAC1=1.0-EX
      BRAC2=BRAC1+PHI*ETA/ETADEL*EX
NOSORT
      X2=BETA/2.0*ETA**2*FPP*BRAC1**2
      EPONU1=ZHOLD((TRANSP-ETA/ETADEL),X2)
      IF(Y)1000,1000,1001
*
*     EQUATION FOR THE INNER REGION
1000  FPPP1=(-F*FPP+LAMDA*(1.0-FP**2)-BETA*FPP**2*ETA*BRAC1*BRAC2)/...
      (1.0+BETA*ETA**2*FPP*BRAC1**2)
      FPPP=FPPP1
      EPONU=X2
      IF(I.EQ.1) ETA16=ETA
      ERRORK=0.0
      GO TO 1002
1001  CONTINUE
      IF(ETA.LT.ETA16) GO TO 1004
      IF((J4-4*(J+1)).EQ. 0) J=J+1
      J4=J4+1
      IF(I.LT.4) GO TO 1004
      K=J
1004  CONTINUE
```

```
          IF(K.LE. 0)K=1
          EPONU=EPONU1
          IF(I.LT.4)ERROR(K)=0.0
*
*         EQUATION FOR THE OUTER REGION
          FPPP2=(-F*FPP+LAMDA*(1.0-FP**2))/(1.0+EPONU)+ERROR(K)
          ERROR1=(0.608-0.1778*ETA+3.394E-3*ETA**2)*1.0E-4
          IF(I.EQ.4)ERROR1=0.0
          FPPP=FPPP2+ERROR1
          ERRORK=ERROR(K)
1002      CONTINUE
          EDEL1=ETA
          EDEL=ZHOLD((FPP-0.001),EDEL1)
          FPP=INTGRL(FPPO,FPPP)
          FP=INTGRL(FPO,FPP)
          F=INTGRL(FO,FP)
          IF(Y)1005,1005,1006
*
*         MEISSINGER INFLUENCE FUNCTION TECHNIQUE
1005      BZ1=BRAC1**2*BETA*ETA**2*FPPP*WPP
          BZ2=BETA*ETA**3*FPP*FPPP/B*(2.0*RE)**0.25/FPPOO**0.5*EX*BRAC1
          BZ=BZ1+BZ2
          CZ=F*WPP+FPP*W+2.0*LAMDA*FP*WP
          DZ1=BETA*ETA*BRAC1**2*2.0*FPP*WPP
```

```
      DZ2=BETA*ETA**2*FPP**2*(2.0*RE)**0.25/B/FPP00**0.5*EX*BRAC1
      DZ=DZ1+DZ2
      EZ1=BETA*ETA**2/ETADEL*EXLO*BRAC1*(PHI*2.0*FPP*WPP + ...
      0.5*(2.0*RE)**0.25/B/FPP00**0.5*ETADEL*FPP**2)
      EZ2=BETA*ETA**2/ETADEL*FPP**2*(EXLO*ETA/2.0*(2.0*RE)**0.25/...
      B/FPP00**0.5)*(1.0-2.0*EXLO)*PHI
      EZ=EZ1-EZ2
      GZ=-1.0-BRAC1**2*BETA*ETA**2*FPP
      WPPP1=(BZ+CZ+DZ+EZ)/GZ
      WPPP=WPPP1
      GO TO 1007
1006  WPPP2=-1.0*(F*WPP+FPP*W+2.0*LAMDA*FP*WP)/(1.0+EPONU)
      WPPP=WPPP2
*
*     STORE PARAMETERS FOR ESTIMATING STREAMWISE TERMS
      IF(I.GT. 3) GO TO 1007
      EPNU(I,J)=EPONU
      F2P(I,J)=FPP
      F1P(I,J)=FP
      F0P(I,J)=F
*
1007  CONTINUE
      WPP=INTGRL(WPP0,WPPP)
      WP=INTGRL(WP0,WPP)
```

```
         W=INTGRL(W0,WP)
         IF(KOUNT4.EQ. 0) GO TO 1020
         EPOUSD=EPONU/((2.0*RE)**0.25*FPP00**0.5*ETADEL)
         YODEL=ETA/ETADEL
*
*        CALCULATE OTHER BOUNDARY LAYER PARAMETERS
         UPLUS=2.0**0.25*RE**0.25*FP/FPP00**0.50
         YPLUS=2.0**0.25*RE**0.25*FPP00**0.50*ETA
         IDISP=1.0-FP
         DISP=INTGRL(DISP0,IDISP)
         IMOM=FP*(1.0-FP)
         MOM=INTGRL(MOM0,IMOM)
1020     CONTINUE
SORT
METHOD   RKSFX
*
TERMIN
      IF(ETA0)100,100,101
*
*     RESET INITIAL CONDITIONS TO VALUES AT ETA=0.50
100   ETAO=0.50
      FPP00=FPP0
      FPP0=FPP
      FP0=FP
```

```
      F0=F
      WPP0=WPP
      WP0=WP
      W0=W
      IF(KOUNT4.EQ. 0) GO TO 103
      DISP0=DISP
      MOM0=MOM
103   DELT=DELT2
      PRDEL=PRDEL2
      OUTDEL=OUTDL2
      FINTIM=FIN1
      GO TO 102
*
101   KOUNT=KOUNT+1
      IF(KOUNT-1)40,40,41
40    WRITE(6,13)
      WRITE(6,14)
41    WRITE(6,15)ETA,FP,WP,FPP,FPP00,ETADEL,EDEL, EZ, PHI
*
*     UPDATE FPP0
      FPP01=FPP00
      FPP00=FPP01+(1.0-FP)/WP
      IF(FPP00.LE. 0.0) FPP00=0.00001
      FPP00=(2.0*FPP00+1.0*FPP01)/3.0
```

```
*
*      RESET INITIAL CONDITIONS FOR NEXT LOOP
       N=J
       J=1
       K=1
       J4=3
       J16=0
       ETAO=0.0
       FPP0=FPP00
       FP0=0.0
       FO=0.0
       WPP0=1.0
       WP0=0.0
       WO=0.0
       DISP0=0.0
       MOM0=0.0
       DELT=DELT1
       PRDEL=PRDEL1
       OUTDEL=OUTDL1
*
       FINTIM=0.50
       FINETA=FIN1+0.50
       IF(KOUNT-40)30,31,31
31     WRITE(6,12)RE,A
```

```
      GO TO 34
*
*     CHECK CONDITIONS FOR CONVERGENCE
30    IF(KOUNT2.EQ. 1) GO TO 60
      IF(KOUNT2.EQ. 0) GO TO 61
60    IF(ABS(FPP01-FPP00)-0.00100)35,35,33
61    IF(ABS(FPP01-FPP00)-0.00100)35,35,33
35    IF((FINETA-EDEL).LT. 0.01 .AND. KOUNT2 .EQ. 0)FIN1=FIN1+ 3.0
      IF((FINETA-EDEL).LT. 0.01 .AND. KOUNT2 .EQ. 1)FIN1=FIN1+1.50
      IF(ABS(ETADEL-EDEL)-0.01)51,51,36
36    EDL2=EDL1
      EDL1=ETADEL
      ETADEL=EDEL
      IF(ETADEL.EQ.EDL2 .AND. ABS(ETADEL-EDL1).LE.0.25) GO TO 51
      GO TO 33
*
51    IF((FINETA-ETADEL).GT. 1.0) GO TO 52
      IF(KOUNT2.EQ.0) GO TO 52
      WRITE(6,10)
      WRITE(6,11)RE,A,LAMDA,ETADEL,KC,B
      IF(KOUNT4.EQ. 0) GO TO 53
      CF=FPP00*(2.0/RE)**0.5
      H=DISP/MOM
      DISP=DISP*(2.0/RE)**0.5
```

```
      MOM=MOM*(2.0/RE)**0.5
      WRITE(6,20)DISP,MOM,CF,H
53    KOUNT4=1
*
*     THIS SECTION CALCULATES THE CORRECTION TERMS
      IF(I-3) 54,55,34
54    RE=RE-DELRE
      GO TO 56
55    RE=RE+DELRE
      ETADEL=0.80*ETADEL
      FIN1=ETADEL+1.0
56    KOUNT=0
      KOUNT2=0
      KOUNT3=0
      KOUNT4=0
      IF(I-3) 58,57,57
57    DO199 L=1,200
199   ERROR(L)=0.0
      DO 200 L=1,N
      DFP=(F1P(1,L)-F1P(3,L))/(DELRE*2.0)
      DF=(F0P(1,L)-F0P(3,L))/(DELRE*2.0)
      ERROR(L)=2.0*RE*(F1P(2,L)*DFP-F2P(2,L)*DF)/(1.0+EPNU(2,L))
200   CONTINUE
58    I=I+1
```

```
      GO TO 33
*
52    FIN1=ETADEL+0.25
      KOUNT2=1
      GO TO 33
10    FORMAT(////,10X,'RE',14X,'A',13X,'LAMDA',9X,'ETADEL',10X,'K',15X,
     $'B')
11    FORMAT(/,6E15.4,////)
12    FORMAT(' EXCEEDED 50 LOOPS   RE=',1E15.4,'   A=',1E15.4)
13    FORMAT(//.'1 THE FOLLOWING VALUES SHOW THE CONVERGENCE TREND')
14    FORMAT(//,8X,'ETA',12X,'FP',12X,'WP',11X,'FPP',10X,'FPPC',8X,
     $'ETADEL',8X,'EDEL',8X,'   EZ',9X,'PHI',//)
15    FORMAT(9E14.5)
20    FORMAT(1X,'DISP =',1E14.4,3X,'MOM =',1E14.4,3X,'CF =',
     $1E14.4,3X,'H =',1E14.4,//)
33    EPONU=0.0
102   CALL RERUN
34    CONTINUE
END
*
PRINT    ETA,F,FP,FPP,FPPP,YPLUS,UPLUS,EPONU
PRTPLT   ERRORK(ETA,FPP,DELT), EPONU(WP,EPOUSD,YODEL)
*
END
STOP
```

Table A-1

Definition of Symbols in Program

Symbol in Program	Symbol in Text or Definition
A	= a
B	= b
BETA	= β
CF	= c_f
DELRE	= Increment of Re to be used for estimation of streamwise terms
DELT1	= Integration step size for $\eta<0.50$
DELT2	= Integration step size for $\eta>0.50$
DISP	= $\delta^* \ (u_\circ/u_a\xi)$
EDEL	= Calculated value of η_δ
EPONU	= ε/ν
EPOUSD	= $\varepsilon/(u_*\delta)$
ERROR1	= Statement to input the estimated streamwise terms in equation form
ERRORK	= Dummy for ERROR(K)
ERROR(K)	= Array for storage of estimated streamwise terms
ETA	= η
ETADEL	= η_δ
EX	= $EXP(-\phi\eta/\eta_\delta)$
F	= f
FIN1	= Value of η at which the integration is to be stopped. Generally start with FIN1 = $\eta_\delta + 3.0$

FP	=	f'
FPP	=	f''
FPPO	=	f_o''
FPPP1	=	f''' for η/η_δ < transition point
FPPP2	=	f''' for η/η_δ > transition point
H	=	H
KC	=	k
LAMDA	=	λ
MOM	=	$\Theta(u_o/u_a)$
OUTDL1	=	Print increment for $\eta < 0.50$
OUTDL2	=	Print increment for $\eta > 0.50$
PHI	=	ϕ
PRDEL1	=	Plot increment for $\eta < 0.50$
PRDEL2	=	Plot increment for $\eta > 0.50$
RE	=	Re
TRANSP	=	Transition point from inner region to outer region of the boundary layer expressed as fraction of η/η_δ
UPLUS	=	u^+
U	=	Meissinger influence function
UPPP	=	U''' (prime denotes differentiation with respect to η)
YODEL	=	y/δ
YPLUS	=	y^+

Appendix B

Meissinger's Influence Function Technique

As stated in Chapter V, due to the length of the equations involved, Meissinger's influence function technique for solving the turbulent boundary layer momentum equation is presented here. This technique provides a means to update f_o'' and η_δ.

Letting

$$Q = \phi\eta/\eta_\delta \tag{B-1}$$

and rearranging the turbulent boundary layer momentum equation as given in Equation 4-20, one obtains

$$\underbrace{f'''}_{A} + \underbrace{(1-e^{-Q})^2\beta\eta^2 f''f'''}_{B_1} + \underbrace{ff'' - \lambda(1-f'^2)}_{C} + \underbrace{\beta\eta f''^2(1-e^{-Q})^2}_{D} + \underbrace{\beta\eta f''^2 Qe^{-Q}(1-e^{-Q})}_{E} = 0 \tag{B-2}$$

The symbols, A, B_1, C, D, and E, are merely used to identify the various terms and have no relation to other parts of the text.

According to Meissinger's influence function technique, Equation B-2 is differentiated with respect to the influence parameter f_o''. Again α will be used to represent f_o'' for convenience. Recalling that

$$U = \frac{df}{d\alpha} \tag{B-3}$$

and noting that

$$\frac{d}{d\alpha} f' = \frac{d}{d\alpha}\left[\frac{df}{d\eta}\right] = \frac{d}{d\eta}\left[\frac{df}{d\alpha}\right] = U' \quad , \tag{B-4}$$

Equation B-2 gives the following when differentiated:

$$\frac{dA}{d\alpha} = U''' \tag{B-5a}$$

$$\frac{dB_1}{d\alpha} = \underbrace{(1-e^{-Q})^2 \beta\eta^2 f''U'''}_{G_\alpha}$$

$$+ \underbrace{(1-e^{-Q})^2 \beta\eta^2 f'''U'' + 2\beta\eta^2 (1-e^{-Q}) e^{-Q} Q_\alpha}_{B_\alpha} \tag{B-5b}$$

$$\frac{dC}{d\alpha} = C_\alpha = fU'' + f''U + 2\lambda f'U' \tag{B-5c}$$

$$\frac{dD}{d\alpha} = D_\alpha = 2\beta\eta(1-e^{-Q})^2 f''U'' + 2\beta\eta f''^2 (1-e^{-Q}) e^{-Q} Q_\alpha \tag{B-5d}$$

$$\frac{dE}{d\alpha} = E_\alpha = 2\beta\eta Q e^{-Q}(1-e^{-Q}) f''U''$$

$$+ \beta\eta f''^2 e^{-Q} Q_\alpha \left[(1-e^{-Q}) - Q(1-e^{-Q}) + Qe^{-Q}\right] \tag{B-5e}$$

where $Q_\alpha = \frac{dQ}{d\alpha} = \left[\frac{1}{2b} (2Re)^{1/4} \eta_\delta \ (\alpha)^{-1/2}\right]$. Solving for U''' in Equation B-5 results in the following:

$$U''' = \frac{B_\alpha + C_\alpha + D_\alpha + E_\alpha}{(1 + G_\alpha)} \qquad \text{(B-6)}$$

where B_α, C_α, D_α, E_α, and G_α are defined by Equation B-5b, c, d, and e. The boundary conditions for Equation B-6 are identical to those derived for laminar boundary layers in Equation 5-8. They are

$$\text{at } \eta = 0 \qquad \begin{cases} U = 0 \\ U' = 0 \\ U'' = 1 \end{cases} \qquad \text{(B-7)}$$

Equation B-7 gives all the boundary conditions necessary for the direct solution of Equation B-6 once f, f', f", and f''' are known. Thus, the influence function which produces successive estimates of f_o'' is given by

$$(f_o'')^{i+1} = \frac{1.0 - (f_\infty')^i}{(U_\infty')^i} + (f_o'')^i \qquad \text{(B-8)}$$

Appendix C

Comparison of Results Using Alternate Eddy Viscosity Distribution with Experimental Data

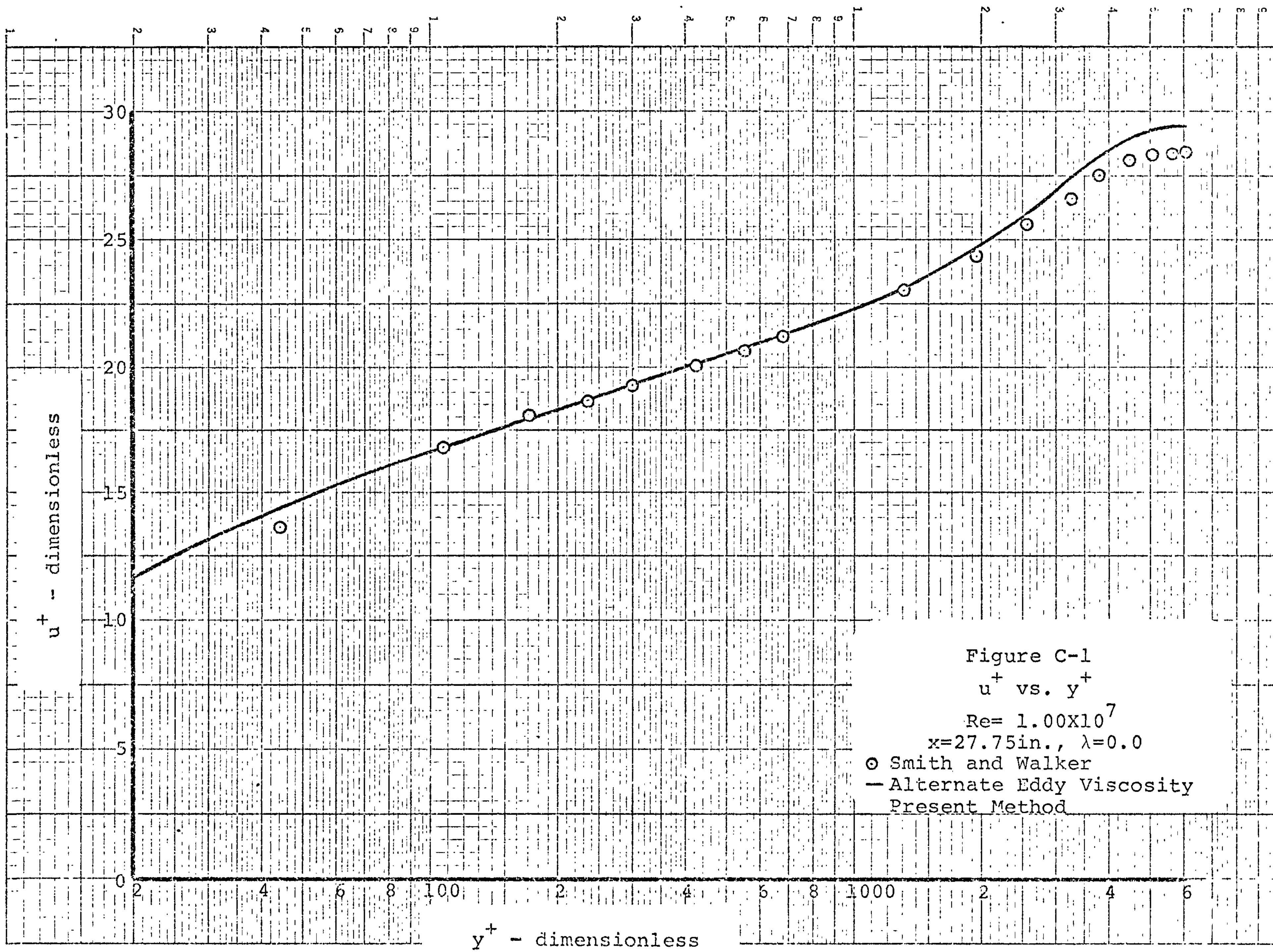

Figure C-1
u^+ vs. y^+
Re= 1.00X10^7
x=27.75in., λ=0.0

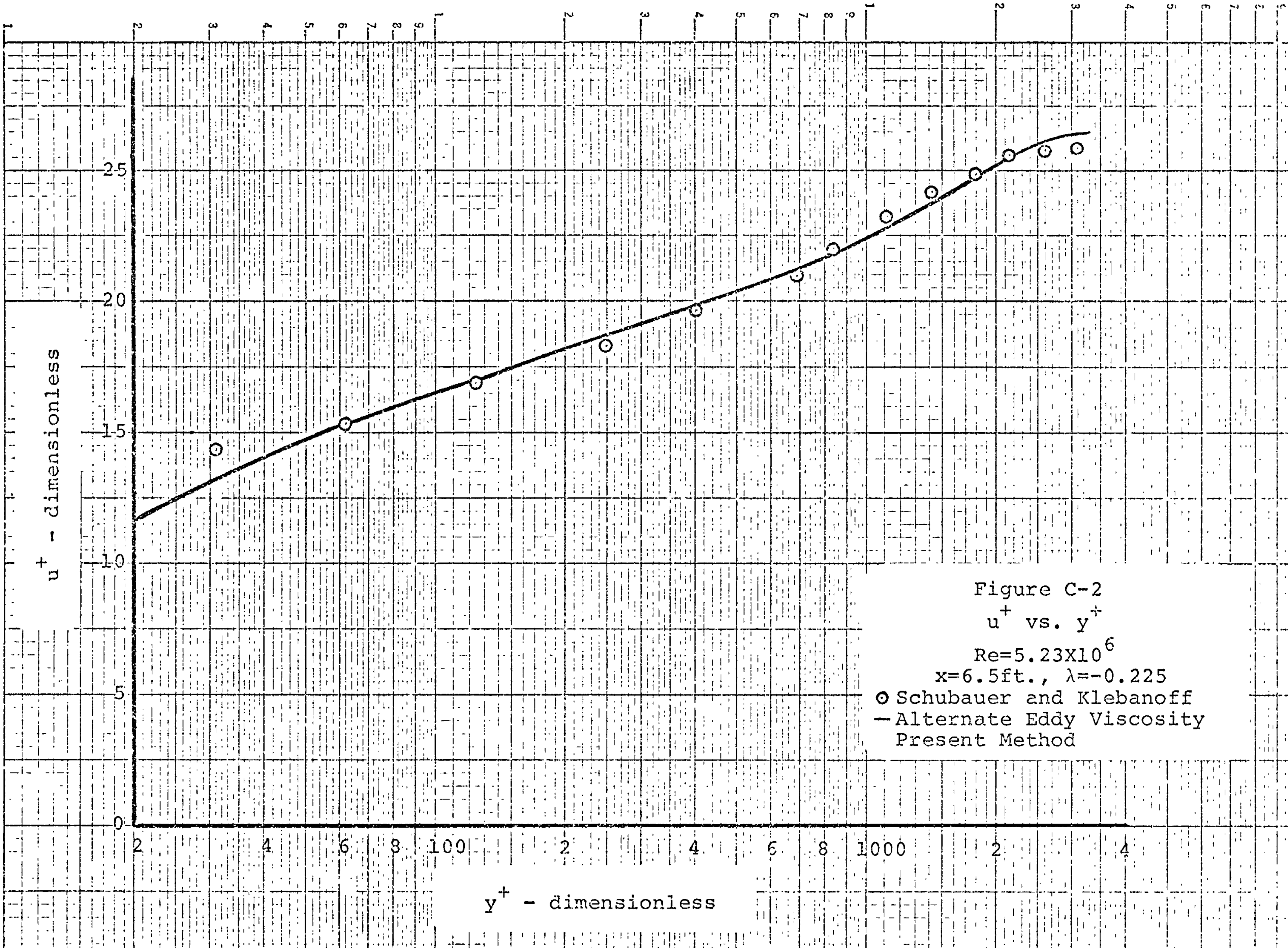

Figure C-2
u^+ vs. y^+
$Re=5.23X10^6$
$x=6.5ft.$, $\lambda=-0.225$

Table C-1

Comparison of Calculations Using Alternate Eddy Viscosity with Experimental Data

SMITH AND WALKER

$Re = 1.0 \times 10^7$ $\lambda = 0.0$

	$c_f \times 10^2$	δ^*, in.	ϕ, in.	H
Experimental	0.249	0.052	0.039	1.33
Calculated	0.233	0.057	0.044	1.32

SCHUBAUER AND KLEBANOFF

$Re = 5.23 \times 10^6$ $\lambda = -0.225$

	$c_f \times 10^2$	δ^*, in.	ϕ, in.	H
Experimental	0.244	0.101	0.076	1.33
Calculated	0.286	0.124	0.094	1.31

Appendix D

Nomenclature

a = Turbulence damping factor, dimensionless

b = Constant in eddy viscosity equation = 25.0, dimensionless

c_{favg} = Average skin friction coefficient = $2\theta/x$, dimensionless

c_f = Local skin friction coefficient, dimensionless

D = Dissipation integral in Equation 1-3

E = Dimensionless pressure gradient which characterizes equilibrium boundary layers

f = Dimensionless similarity variable

f''_o = Value of f'' at the wall, dimensionless

H = Shape factor = δ^*/θ, dimensionless

k = Constant in eddy viscosity equation, dimensionless

k_2 = Constant in Clauser's eddy viscosity equation for the outer region, dimensionless

L = Mixing length, ft.

P = Pressure, psi

Re = Reynolds' number

u = Velocity in streamwise direction, ft./sec.

u' = Fluctuating component of velocity in x-direction

u_a = Streamwise approach velocity, ft/sec.

u_o = Streamwise velocity at the outer edge of boundary layer, ft/sec.

u^+ = Velocity in terms of wall law, dimensionless

U = Dummy variable used in Meissinger's influence function technique, defined by Equation 5-6, dimensionless

v = Velocity in y direction, ft/sec.
v' = Fluctuating component of velocity in y-direction
x = Coordinate in direction of streamwise flow, ft.
y = Coordinate in direction normal to surface along which the boundary layer flows, ft.
y_m = Value of y at outer edge of boundary layer
y^+ = Distance in y-direction in terms of wall law, dimensionless

Greek Symbols

α = Dummy variable for f_o'', dimensionless
β = Constant = $2(2\ Re)^{1/2}k$, dimensionless
γ = Klebanoff's intermittency factor, dimensionless
Δ = Finite difference
Δ_c = Symbol for streamwise terms in momentum equation, defined by Equation 5-14, dimensionless
ψ = Stream function
η_1 = Intermediate variable in developing η, (Equation 4-3)
η = Dimensionless similarity variable
η_δ = Value of η at outer edge of boundary layer, dimensionless
θ = Momentum thickness, in.
δ^* = Displacement thickness, in.
δ_c^* = Displacement thickness as calculated by Clauser's eddy viscosity equation (Equation 3-3), in.
ρ = Density, lb/ft.^{3}
τ_w = Shear stress at the wall, lb/ft.^{2}
μ = Absolute viscosity, lb/ft.sec.

ν = Kinematic viscosity, lb/ft.^{2}

δ = Boundary layer thickness, in.

δ^{**} = Dissipation energy thickness, in.

ε = Eddy viscosity, lb/ft.^{2}

λ = Dimensionless pressure gradient, defined by Equation 4-10

ξ = Independent similarity variable in x-direction, ft.

ϕ = Expression in Gill and Sher eddy viscosity distribution, defined in Equation 3-1

Subscripts

$(\ )_i$ = Denotes inner region of boundary layer

$(\ )_o$ = Denotes outer region of boundary layer

$(\ )_\eta$ = Denotes differentiation at constant η

$(\ )_\infty$ = Denotes evaluation at $\eta = \infty$

Superscripts

' = Prime denotes differentiation with respect to η

$\overline{(\ )}$ = Time averaged